Paleocene-earliest Eocene Larger Benthic Foraminifera and *Ranikothalia*-bearing carbonate paleo-environments of Costa Rica (South Central America)

Claudia Baumgartner-Mora and Peter O. Baumgartner
Institut des Sciences de la Terre, Université de Lausanne, Géopolis, CH 10156 Lausanne Switzerland
email: claudia.baumgartner@unil.ch

ABSTRACT: Here we present a biostratigraphic and systematic revision of American *Ranikothalia*, based on outcrop collections form Costa Rica end westernmost Panama and on type collections of the Naturhistorisches Museum Basel. Paleocene-lowermost Eocene *Ranikothalia*-bearing shallow-water limestones occur in three distinct palaeogeographic settings along the Southern Central American convergent margin:

1. The Barra Honda Limestone (Tempisque Basin, Costa Rica) is, according to $^{87}Sr/^{86}Sr$-ratios and biostratigraphy of mid Selandian to late Thanetian (? earliest Ypresian) age. Tectonic uplift and temporary demise of a Middle American Arc segment during the Selandian allowed the formation of the pure carbonates of the Barra Honda Limestone. The upper well-bedded subunit exposes a higher energy facies, in which *Neodiscocyclina* spp. and *Ranikothalia catenula* group (redefined here) are locally abundant. Open marine facies with *Morozovella velascoensis* interfinger in a small scaled facies pattern in the topmost part. Tectonic subsidence and resumed arc activity resulted in rapid eutrophication/drowning.

2. Herradura – Quepos carbonate shoals on oceanic seamounts. The Herradura and Quepos terranes may represent the earliest seamounts formed by the Galapagos hotspot plume tail activity, >1000km to the SW of their present-day position. Pillowed lava flows and subaerial volcanic breccias occur with Upper Palaeocene-lowermost Eocene shallow-water limestones rich in *Ranikothalia* gr. *catenula*, *Neodiscocyclina* spp. and coralline algae.

3. Burica Peninsula – carbonate shoal on an accreted oceanic plateau. An Upper Paleocene carbonate shoal established on part of the Inner Osa Igneous Complex after its accretion to the western edge of the CLIP (Caribbean Large Igneous Province) and its possible emersion. *In situ* rhodoid limestones of the Río Palo Blanco (W-Panama) contrast with redeposited material in turbidites and debris flow breccias, interbedded with siliceous pelagic limestones and arc-derived mudstones.

A morphometric study on 150 axial sections of *Ranikothalia* spp. from all studied settings reveals a morphologic continuum between megalospheric (A) forms and microspheric (B) forms previously described as several species, here grouped as the *R.* gr. *catenula.* We conceive that these co-occurring morphotypes belong to one biological species. The separation of this group into 2 or 3 genera seems highly artificial, since many samples contain transitional forms between the "sub-evolute" microsphreric forms "*Caudrina*" *soldadensis* (*R. catenula soldadensis* herein) and the involute "*Chordoperculinoides" bermudezi* (*R. c. bermudezi* herein). Neither from previous studies nor from our material we can conclude on a biostratigraphic relevance of the various morphotypes. In particular, we cannot confirm a stratigraphic succession from flatter (*R. c. soldadensis*) to more robust (*R. c. bermudezi*) forms.

Shape and shell thickness distribution of morphotypes of the *Ranikothalia* gr. *catenula* can be interpreted in terms of hydrodynamic energy and light availability in their habitat, in comparison with observations made on living LBF. This interpretation matches the hydrodynamic energy deduced from the microfacies and the abundance of photosynthetic red algae in our thin sections. Flat lenticular delicate A-forms (*R. c. catenula)* occur together with delicate B-forms (*R. c. soldadensis)* both in shallow protected and deeper off-shore calm water areas. The most robust B-form *R.c. bermudezi* may be a good indicator of shallow, high energy palaeo-environments. Possible Paleoceme dispersal routes for Amerucan *Ranikothalia* are discussed.

INTRODUCTION

Southern Central America is composed of a puzzle of oceanic terranes that extend between the North American continental slivers of Chortis s.str., forming the mountains of NW-Nicaragua, and the South American Plate, represented by the Columbian Andes (text-fig. 1 A). No ancient continental basement is known from these South-Central American terranes, here called "oceanic Central America". The basements are oceanic in origin, including the southern half of the classical "Chortis Block" formed by subduction/accretion mélanges that we called Mesquito Composite Oceanic Terrane (MCOT, Baumgartner et al. 2008). The rise of these oceanic basements into the photic zone and the formation of neritic carbonates was controlled by convergent, collision tectonics, and/or arc development. In this context, shallow carbonate paleo-environments were short-lived and formed not only on uplifted basements and arcs, but also on (now accreted) volcanic edifices of Pacific oceanic seamounts.

Mesozoic pelagic paleoenvironments are represented by radiolarites of Late Triassic to Late Cretaceous age in the Mesquito Composite Oceanic Terrane of Nicaragua and the Nicoya Terrane of Northern Costa Rica (Denyer and Baumgartner 2006, Baumgartner et al. 2008, Bandini et al. 2008, 2011). The oceanic basements cropping out from Central Costa Rica to Panama and to Eastern Colombia are Late Cretaceous in age and remain in the pelagic realm until the early Cenozoic.

The Late Cretaceous-Paleogene history of the southern Central American land bridge is characterized by a subduction-related tectonic environment with the accretion of oceanic terranes to the western edge of the CLIP (Caribbean Large Igneous Province), the oceanic part of the Caribbean Plate (Bourgois et al. 1984, Baumgartner et al. 1989, 2008, Di Marco, Baumgartner and Channell 1995, Buchs et al. 2009, 2010, 2011a, b).

Age and distribution of shallow carbonates in oceanic Central America and the Caribbean

Shallow carbonate paleo-environments in the area were mostly ephemeral and restricted to phases of tectonic uplift or volcanic build-up, which created short-lived and mostly disconnected carbonate shoals, unlike the large carbonate platforms on continental margins. Major drops in sea-level may have enhanced short-lived shallow-water conditions. Most of the limestones formed on these shoals are dominated by Larger Benthic Foraminifera (LBF) and coralline algae, rather than coral build-ups, which are rare.

LBF are very important both for biochronology and paleo-environmental interpretation. Shape and test thickness of LBF are extremely dependent of the habitat in which each species may have lived (Hallock 1985, 1987, Hallock, Röttger and Westmore 1991, Hottinger, Haliez and Reiss 1993; Hohenegger 2000, 2004). The resulting high morphological variability led to endless taxonomic discussions, which in turn, were not favourable to the consolidation of a standard biozonation for Western Hemisphere, such as the one established for the Eastern Hemisphere (Serra-Kiel et al. 1998; Peybernès et al. 2000). Additional difficulties arise form the fact that many of the low latitude LBF occurrences lack entire groups, such as the Alveolinids, or the agglutinated forms which are absent in the Paleogene of oceanic S-Central America and the southern Caribbean. Much of the classical work on American LBF was based on discontinuous sections and on resedimented material (Caudri 1974, 1975, 1996) in which the age calibration was based on regional geologic concepts and occasionally associated other macro- and microfossil groups. Physical superposition of samples and fossil assemblages, essential in modern biochronoloy, has rarely been used in the study area. This situation led often to circular reasoning concerning biostratigraphic ranges. The best biozonation, so far, was published by Butterlin (1981). It is mainly based on observations in the large and long lasting carbonate realms of Mexico. Many species used in his zonation are absent from our study area. Nevertheless, some synthetic ideas on shallow carbonate occurrences in oceanic central America will be sketched here.

In oceanic Central America, i.e. from northeastern Nicaragua (NW) to eastern Panama (SE) we observed a systematic younging of the first shallow-water carbonate facies encroaching on oceanic basements and/or older deep-water formations (text-fig. 1b, Baumgartner-Mora, Baumgartner and Barat 2013). Here is a short inventory of shallow carbonate occurrences in this area.

Aptian-Albian. Shallow-water limestones (Cerro Vailavas, Siuna area, NE Nicaragua) are dated by rudists and Albian LBF such as *Orbitolina (Mesorbitolina) texana* (Roemer 1849) (Vaughan 1932, Vaughan and Cole 1941), rest unconformably on Lower Cretaceous deep water sediments which seal the exhumation of the Siuna Serpentinite Mélange, part of the MCOT (Baumgartner et al. 2008, Flores et al. 2015).

Middle Campanian - lower Maastrichtian. The shallow-water El Viejo Formation (N-Costa Rica, Schmidt-Effing 1975; Pons, Vicens and Schmidt-Effing 2016), dated by rudists and LBF, such as *Pseudorbitoides rutteni, Pseudorbitoides israelskyi, Sulcoperculina globosa* and *Sulcoperculina* sp. (Baumgartner-Mora and Denyer 2008), unconformably encroaches on the Nicoya- and Santa Elena basement complexes, with rudistid biostromes followed by open platform bioclastic limestones, wich are in turn overlain by pelagic upper Maastrichtian-Paleocene sediments. Campanian- Maastrichtian shallow-water material including LBF was also found re-deposited in deep water sediments in the Herradura and Quepos promontories (central Pacific coast of Costa Rica, text-fig. 1.). Azema et al. (1979) described limestone clasts containing *Pseudorbitoides* sp. and *Sulcoperculina* sp. from Punta Quepos. This material was probably derived from a chain of seamounts (the Herradura-Quepos Terrane, see below), now accreted to the trailing edge of the Caribbean Plate.

Lower Paleocene. No shallow carbonates of the lower Paleocene are known so far from oceanic S-Central America and the Caribbean.

Upper Paleocene/lowest Eocene. Ranikothalia-bearing shallow-water carbonates, of the upper Paleocene, the subject of this chapter, are only known from few localities in oceanic S-Central America, namely from Costa Rica and W-Panama (text-fig. 1.). Two main, distinct geological settings can be observed: 1. The Barra Honda Formation (Dengo 1962), preserved as remnants in the Costa Rican Tempisque Basin (text-fig 1.b, 2). It rests unconformably on Upper Cretaceous to lower Paleocene deep-water formations forming an eroded structural high (Jaccard et al. 2001). As we shall discuss in detail in this chapter, the main body of the Barra Honda carbonate platform (originally >900 km^2) is made of mostly restricted, pure carbonate facies dated as late Paleocene (Thanetian) by ^{87}Sr / ^{86}Sr ratios, LBF such as *Ranikothalia catenula* group and planktonic foraminifera. Barra Honda is covered by Eocene turbidites. 2. Other upper Paleocene – lowest Eocene shallow carbonates occur mainly as resediments exposed in the Herradura area, the Quepos promontory and the Osa and Burica peninsulas along the Pacific coast of southern Costa Rica/western Panama. They are associated to deep water sequences and are interpreted as resediments transported down slope from insular carbonate shoals. All these occurrences are related to oceanic terranes that are exotic with respect to the early Cenozoic W-margin of the Caribbean Plate. They are characterized by a complex accretionary history (Buchs et al. 2009, 2010) that will be dealt with below under “geological setting” of each area.

To the SE of the S-Nicoya fault line (Central Costa Rica, text-fig. 1.) Late Cretaceous oceanic plateaus may represent actual outcrops of the trailing edge of the Caribbean Large Igneous Province (CLIP). These include the SE corner of the Herradura Promontory (text-fig. 1, Denyer and Gazel 2009) and the Azuero Plateau cropping out in Coiba, Soná and Azuero (Panama, Buchs et al. 2010). The Upper Cretaceous formation of the CLIP triggered a new, E-dipping subduction zone, the Middle American Trench, and Campanian-Maastrichtian arc initiation on the trailing CLIP edge (Buchs et al. 2009, 2010). Shallow carbonates do not occur until the Eocene, when the volcanic arc became more mature (Alvarado et al. 2007) and when the collision of Pacific terranes created tectonic uplift.

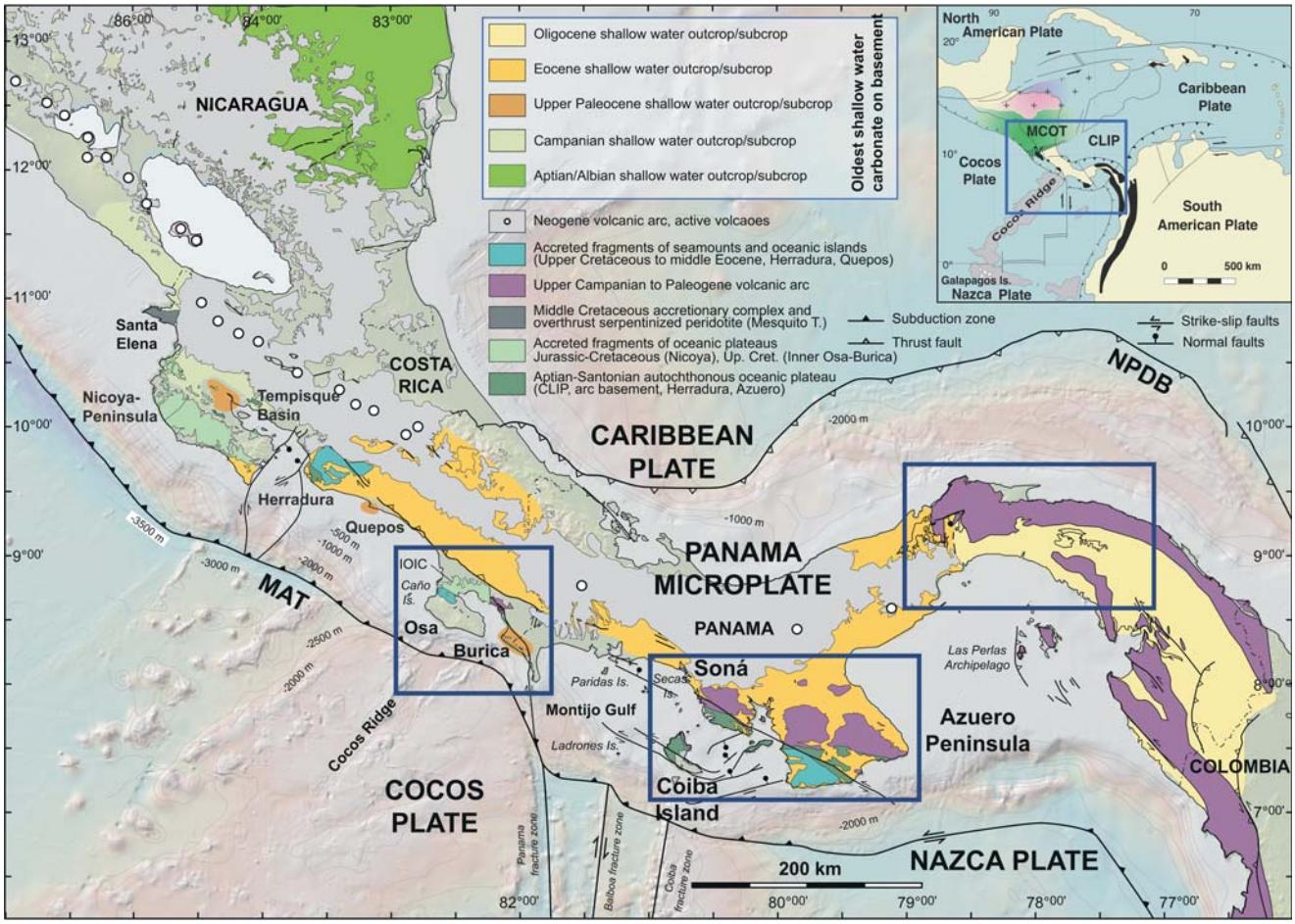

TEXT-FIGURE 1
A. Plate tectonic situation of Central America with the new subdivision of the Chortis Block according to Baumgartner et al. (2008). B. Terrane map of E-Panama, Costa Rica and Nicaragua, modified after Andjic, Baumgartner-Mora and Baumgartner (2016). Geological sketch map of South-Central America. Main map: Principal igneous basement and arc units modified after Buchs et al. (2010). Sediments are illustrated as a theoretical subcrop map of the oldest shallow-water carbonates on basements or older oceanic formations. Areas discussed in this paper in blue rectangles.

Middle to Upper Eocene. Carbonate banks/ramps of the Middle to Upper Eocene are widespread along the Middle American Arc and forearc areas, that reached the photic zone due to uplift during collisional events (Andjic, Baumgartner-Mora and Baumgartner 2016) or buoyancy of the evolving arc. Shallow carbonates of this age occur also on the Hess Escarpment and the lower Hess Rise (Baumgartner and Baumgartner-Mora *in*: Werner et al. 2010, Weber 2013), Jamaica, Puerto Rico, Hispaniola, Saint Barthélemy, Carriacou, Trinidad, N-Venezuela and NW-Colombia (text-fig. 1A). They are dated by a variety of LBF of the genera *Amphistegina, Asterocyclina, Discocyclina, Eoconoloides, Eofabiania, Fabiania, Gypsina, Helicolepidina, Heterostegina, Lepidocyclina, Linderina, Neodiscocyclina, Nummulites, Operculina, Orthophragmina, Polylepidina, Proporocyclina,* and *Sphaerogypsina* (Baumgartner-Mora, Baumgartner and Tschudin 2008). The first shallow carbonates that encroach on arc/forearc basements in Panama are dated as Upper Eocene in Azuero and the Canal Basin (Cole 1959, Buchs et al. 2010, Montes et al. 2012a).

Oligocene - lower Miocene. carbonate shoals, dated by *Lepidocyclina miraflorensis, L. giraudi,* and *L. canellei* as upper Oligocene - lower Miocene are the first shallow carbonates that encroach on arc-derived conglomerates and breccias around the Chucunaque Basin of Eastern Panama (Barat et al. 2014). Upper Oligocene carbonate shoals are known from N Costa Rica (Andjic, Baumgartner-Mora and Baumgartner 2016) and the Nicoya Peninsula (Baumgartner-Mora, Baumgartner and Tschudin 2008).

STUDIED LOCALITIES AND SAMPLES

This report is based on our own collections, as well as on field work shared with several PhD-students between 1983 and 2015. We use data and samples collected by them. in particular, by Obando (1986), Di Marco (1994), Di Marco, Baumgartner and Channell (1995), Jaccard et al. (2001) Jaccard and Münster (2001), Arias (2000, 2003), Buchs (2009, 2010, 2011), and Andjic, Baumgartner-Mora and Baumgartner (2016). All samples used in this report are listed in table 1, including information of the location, age and microfacies, as well as fossil content. In the early years we obtained determinations of microfossils in thin sections from J. Azéma, J. Butterlin, G. Glaçon, and J. Sigal. This data was used for a first synthesis of the stratigraphy and paleogeography of the Pacific side of Costa Rica (Baumgartner et al. 1984). Some of this data is also used in

TABLE 1
List of studied samples. Location of samples from Cerro Espiritu Santo are given in Lambert coordinates (for N-Costa Rica, see text-fig. 3).

Sample	Nb. of thin sections (coll.)	Locality, Age, Sr87/Sr86: Ma	Coordinates	Microfacies in thin section	Microfossils (abundance estimate: %)
Barra Honda Formation, Tempisque area, N-Costa Rica					
4,1B	1 (Jaccard et al.)	Laguna Jicote, Early - Mid. Eocene, 50+4-5	381.8/266.2	LBF - coralline algae - echinoderm packstone	*Neodiscocyclina sp.(30),* Melobesioideae *(40)* echinoderms *(30),*Nummulitidae, *Eoconoloides wellsi,*
8-2D	1 (Jaccard et al.)	Cerro Alto Viejo, Late Palaeocene	385.8/260.9	pelagic lime-wackestone	*Morozovella velascoensis*
15.1	1 (Jaccard et al.)	Cerro Corralilio, Late Paleocene	388.4/241.8	pelletal mudstone	*Praealveolina sp.*
23.8		Pochote, Late Palaeocene, 58+4-2	395.6/236.6	corallinacean wackestone	*Polystrata alba,* geniculate corallines, *Sporolithon, Melobesioideae*
6.8	1 (Jaccard et al.)	Espiritú Santo, Late Palaeocene, 56+6-2	388.1/263.1	corallinacean - *Polystrata alba* wackestone	*Ranikothalia catenula* group, *Polystrata alba,* geniculate corallines, *Distichoplax biserialis, Sporolithon,* Melobesioideae
6.7A	1 (Jaccard et al.)	Espiritu Santo, Late Palaeocene, 57+8-3	388.1/263.1	corallinacean - *Polystrata alba* wackestone	*Ranikothalia catenula* group, *Polystrata alba,* geniculate corallines, *Distichoplax biserialis, Sporolithon, Melobesioideae*
CM 1533	3 (CBM)	Espiritu Santo, Late Palaeocene	388.1/263.1	*in situ* corallinacean - LBF packstone - rudstone, stromatilite clast, rhodoids	*Ranikothalia catenula* group (10), geniculate corallines *(20), Distichoplax biserialis (10),Sporolithon (20) Polystrata alba (10),* Melobesioideae *(10)*
CM 1534	3 (CBM)	Espiritu Santo, Late Palaeocene	388.1/263.1	*in situ* geniculate coralline - LBF packstone - wackestone,	*Ranikothalia catenula group (2), geniculate corallines (20), Distichoplax biserialis (20),Melobesioideae (10),* miliolids, *Morozovella sp. cf. M. velascoensis*
Santo 02	3 (CBM)	Espiritu Santo, Late Palaeocene	388.1/263.1	*in situ* rhodoid-*Polystrata* bafflestone	rhodoids: Melobesioideae (30), *Polystrata alba* (10), solenoporid algae,*Ranikothalia catenula* group (10), geniculate corallines (10), *Distichoplax biserialis* (10)
JMIII6	1 (Jaccard et al.)	Cerro Guayacán, Late Paleocene	390.3/259.2	bioclastic wackestone	*Polystrata alba*, Miliolidae, *Sigmoilopopsis* sp., *Distichoplax biserialis*
6.9	1 (Jaccard et al.)	Espiritú Santo, Late Plaeocene	388.1/263.1	pebble of white micrite encrusted by coralline algae	Miliolids, Melobesioideae
Herradura Quepos Terranes, Central Costa Rica					
Esp084	2 (CMB)	N-end of Playa Espadilla, Quepos, Late Paleocene	N 9°23'48" W 84°09'48"	redeposited blocks of limestone breccia: coralinacean-LBF rudstone	Melobesioideae (20), geniculate corallines (30), LBF (10): *Neodiscocyclina* sp., *Ranikothalia cat*enula group, crinoids
Esp004	1 (CMB)	N-end of Playa Espadilla, Quepos, Late Paleocene	N 9°23'48" W 84°09'48"	redeposited blocks of limestone breccia: coralinacean-pelagic clast rudstone	pelagic clasts*: Morozovella velascoensis,* geniculate coralines, Melobesioideae
QC15	2 (CMB)	Quebrada Camaronera, Quepos, Late Paleocene	N 9°23'51" W 84°08'22"	redeposited LBF-corallinacean grainstone, current sorted and oriented LBF	geniculate corallines (20), *Neodiscocyclina* sp. (30), *Ranikothalia catenula antillea-tobler*i A-forms (30), *Lithophyllum*
QC 16	1 (CMB)	Quebrada Camaronera, Quepos	N 9°23'51" W 84°08'22"	redeposidted melobesioidean-LBF rudstone - stylobreccia	Melobesioideae (70), *Neodiscocyclina* sp. (20)
CM806	1 (CMB)	Playa Macha Sur, Quepos, Late Paleocene	N 9°24'49" W 84°09'52"	redeposidted coraline-LBF rudstone olivine reworked from seamount basement	geniculate coralines (40), Melobesioideae (30), *Lithophyllum, Neodiscocyclina* sp. (10), *Ranihothalia catenula anillea, tobleri, bermudezi* (1) dasycladacean
OA63	3 (O. Arias)	Río Cañas, Herradura Terrane	N 9°32'52" W 84°07'50"	redeposited rhodoid-LBF rudstone - stylobreccia.	rhodoids (90): mainly *Mesophyllum, Lithophyllum, Ranikothalia catenula antillea (5) Discocyclina* sp.*(5),* bivalve fragments, bryozoans.
OA64	5 (O. Arias)	Río Cañas, Herradura Terrane	N 9°32'52" W 84°07'50"	resedimented LBF-coralline rudstone, large size sorting	LBF(70): *Ranikothalia catenula* ssp.: *antillea, bermudezi, soldadensis,* geniculate corallines (20), oyster fragments, bryozoans
OA65BB	15 (O.Arias)	Río Cañas, Herradura Terrane	N 9°32'52" W 84°07'50"	resedimented LBF-coralline packstone small size sorting	LBF(70): *Ranikothalia catenua antillea* (60), *Discocyclina* sp. (10), geniculate corallines (20), oyster fragments, bryozoans
OA65CC	15 (O.Arias)	Río Cañas, Herradura Terrane	N 9°32'52" W 84°07'50"	resedimented LBF-coralline packstone large size sorting	LBF(70): *Ranikothalia catenua* ssp.: *antillea*, *bermude*zi, *soldadensis*, geniculate corallines (20), oyster fragments, bryozoans

TABLE 1 (continued)
List of studied samples. Location of samples from Osa and Burica Peninsulas (see text-fig. 7).

Osa Mélange. Osa Peninsula, S-Costa Rica					
CM 856	2 /CBM)	Brazo Derecho del Río Tigre, Osa Peninsula, Late Paleocene reworked	N 8°31'07.24" W 83°26'39.30"	redeposited LBF-corallinacean grainstone, size sorted, basalt clast reworked from basement	*Ranikothalia catenula*, mainly *antillea* A-forms (50), geniculate and melobesian corallines (30)
Burica Terrane, Burica Peninsula, S-Costa Rica and W-Panama					
CM 316, CM324	12 (CBM)	Playa Mangle, Burica Peninsula, Costa Rica, Late Palaeocene	N 8°24'13" W 83°07'44"	redeposited LBF-rhodoid grainstone-rudstone, basalt clasts reworked from basement, current size sorted	*Ranikothalia catenula* ssp. *antillea, tobleri* equatorial sections (50), *Discocyclina* sp. (30), Melobesioideae (30), geniculate corallines (5), bryozoans
CM 314	12 (CBM)	Playa Mangle, Burica Peninsula, Costa Rica, Late Palaeocene	N 8°24'13" W 83°07'44"	washed sample	*Ranikothalia catenula* group, *Neodiscocyclina* sp.
GDM 92-41	2 (G. DiMarco)	headwaters of Río Palo Blanco, Burica, Peninsula, Pamana	N 8°20'08" W 83°01'35"	*in situ* melobesian bafflestone to boundstone with LBF, mixed large and small forms	Melobesioideae (60): *Sporolithon, Mesophyllum, Ranikothalia catenula* ssp:(40) *antillea, sodadensis, bermudezi, Neodiscocyclina* sp.(5), bryozoans
JOR 55	1 (J. Obando)	Playa Mangle, Burica, Middle Eocene	N 8°24'15" W 83°07'41"	calciturbidite with LBF	*Asterocyclina monticellensis, Pseudophragmina* sp. *Amphistegina* sp.
JOR 56a	1 (J. Obando)	Playa Mangle, Burica, CR, Late Paleocene-earliest Eocene	N 8°24'13.3" W 83°07'44.7"	pelagic limestone	*Morozovella velascoensis*
JOR 220	1 (J. Obando)	Q. Piedra Azul, top section, reworked Late Paleoc. clast in mid. Eocene	N 8°23'06" W 83°01'08"	LBF rudstione in clast	*R. catenula* group,*N. barkeri, Amphistegina*
JOR 254	1 (J. Obando)	Q. Piedra Azul, 5m below top, reworked Late Paleoc. clast in mid. Eocene	N 8°23'06" W 83°01'08"	LBF rudstione in clast	*R. catenula* group,*N. barkeri, Amphistegina*
JOR 256	1 (J. Obando)	Q. Piedra Azul, 35m below top, reworked Late Paleoc. clast in mid. Eocene	N 8°23'04" W 83°01'07.6"	LBF rudstione in clast	*R. catenula* group,*N. barkeri, N. cristensis* ? Melobesiae, *Amphisteginae*, bryozoans
JOR 258	1 (J. Obando)	Q. Piedra Azul, 120 m below top, Burica Peninsula, CR, early middle Eocene	N 8°23'00" W 83°01'07"	calciturbidite reworking middle Eocene platform material	*Amphistegina, Asterocyclina, Neodiscocyclina marginata, Pseudophragmina* (?) *flintensis, N. aster*, Melobesiae.
JOR 260	1 (J. Obando)	Q. Piedra Azul, 185 m below top, Burica Peninsula, CR, Late Paleoc.- Early Eocene	N 8°28'49" W 83°01'04"	Rresedimented LBF rudstone, with pelagic material	*R. catenula* group, *N. barkeri, M. weaveri,* radiolaria, *Morozovella* sp. globigerinids
JOR 261	1 (J. Obando)	Quebrada Piedra Azul, 225 m below top, Burica Peninsula, Late Paleoc. - Early Eocene	N 8°22'51" W 83°01'16"	planktonic foraminifer-radiolarian packstone	
JOR 281	1 (J. Obando)	Playa Mangle, Burica, CR, Late Paleocene-earliest Eocene	N 8°24'13.3" W 83°07'44.7"	pelagic siliceous limestone planktonic foraminifer wackestone	*Morozovella velascoensis*

this report. All illustrated thin sections are deposited at the Musée Cantonal de Géologie, Anthopole, University of Lausanne, Switzerland under the numbers MGL 96734 to MGL 96753

METHODS

Transmitted light microscope scanning of thin sections

Standard, polished geological thin sections were prepared oriented parallel and perpendicular to the bedding of all samples and were scanned with an Olympus VS110 slide scanner. A motorized z-stage allows an extended depth of focus over the thickness of the thin section by extracting the in focus features of several images with a different focal point. The motorized x-y-stage allows to take several hundred overlapping individual images, stiched together by the software to produce an image of approximately 12'000 x 26'000 pixels with the 4x objective. The resolution is about 622 pixels/mm for the 4x objective, 1555 pixels/mm for the 10x objective, and 3100 pixels/mm for the 20x objective. All thin sections were routinely scanned with the 4x objective, which gives a pixel size of about 1.6 µm. In general, this resolution is enough to allow for detailed analysis of microfossils on the whole surface of the thin section on the computer. The over 1 Gb scans were usually compressed as high quality .jpg files of 100-200 Mb, that could be analysed on a standard PC. Most transmitted light images of the plates were extracted from this type of scans. Transmitted light images were taken along with cathodoluminescence images at the same position and optical settings.

Optical cathodoluminescence

Cathodoluminescence (CL) in minerals depends on the presence trace elements that act as activators, which are stimulated to emit light when bombarded with energetic electrons. In carbonates the most common activator is bivalent manganese (Mn^{2+}). Bivalent iron (Fe^{2+}) is the most important quencher ion (Sommer 1972). CL has been widely used to visualize zoning of minerals (e.g. zircons, carbonates). In carbonate minerals CL has allowed to better understand diagenetic processes. Reviews were presented by Marshall (1988), Machel et al. (1991), Pragel et al. (2000) and Scholle and Ulmer-Scholle (2003). CL has been widely applied to establish cement stratigraphy (Meyers 1974, 1978; Bruckschen, Neuser and Richter 1992).

CL responses are normally described as brightly luminescent, dully luminescent, or nonluminescent, although modern equipment allows more detailed measurement of intensities and spectral information on CL (Cazenave, Chapoulie and Villeneuve

2003). In general, incorporation of Mn^{2+} into the calcite lattice stimulates luminescence and incorporation of more than 200 ppm of Fe^{2+}, reduces or quenches luminescence. Qualitative interpretation of CL assigns dull blue, intrinsic luminescence to oxidizing environments in which the reduced forms of both Mn and Fe are unavailable for incorporation into the crystal lattices of calcite or dolomite. Oxidized forms of these elements are not incorporated into calcite or dolomite crystals. Bright yellow-orange luminescence is associated with crystals with relatively high Mn/Fe trace element ratios, typically achieved under reducing conditions during early to intermediate stages of burial diagenesis (Scholle and Ulmer-Scholle 2003).

The relationship between CL emission intensities and trace-element concentration has been controversial, principally because results were reported as qualitative (visual) estimates of CL intensity and color. In addition, Mn^{2+} concentrations in luminescing calcites have been near or below the practical detection limit of the electron microprobe.

In recent work both on natural and synthetic calcites (El Ali et al. 1993, Cazenave et al. 2003) it has become clear that for low Fe^{2+} contents the lower detection limit of orange (600 nm) CL activation is around 10-20 ppm Mn. A slightly higher Mn concentration required in dolomites reflect the less effective activation by Mn^{2+} incorporated on the Mg^{2+} site than on the Ca^{2+} site of dolomite (Sommer 1972, Cazenave et al. 2003).

Moderate CL intensities were reported from calcites containing 200 to 700 ppm and bright intensities from calcites with more than 700 ppm Mn^{2+}. A linear relationship between Mn^{2+} concentration and photometrically measured CL intensity can be observed at low concentrations. Above 400-600 ppm, the increase of CL intensity is less than the linear trend, perhaps due to the beginning of concentration quenching. Data on the effect of Fe^{2+} quenching are still controversial, although CL intensity of calcite seems to be more sensitive to Mn^{2+} activation than Fe^{2+} quenching.

Increased Fe/Mn ratios result in steeper slopes of the Mn luminescence linear trend. However, below 200 ppm no quenching occurs, and no extinction, even for low Mn values, was observed up to 3000 ppm of Fe. In general, more than 10,000 ppm (1 wt.%) of Fe_2 are needed to extinguish Mn-activated CL. Mn-free and Fe-poor calcites show a dull intrinsic blue (410-430 nm) CL. Violet-mauve colours arise from the combination of intrinsic CL and low Mn^{2+} activation.

Recent biogenic carbonates show a wide range of CL intensities (Barbin et al. 1991a). Both metabolic processes and changes in the environment can be invoked to explain Mn-variations during growth of calcareous shells (Barbin et al. 1991b). Comparatively few CL-work has been dedicated to the detection of microfossils in recrystallized rocks and the biomineralisation and earliest diagenesis of recent and fossil material (Amieux 1987; Martini et al. 1987, Baumgartner-Mora and Baumgartner 1994, Green 2001, Kolodziej et al. 2011). Barbin et al. (1989) interpreted variable CL response of larger foraminifers within the same population as the result of synsedimentary mixing of specimens from different environments.

For us, CL analysis of polished thin sections has become a routine method (Baumgartner-Mora and Baumgartner 1994) for the observation of microfossils in recrystalized limestones recovered from accreted terranes of Costa Rica and the Caribbean (Baumgartner-Mora et al. 2008, Baumgartner-Mora and Baumgartner 2011).

Optical microscopy of microfossils in thin sections of carbonates allows observing the carbonate crystal architecture resulting form diagenetic modification of original biominerals. Only physical grain size and orientation fabrics, as well as major impurities, such as clays in the matrix and oxide stains can be visualized. In contrast, CL detects very minor variations in the trace-element concentrations of Mn^{2+} within crystals. These are a result of either variable incorporation of Mn^{2+} during biomineralization (cf. Barbin 2000), or represent earliest diagenetic modifications of biominerals and the precipitation of the first cements under variable redox conditions in the post-mortem microenvironment. Luminescent zonations in carbonates reflect differential Mn^{2+} uptake during crystal growth which can be caused by: (1) changes in trace element composition of the precipitating fluid, or (2) changes in the crystal growth rate independent of the Mn^{2+} concentration in the fluid. Hence, CL is an excellent method to analyze the original microscopic architecture of Larger Benthic Foraminifera, since original, biomineralized material can be distinguished from diagenetic cements. CL in thin sections of rocks may rival with SEM observation of well-preserved, isolated material in revealing original lamellar structures and stoloon/pore systems in LBF (plate 7, text-fig. 10). CL permits safe systematic description of benthic and planktonic Foraminifera even in highly recrystallized rocks. Systematic definitions of larger foraminifer species may need revision as a result of the gain in morphologic resolution. The dark/bright CL banding parallel to the lamellar structure observed in many nummulitid specimens (Pl. 7.) is interpreted as a primary growth structure. It resulted from variable incorporation of Mn^{2+}during phases of biomineralisation due to changing environmental and/or metabolic conditions.

Preservation of fine growth structures in LBF seems to be better in carbonate material penecontemporaneously displaced into deeper water environments. Even under this condition, the majority of LBF preserved only a partially or completely recrystallized test. Growth structures are usually destroyed in shallow water limestones, where *in situ* material underwent lithification in the shallow environment. We conclude that the preservation of growth structures is the result of displacement of tests into deeper water. In the open marine, carbonate bank environment, recent tests that had undergone the earliest diagenetic plugging of microporosity only, must have coexisted with already transformed material. The resedimentation process sampled such a mixture and displaced it into a deep water environment, which preserved the earliest stages of diagenesis. In contrast, high fluxes of seawater through consolidated sediment in shallow bank environments may lead to total recrystallization of all tests and to rapid early lithification under homogeneous Eh/pH conditions resulting in undifferentiated CL.

Laboratory procedure. For cathodoluminescence 40 µm thick thin sections were highly polished with diamond paste. A good polish is essential to achieve high resolution and well focused images. CL images were obtained in using the electronics and electron gun of OPEA adapted to The vacuum chamber of CTTL, Technosyn 8200 MkII, mounted o n an Olympus light microscope with a mobile tubus and an object stage fixed in height. The OPEA was operated at 15-20 kV and 0.4 - 0.5 mA

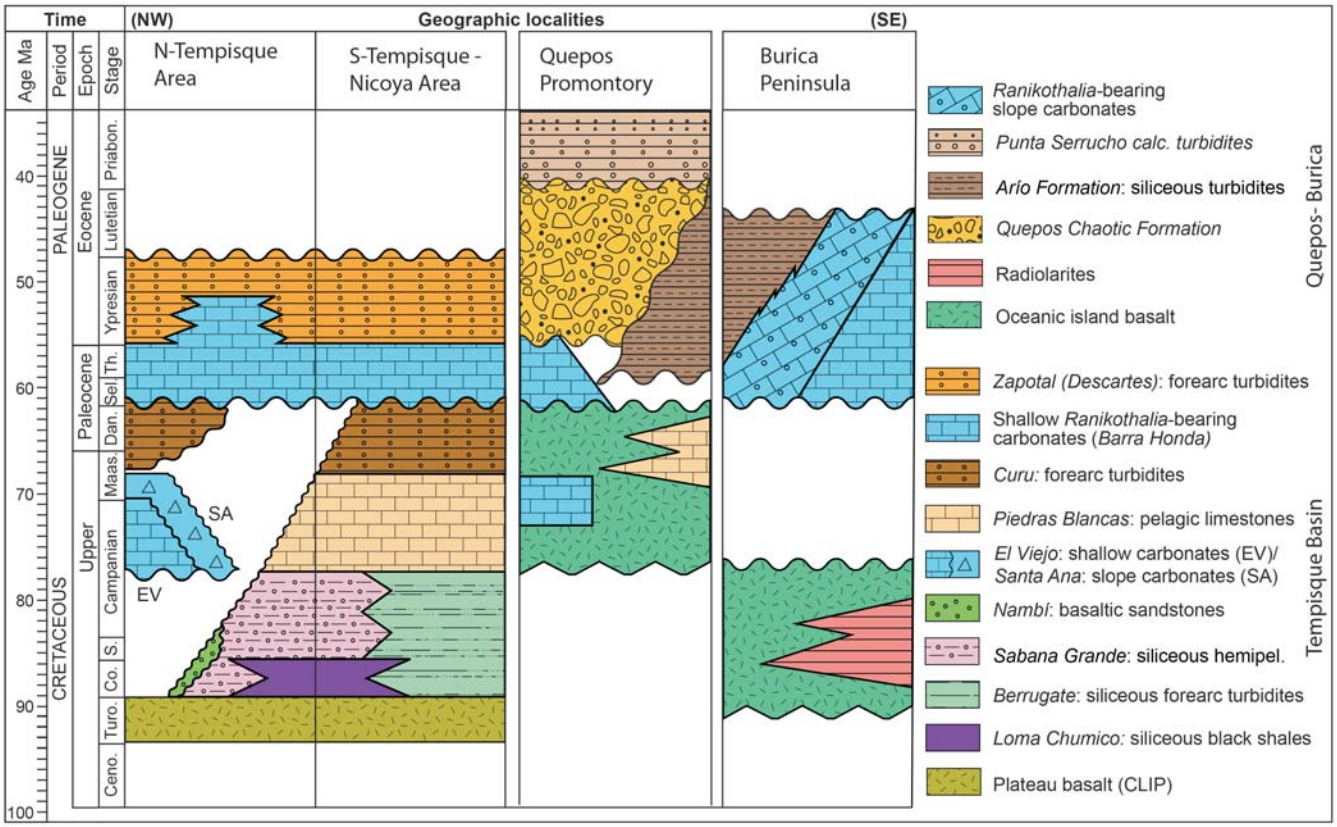

TEXT-FIGURE 2
Simplified chronostratigraphic logs of the Tempisque area, Quepos-Herradura and Burica Peninsula. Formation names are indicated in italics. Based on data by Baumgartner et al. (1984), Bandini et al. (2008), Buchs et al. (2009), Denyer, Aguilar and Montero (2013, 2014) and Andjic, Baumgartner-Mora and Baumgartner (2016).

with an unfocused cold cathode electron beam under an air atmosphere at 0.2 torr. The CL intensity of natural limestones varies greatly and weakly luminescent objects are at the limit of colour CCD-capture. Specialized CCD-cameras provide high sensitivity, nevertheless, exposure times of up to several seconds are needed to capture the very dim blue intrinsic CL of calcite.

Principles of dating by means of $^{87}Sr/^{86}Sr$ stable isotope geochemistry

Strontium (Sr) is a member of alkaline earths group (along with Be, Mg, Ca, Sr, Ba and Ra). The ionic radius of Sr^{2+}, which is about 1.13 Å, is close to the one of Ca^{2+} that is around 0.99 Å. Consequently, strontium can replace calcium in minerals. The replacement of Ca^{2+} by Sr^{2+} is restricted the eightfold coordinate sites, whereas calcium can be incorporated in six and eightfold coordinate sites because of its smaller size (Faure and Mensing 2004). Strontium has four naturally occurring stable isotopes (^{84}Sr: 0.56%; ^{86}Sr: 9%, ^{87}Sr: 7.04% ^{88}Sr: 82.53%) from which only ^{87}Sr is radiogenic and derives from ^{87}Rb (Faure 1986; Veizer 1989).

The decay of ^{87}Rb produces his daughter isotope, ^{87}Sr, by emission of a Beta particle (electron), with a half-life period of 58.8 Ga. ^{87}Rb is incompatible in the mantle; this is why the upper crust is enriched. Because of this very long half live, old cratons have relatively higher ^{87}Sr contents, hence high $^{87}Sr/^{86}Sr$ ratios, compared to the average sea-water strontium ratio (Faure 1986; Veizer 1989; Faure and Mensing 2004). The abundance of the ^{87}Sr isotope can vary because of its radiogenic origin (Capo, Stewart and Chadwick 1998) and the strontium isotopic composition of a mineral or rock containing Rb then depends on its age and Rb/Sr ratio (Faure and Mensing 2004). But in general, globally increased rates of erosion of ancient shields provoke a tendency towards higher $^{87}Sr/^{86}Sr$ ratios in the world ocean waters (Veizer, 1989).

On the other hand, ^{86}Sr is a stable isotope relatively enriched in the mantle. Hence, increased mid- ocean ridge or oceanic plateau activity, hydrothermal alteration of oceanic crust, and an increased rate of erosion of ancient plateaus and volcanic arcs will produce a tendency towards lower $^{87}Sr/^{86}Sr$ ratios in sea water.

Strontium flux from geosphere to hydrosphere. Because of the radiogenic decay, which produces ^{87}Sr, the alteration product of cratons will provide a $^{87}Sr/^{86}Sr$ influx that is above the marine average, between 0.710 (McArthur 1998) and 0.7116 (Banner 2004). High $^{87}Sr/^{86}Sr$ ratios are characteristic for a river influx from cratonic areas, but they depend on the mineral composition and the alterability of bedrock and climatic factors (Palmer and Osmond 1992). Low $^{87}Sr/^{86}Sr$ ratios can be expected in

rivers draining oceanic or arc terranes. The chemical composition of the river influx depends on the chemical and isotopic composition of drainage basins. On the contrary, mid ocean ridge activity and extrusion of large ifneous provinces, will considerably lower the average marine $^{87}Sr/^{86}Sr$ ratios. If there was no alteration/erosion of cratonic material, the inherited strontium isotopic signature would tend towards the ratios of the depleted mantle between 0.703 (McArthur 1998) and 0.7037 (Banner 2004). Also, the diagenesis of marine carbonates is considered as being important to the general $^{87}Sr/^{86}Sr$ variations in seawater. The average value of this source is ~0.708 (McArthur 1994). Another source that can be separately discussed is the dissolution of carbonate and evaporitic rocks, which may be considered as the major source for strontium in the oceans because of their high strontium content and high solubility (Brass 1976; Shields 2007). However, the strontium isotope ratio resulting from this dissolution (~0.708) is close to that of Phanerozoic seawater ($\sim 0.708 \pm 12 * 10^{-6}$) (Peterman et al. 1970) and is not taken into account when interpreting $^{87}Sr/^{86}Sr$ trends (Veizer and MacKenzie 2003; Shields 2007).

In summary, the two main poles for the variation of strontium isotopic ratios in seawater are mantle-derived hydrothermal and alteration sources, vs. continental weathering/erosion of cratonic areas, owing to their extreme contrast in strontium isotope ratios.The strontium isotope ratio of sea water is considered to be the same worldwide for a given time, because the residence time of Sr is about 10^6 years, far longer than the mixing time of the ocean waters, which is in the order of 10^3 years (Raymo, Ruddmann and Froelich 1988, Palmer and Edmond 1989; Holland 1984; Hodell et al. 1989; Berner and Rye 1992; McArthur 1994; Banner 2004). Sr is present in sea water as a trace element with concetrations around 7-8 mg/l (ppm). The modern Sr-concentration in tropical rivers varies between 8-22 µg/l (Viers et al. 2000) and world average Sr-concentration in rivers is 100 µg/l (ppb) (Meybeck 1987, Palmer and Edmund 1989)

The strontium records of seawater show a cyclicity of about 60-70 Ma throughout the Phanerozoic (Prokoph, Shields and Veizer 2008), which is superimposed on the major fluctuations of the Wilson cycle with a cyclicity of about 250 Ma (Vérard et al. 2015). In addition, irregular variations of the strontium isotope ratio can be observed through time (Prokoph, Shields and Veizer 2008; McArthur 1994, 1998; Faure and Mensing 2004). Variations can be explained by major volcanic/tectonic/orogenic events (McArthur 1994; Vérard et al. 2015).

Age determinations are based on comparison of strontium isotope ratios of dated marine fossils/bulk sediment, and can only be measured in marine sediments, preferably carbonates, rich in strontium, (up to 7000 ppm, Faure et al. 1978, Shields 2007). Biominerals are very important to $^{87}Sr/^{86}Sr$ dating because they are thought to have precipitated in equilibrium with seawater and should therefore reflect the original marine seawater $^{87}Sr/^{86}Sr$ ratio. For a given age, there is a "unique" value of the strontium isotope ratio, whereas for a given strontium ratio, multiple ages are possible, because the curve has minima and maxima. This has to be considered when working with $^{87}Sr/^{86}Sr$.

We used the LOWESS reference curve published by McArthur, Howrath and Bailley (2001). This curve takes statistically into account the quantity of the data for a given age, as well as the quality of both the $^{87}Sr/^{86}Sr$ measurements and chronostratigraphic calibrations of each sample. A specific 2 uncertainty is given for each $^{87}Sr/^{86}Sr$ value of a given age. $^{87}Sr/^{86}Sr$ values versus age show a broad peak in the studied Late Cretaceous – Early Tertiary time interval. From a maximum at the K/T-boundary vaules drop thoughout the Paleocene, reach a minimu minimum in the Ypresian and rise again during the Eocene to identical valueas as seen in the Paleovene. Consequently, each measured value corresponds to two or more possible ages. In addition, the Palaeocene segment of the curve is poor in quantity of data as well as in age constraints, thus permitting a far lower precision of the curve than at other ages (like in the Cretaceous or the Neogene). However, the results may improve the precision of the micropaleontological ages obtained (Baumgartner-Mora, Baumgartner and Tschudin 2008).

$^{87}Sr/^{86}Sr$ Laboratory procedures

All analyses were performed on samples with a known paleontological age (at least Mesozoic or Cenozoic). This allowed to know on which side of the relative maximum at the Cretaceous/Tertiary boundary of the LOWESS-curve, the sample is located. Selected samples were extracted from individual bioclasts with a dentists microdrill after excluding any detrital contamination by examination under the optical microscope and in cathodoluminescence.

Reconnaissance studies of pilot samples on slightly etched surfaces by SEM (secondary and backscattered electron beam and energy dispersive analysis) showed no contamination by clay minerals or detrital grains.

Powdered samples were dissolved in 2N HCl, then rapidly centrifuged. The residue of the evaporated solution was then re-dissolved in 3N HNO3, Sr was separated in a Sr-Spec® Han ion separation column. Measures were done in November 2000 in the Mass Spectrometry Laboratory of professor Jan Kramers at the Institute of Mineralogy and Petrology of the University of Bern (Switzerland) with a Nu Instruments® ICPMS multicollector in static mode. Over 50 alternate measures of the standard and the sample were taken into account for defining the standard deviation σ from the mean $^{87}Sr/^{86}Sr$-ratio measured.

GEOLOGICAL SETTING OF *RANIKOTHALIA*-OCCURRENCES IN COSTA RICA AND W-PANAMA

Geological setting, age and facies of the Barra Honda Formation

The Barra Honda Formation, originally defined by Dengo (1962b), is a carbonate platform cropping out mainly in the Tempisque Basin of N-Costa Rica (text-figs. 1, 2). Its original surface may have exceeded 900 km^2, but today it is exposed as remnants in the hills N and S of the Tempisque river and in the northeastern Nicoya Peninsula (Text-fig. 2, 3). Mora (1981) distinguished two subunits, a lower poorly stratified massive white limestone composed of algal boundstones and some peloid wackestones, and an upper stratified unit of peloidal packstones and oolitic grainstones.

Pre-Barra Honda stratigraphy of the Tempisque area

The outcrops of the Nicoya Peninsula and the Tempisque area represent a collage of Mesozoic plateau-type (Sinton, Duncan and Denyer 1997) oceanic terranes that assembled during the late Cretaceous (De Boer 1979) along the western edge of the

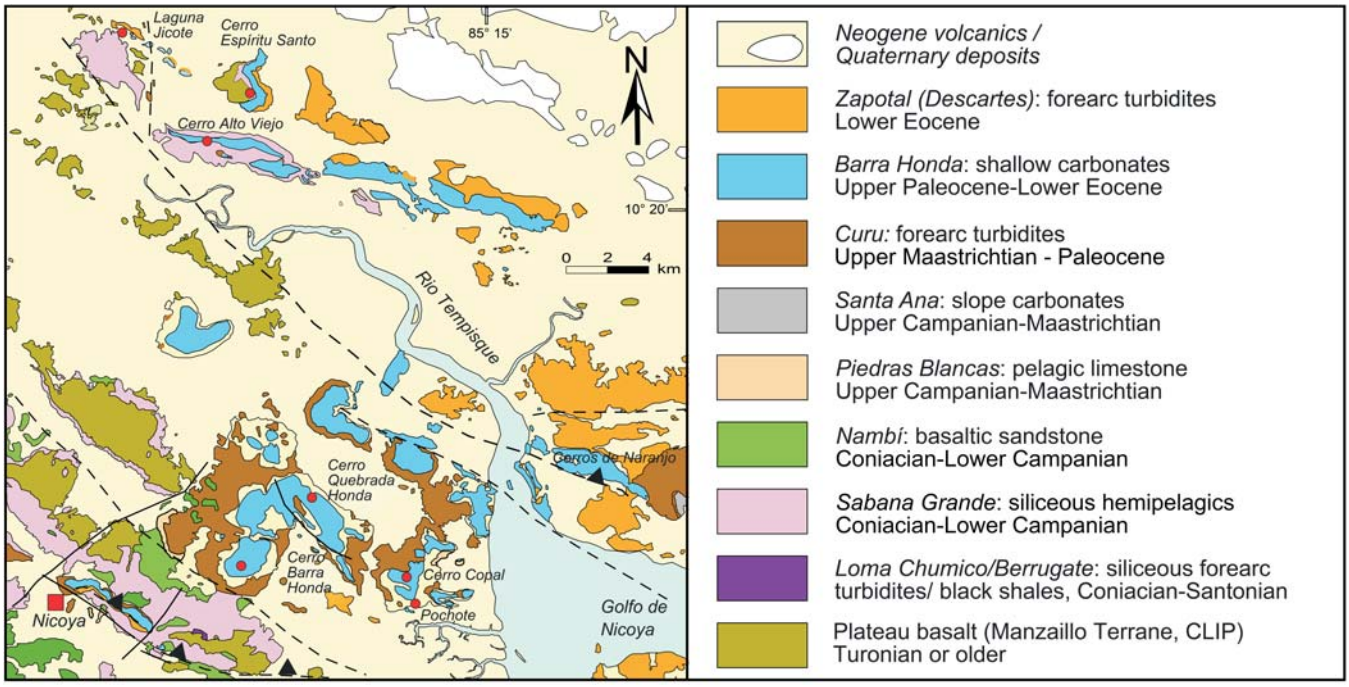

TEXT-FIGURE 3
Geological map of the Lower Tempisque Basin showing the outcrops of the Barra Honda Formation and its stratigraphic substratum. The location of the studied sections is indicated. Map compiled by K. Flores, with modifications after Denyer, Aguilar and Montero (2013). Terrane terminology after Andjic, Baumgartner-Mora and Baumgartner (2016).

Caribbean Plate, at a major boundary between the Caribbean Large Igneous Province s.s. (CLIP s.s.) to the south and the Mesquito CompositeOceanic Terrane (MCOT, Baumgartner et al. 2008) to the north (text-fig. 1.B). The exact nature, age and assembly of these basements in the Nicoya-Tempisque area is still a matter of debate. In previous studies, our subdivision of terranes in the area was three-fold (Bandini et al. 2008): (1) the Nicoya Complex s.s., a deformed igneous mélange of pre-Campanian plateau-like basalts and gabbros that intruded and extruded into Middle Jurassic to Santonian ribbon radiolarites (Denyer and Baumgartner 2006); (2) the Matambú Terrane, a "pre-Albian" oceanic basement covered by Upper Cretaceous hemipelagic/turbiditic sediments and characterized by the occurrence of the "Albian" Loma Chumico Formation; (3) the Manzanillo Terrane, a pre-Turonian oceanic basement intruded by the Turonian Tortugal picritic suite. The Manzanillo Terrane was regarded as the westernmost outcrop of the CLIP s.s. and is overlain by the Coniacian-lower Campanian (Bandini et al. 2008) arc-derived Berrugate Formation (Flores, Denyer and Aguilar 2003) cropping out in the southeastern and eastern Nicoya Peninsula and in the Nicoya Gulf area.

Recent radiolarian biostratigraphic work by Andjic and Baumgartner (2015) and Andjic, Baumgartner and Baumgartner-Mora (submitted) on hemipelagic, tuffaceous siliceous mudstones exposed in the southeastern and central Nicoya Peninsula revealed interbedded green, often organic-rich cherts, shales, tuffacous siliceous mudstones and volcanic sandstones in outcrops mapped as the "Albian" Loma Chumico Formation (Denyer, Aguilar and Montero 2013). However, lithostratigraphy, microfacies and geochemistry indicate that these rocks are distal equivalents of the Berrugate Formation defined in the Nicoya Gulf area in a more proximal facies including volcaniclastic turbidites and debris flows (Flores, Denyer and Aguilar 2003). The tuffaceous lithologies contain well-preserved, Coniacian – Santonian radiolarian assemblages, very similar to those described by Bandini et al. (2008). In the type area of the Loma Chumico Formation, where allegedly, ammonite fragments of late Albian age were found (*Neokentroceras* sp., Azéma, Sornay and Tournon 1979), we retrieved very similar Coniacian – Santonian radiolarian assemblages. As a consequence, the Loma Chumico organic-rich shales are a facies that is coeval with the predominantly arc-derived Berrugate Formation and the latter should be considered as a facies variation. The roughly coeval Sabana Grande and Nambí formations (text-fig. 2, 3.) may also be lateral facies variations probably formed more distally with respect to the arc activity recorded in the Berrugate facies. Andjic and Baumgartner (2015) concluded that the former Matambú and Manzanillo Terranes should represent one paleogeographic fore-arc domain, the Manzanillo Terrane, with a CLIP-like basement overlain since the Coniacian by siliceous organic-rich shales, arc-derived, or siliceous/calcareous hemipelagic formations (organic-lean facies of Ehrlich et al. 1996) depending on the proximity and activity of an early intermediate volcanic arc. The CLIP-like basement became accreted in latest Turonian-earliest Coniacian time, shortly after the Tortugal picritic intrusion wich is dated as 89 Ma (Alvarado, Denyer and Sinton 1997).

While Denyer and Gazel (2009) and Denyer, Aguilar and Montero (2013, 2014) include all basement outcrops of the Nicoya-Tempisque area with the Nicoya Complex, we restrict the term Nicoya Terrane to the NW corner of the Nicoya Penin-

sula (text-fig.1. A, B). This domain is clearly exotic with respect to the Manzanillo Terrane, since it contains Middle Jurassic to Santonian ribbon-bedded radiolarites of open oceanic origin, devoid of any arc influence. Here, the youngest plateau-like intrusions are dated around 80 Ma (early Campanian, Sinton, Duncan and Denyer 1997, Madrigal et al. 2016). We conclude that the Nicoya Complex *sensu stricto* became accreted in the early- middle Campanian, causing the temporary cessation of the arc activity in the area. The extinction of the arc volcanoes gave rise to a late Campanian-Maastrichtian pelagic limestone sequence, the Piedras Blancas Formation, typical for the southern and central Nicoya Peninsula (text-figs. 2, 3). At the same time, tectonic uplift and emersion of the basements to the north is documented by boulder conglomerates and the unconformably overlying middle Campanian shallow-water El Viejo Formation (Pons, Vicens and Schmidt-Effing 2016) (text-figs. 2, 3). Shallow-water conditions of the middle-late Campanian were ephemeral and were soon replaced by hemipelagic/turbiditic facies of the Maastrichtian-early Paleocene that often contain reworked shallow-water material of the El Viejo Formation (Cerro Cebollín, Jaccard et al. 2001, Santa Ana Formation, Denyer, Aguilar and Montero 2014). By the late Maastrichtian, the arc activity resumed and produced the forearc turbidite Curu Formation (Denyer, Aguilar and Montero 2014) that ranges into the Lower Paleocene.

Barra Honda stratigraphic framework

On a regional scale, the Barra Honda Formation rests with an erosive unconformity on the older Upper Cretaceous to Paleocene formations, namely from N to S: the Sabana Grande (siliceous hemipelagics, at Cerro Espíritu Santo, text-figs. 2, 3, 4), the Piedras Blancas (pelagic limestones) and the Curu (fore-arc turbidites) formations (at Pochote, text-fig. 4.) . Due to important differences in competence between the early lithified limestones and the underlying, clay-rich, often poorly lithified formations, the basal contact of the Barra Honda limestones is generally affected by gravitational and tectonic deformation including slumping and injection of detrital lithologies into the karstified limestone bodies. In the quarries of the Cerros de Naranjo (easternmost outcrops of Barra Honda, text-fig. 3) and in the Cerro Calera (facing the town of Nicoya) the limestones rest with a S-SW vergent thrust contact on the underlying detrital lithologies (Denyer, Aguilar and Montero 2014). Based on planktonic foraminifera, such as *Globorotalia formosa formosa* Bolli 1957*, Globorotalia aragonensis* Nuttall 1930 and *Globorotalia formosa gracilis* Cushman 1925, Rivier (1983) dated these detrital turbidites as Eocene and hence, inferred an Eocene or younger age of the Barra Honda Formation. The detrital turbidites are now mapped as the Lower Eocene Zapotal Member by Denyer, Aguilar and Montero (2013), which corresponds to the stratigraphic cover of the Barra Honda Formation, text-fig. 2). Instead, Sprechmann (1984) and Sprechmann et al. (1987) assumed an Upper Cretaceous age for Barra Honda and implied a tectonic or gravitational emplacement of the whole platform over the underlying rocks. However, there are places, where the basal, stratigraphic contact of the formation is well preserved.

Cerro Espiritu Santo (text-figs. 3, 4). In the northernmost occurrences of Barra Honda an outcrop near the top of the hill (coord.: 388.1/263.1, Jaccard et al. 2001) exposes a transgressive contact of Barra Honda limestones on altered hemipelagic mudstones of the Sabana Grande Formation. Further to the W altered outcrops of the basaltic basement (Manzanillo Terrane) occur beneath 60-80 m of Sabana Grande. The top of the hemipelagic/turbiditic sediments is deeply altered and overlain by a brownish layer, interpreted as paleosoil (Di Marco, Baumgartner and Channell 1995, Jaccard et al. 2001, here: text-fig. 4, section A). This horizon is overlain by a meter-thick layer of well-rounded and bored pebbles and cobbles of shallow-water limestone (text-fig. 4, image top left) set in a sandy matrix, in turn overlain by lenses of cross-laminated oolitic packstones and grainstones containing orthophragminas, such as *Neodiscocyclina grimsdalei*, thick-shelled *Ranikothalia catenula, antillea* and *R. c. tobleri* and the squamariacean algae, *Polystrata* (= *Ethelia*) *alba* Pfender 1936*,* which encrusts large melobesian rhodoids forming bafflestones*.* The described contact and the overlying facies is clearly transgressive/progradational over a deeply eroded surface that was probably subaerially exposed prior to the onset of a high-energy beach paleo-environment. These relatively well-washed facies are overlain by calm-water micritic wackestones rich in *Distichoplax biserialis* (Dietrich), which is a common micro-*problematicum* (coralinacean alga?) in middle to late Paleocene carbonate environments, and thin-shelled *Ranikothalia,* such as *R. catenula catenula* and *R. c. soldadensis*. Calvo and Bolz (1991) recognized the late Paleocene – early Eocene age of the Espiritu Santo limestones but did not relate them with the Barra Honda Formation.

Pochote (text-fig. 3, 4. section B, coord.: 395.6/236.6). South of the Cerros Copal. Jaccard et al. (2001) studied a sequence which shows the reworking of pelagic Upper Cretaceous limestones in an Upper Paleocene fore-slope matrix at its base, and which grades upsection into typical Barra Honda facies. Over a sharp, but apparently conformable change from turbiditic sandstones of the Curu Formation the carbonate section begins with a polymict breccia, containing pelagic limestone clasts and Barra Honda-type packstone clasts with red algae. The matrix is abundant in the lower part of the section and consists of an offshore crinoidal packstone, containing planktonic foraminifera and red algae. It disappears near the middle of the section. The matrix namely contains *Morozovella velascoensis* Cushman 1925, and *Pseudohastigerina* sp.; *Polystrata alba* is present in both the matrix and the platform clasts. The pelagic lithoclasts are the largest and mostabundant at the base. Higher in the sequence, they become smaller and finally disappear, while platform-type clasts increase in size and abundance upsection. The angular pelagic lithoclasts contain planktonic foraminifera, such as *Globotruncana ventricosa* White 1928, ranging from the late Campanian to the early Maastrichtian (Jaccard et al. 2001, pl. 2-2) and some of them are bored by bivalves. These clasts were certainly derived from the Piedras Blancas Formation which was uplifted and lithified before being eroded, bored and redeposited. Towards the top of the section, only intraformational platform clasts remain in a massive, poorly bedded limestone without an open-marine influence.

Jaccard et al. (2001) interpreted this section as a fore-slope environment, which collected both lithoclasts eroded from the Upper Cretaceous substrate of the Barra Honda Fm. and slightly indurated platform sediments in an open marine environment (see model text-fig 4.). The shallowing upwards trend is marked by the dominance of intraformational platform breccias towards the top of the section. The Pochote section records the Late Paleocene southward progradation of the Barra Honda platform over a deeper marine, detritally dominated paleo-environment of the Curu Formation. Although the Pochote section is not in

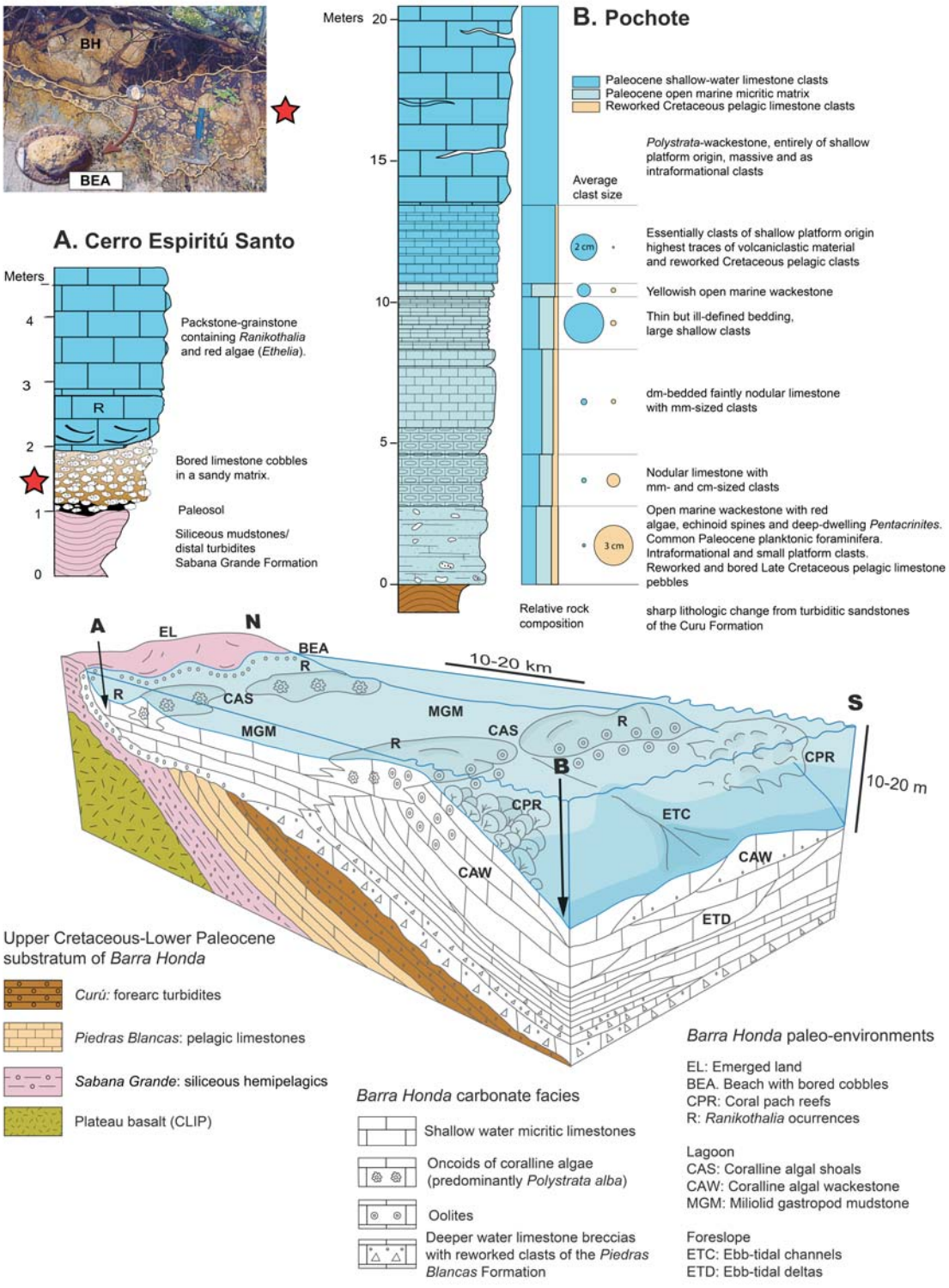

TEXT-FIGURE 4
Stratigraphic key sections and depositional model of the Upper Paleocene Barra Honda Formation. Top left: image of transgressive contact of the Barra Honda limestones (BH) over a beach conglomerate with bored cobbles (BEA), Cerro Espiritu Santo, after Jaccard and Münster (2001). Section A: Cerro Espiritu Santo, Section B: Pochote, both after Jaccard et al. (2001). 3-D depositional model after data presented in Jaccard et al. (2001) and own interpretations. Towards the S (section B) Barra Honda limestone breccias encroach in an off-shore environment of the Curu forearc turbidites reworking Upper Cretaceous lithoclasts from the underlying erosional surface cutting into the older (Sabana Grande, Piedras Blancas and Curu) formations. Upsection, massive intraclast breccias give way to platform sediments organized in ebb-tidal fans (ETF). Towards the N (section B) Barra Honda lagoonal micritic facies (MGM) progressively onlap on higher-energy beach and foreshore sediments (BEA) during relative sealevel rise on the eroded structural high. The higher (younger?) stratigraphic levels of Barra Honda show patchy shoals of coralgal oncoid grain- and packstones (CAS) with Ranikothalia sp. (R). and sometimes oolites. Rare coral patch reefs (CPR) occur toward the more open marine environments to the south.

outcrop continuity with a major limestone body, its geographic position, sedimentology and age reveal important data for the understanding of the Barra Honda platform history.

In summary, a general allochthony of the Barra Honda Formation cannot be confirmed. The basal onset of the formation is clearly transgressive over deeply altered, probably subaerially exposed Upper Cretaceous-lower Paleocene formations in the northern outcrops of Barra Honda. Towards the southern edge of the Barra Honda outcrops, the onset of the micrite sediments from platform environment is progradational over open marine upper Paleocene calcarenites. Reworked and bored Upper Cretaceous lithoclasts are very common in the basal outcrops of Barra Honda. They record lithification and tectonic exposure of the underlying formations, prior to the sedimentary onset of Barra Honda.

The top of Barra Honda. Between the Laguna de Jicote (text-fig. 3) and the upper Tempisque River isolated outcrops in small hills yielded massive wackestones rich in echinoderms, red algae and some age-diagnostic LBF, such as *Neodiscocyclina bullbrooki* (Vaughan, Cole and Grimsdale 1941) and *Eoconuloides* cf. *wellsi* Cole and Bermudez 1944 (see Jaccard et al. 2001, Pl. 3-5, 6) indicating an Early-Middle Eocene depositional age. This age is confirmed by a single $^{87}Sr/^{86}Sr$ stable isotope ratio measured in an echinoderm fragment (sample 4,1 B, Tab. 1) which gave a numerical age of 50 Ma +3.8 - 5.3 (late Ypresian – early Lutetian). Although this age is poorly constrained, it is statistically younger than all the other ages obtained for Barra Honda (see below). Apparently, these limestones overlie the basaltic basement or a veneer of Sabana Grande siliceous mudstone (text-fig. 3). They are in turn overlain to the north by the Zapotal forearc turbidites. Hence, they have a stratigraphic position like the main bodies of Barra Honda. these sediments could represent the youngest parts of the platform that encroached on the tectonic paleohigh and survived until the early/middle Eocene before they were drowned by renewed subsidence.

To our knowledge, there is, at present, only one place, where the contact between Barra Honda and the stratigraphically overlying Zapotal Member of the Descartes Formation can be directly observed. It is in the "Teresita" quarry located about 4 km east of the Nicoya town center (10° 08' 85''N, 85° 85' 26''W, text-fig. 3, plate 1, figs 1, 2). On the eastern side of the Quarry, thin-bedded volcaniclastic turbidites conformably overlie the topmost limestone of the Barra Honda Formation (mentioned in Denyer, Aguilar and Montero 2014). The top 20-30 m of Barra Honda are characterized by dm-bedded yellowish white and alternating grey (tuffaceous?) limestone. The topmost beds contain replacement chert nodules arranged in irregular layers (plate 1. text-fig. 2). Above a sharp contact, a 30-50 cm thick greenish interval rich in tuffites and/or glauconite (analyses are in progress) and thin cherty limestone marks the boundary with the overlying, distinctly orange-red base of the Zapotal Member (Denyer, Aguilar and Montero 2014). The first meters are composed of red siliceous mudstone and 5-10 cm thick chert beds. Upsection, distal volcaniclastic, siliceous distal turbidites are interbedded with brownish-red claystones. This contact is best observed along the road leading to the quarry. This section is interèpreted as the drowning of the Barra Honda platform brought about probably by eutrophication resulting in a change from carbonate to biosiliceous sedimentation and the onset of arc-derived tuffites and turbidites some time later. The lowest levels of the Zapotal Formation are reminiscent of the upper Thanetian-lower Ypresian siliceous Buenavista Formation (Baumgartner et al. 1984, Andjic, Baumgartner-Mora and Baumgartner 2016) that intervenes between the Curu and Descartes formations along the northern shores of the Santa Elena Peninsula. Paleoclimatic changes around the Paleocene/Eocene boundary are recognised worldwide by major carbon and oxygen stable-isotope shifts (e.g. Vandenberghe et al. 2012). These changes may have caused intensified weathering, runoff and eutrophication of the forearc area causing the demise of carbonate production and the enhancement of biosiliceous productivity (an event recognized elsewhere in the Eastern Pacific realm). At the same time, arc volcanic activity resumed after arelative quiescence during the Late Paleocene.

Biostratigraphic age of the Barra Honda Formation

Originally, Rivier (1983) suggested a middle Eocene or younger flooding of a slightly deformed area to explain the unconformable, but depositional contact of the Barra Honda Formation. Sprechmann et al. (1987) correlated the Barra Honda limestones with the rudist-bearing limestones of Santa Elena (El Viejo Formation; Schmidt-Effing 1975) on the basis of early Maastrichtian globotruncanids recovered from sheared rudstones below the base of Barra Honda. They also mentioned Campanian LBF recovered from unspecified limestones. Sprechmann et al. (1987) did not provide exact sample locations that would show how the reported Upper Cretaceous fossils related to the micritic Barra Honda limestones, generally devoid of age-diagnostic fossils. Upper Cretaceous reworked shallow- and deep-water material is, however, quite common in the lower Paleocene sequences that underlie the Barra Honda limestones (Seyfried and Sprechmann 1985; Winsemann 1992). The presence of reworked Campanian LBF and rudists in Paleocene-Eocene mass flows demonstrates the erosion of Campanian carbonates produced in an open marine, high energy environment that is distinct from the mud-dominated Barra Honda environment. Sprechmann et al. (1987) assumed that the rudist-foraminiferal facies is marginal to the restricted Barra Honda facies, but provided no evidence of lateral continuity between the two formations. In the Bajo Tempisque area rudistis and Campanian LBF are found reworked into coarse basaltic conglomerates that directly overlie the Manzanillo basaltic basement (Barbudal Formation, Rivier 1983; Seyfried and Sprechmann 1985). These deposits formed during the late Campanian, but do not contain clasts of Barra Honda-type carbonates. The first appearance of Barra Honda-type clasts in coarse mass-flow and channel-fill deposits associated with deep-water formations is systematically middle-late Paleocene in age (Cerco de Piedra Formation; Sprechmann 1982, Sprechmann et al. 1987, Winsemann 1992). The Barra Honda-type micrites are therefore unlikely to be much older than middle-late Paleocene.

The occurrence of *Ranikothalia* gr. *catenula* and orthophragminas, as well as planktonic foraminifera such as *Morozovella velascoensis* in several localities of the Barra Honda Formationclearly indicates an Upper Paleocene to perhaps lowest Eocene age at least for the upper, datable part of the formation. These results will be discussed below under "biostratigraphy" for all Costa Rican occurrences in Paleogene shallow carbonate deposits.

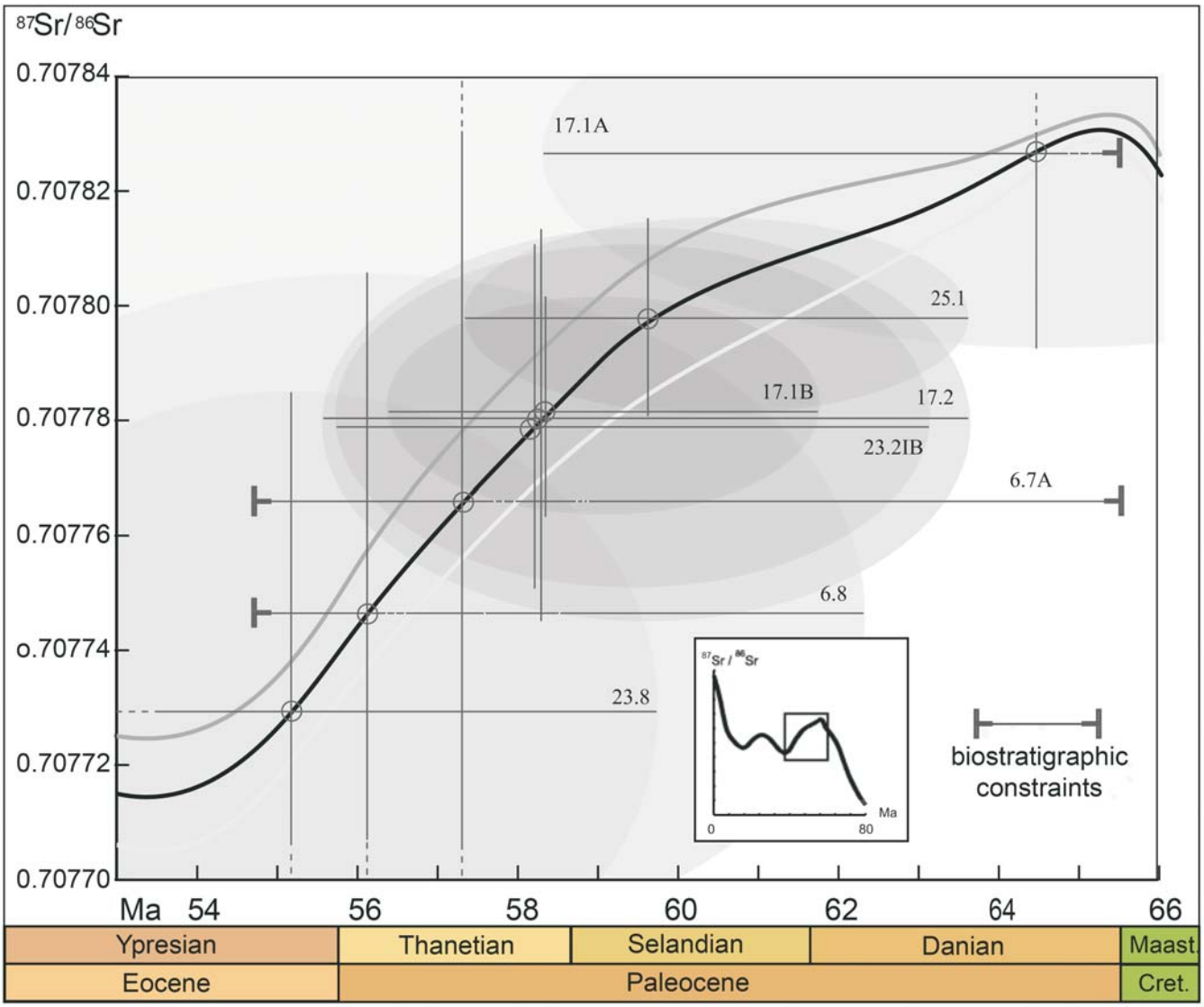

TEXT-FIGURE 5
Plot of the $^{87}Sr/^{86}Sr$ ratios obtained by Jaccard and Münster (2001, modified) from samples of the Paleocene Barra Honda Formation against the LOWESS curve (McArthur, Howrath and Bailley 2001). Biostratigraphic constraints are the range of *Morozovella velascoensis* and *Ranikothalia* sp. (see text).

Age of the Barra Honda Formation by $^{87}Sr/^{86}Sr$ ratios

Jaccard and Münster (2001) measured $^{87}Sr/^{86}Sr$ stable isotope ratios in a variety of bioclasts sampled in the Barra Honda, Santa Ana and El Viejo formations. The aim of these measures was to better constrain the age of micropaleontologically dated samples and to better estimate the duration of the platform development. For the theory of Sr-isotope stratigraphy and laboratory procedures the reader is referred to "methods" above.

Here we publish for the first time the results concerning the Barra Honda Formation given in text-figure 5. At first sight, the values seem to be scattered through the whole Paleocene, but a more careful examination taking into account the 2σ cumulated uncertainties of the measures and of the curve shows two tendencies: Four data points (23.8, 6.8, 6.7A, 17.1A) (Tab.2) have relatively large uncertainties and do not group together. The other three (23.2IB, 17.2, 17.1B) have significant lower uncertainties, and cluster between 56 and 59 Ma. We think that the first group of samples considerably lacks precision and accuracy; they could therefore also well be of an age between 56 and 59 Ma, by taking their large uncertainty into account. The values with the lowest uncertainties come from three different localities and from four very different facies. The interval 56 to 59 Ma corresponds to a latest Selandian- Thanetian age according to the time scale adjustments by Ogg (2004) used to calculate the numerical ages of the LOWESS-curve (McArthur, Howrath and Bailley 2001), which is in agreement with the Late Paleocene micropaleontological ages (see biostratigraphy below). A secure interpretation is that the Barra Honda platform, as far as dated by these samples, would be restricted to the Upper Paleocene. In the ICS International Chronostratigraphic Chart v2015.1, the Selandian/Thanetian boundary was slightly

shifted towards 59.2 Ma, which does not change much for this interpretation. In conclusion, although these data are now 15 years old and could be measured today with more precision, they give a significant confirmation of ages established by biostratigraphic ranges of microfossils.

Discussion: Barra Honda facies distribution and model

The sections (text-fig. 4. A, B) described above show two different phases of the Barra Honda platform evolution. Towards the south (section B, Pochote) the Barra Honda Platform progrades over open marine facies with redeposited intraformational breccias that reveal an abundant, restricted shallow-water carbonate production on a nearby shoal. The microfacies of both the matrix and the clasts are rich in micrite (pack- to wackestone) and in *Polystrata* (=*Ethelia*) *alba* (Pfender 1936) Denizot 1968, very common in most lithologies of Barra Honda. This squamariacean (red) alga grew encrusting on rhodoids, or on any other firm substrate. It is typical for uppermost Cretaceous and Paleocene algal platforms, although its range extends from the Barremian to the Eocene (Massieux and Denizot 1964, Praturlon 1966). In the lower part of the Pochote section crinoids and planktonic foraminifera are frequent in the matrix, and underline the open marine slope environment of deposition. This matrix disappears completely upsection and the typical algal wackestone facies becomes dominant. No LBF were found in the Pochote section. Dating resides on the presence of *Morozovella* sp. in the matrix, $^{87}Sr/^{86}Sr$-ratios measured in the matrix (sample 23.21B and 23.8, table 1) and in *Polystrata alba* from the nearby Cerro Copal (sample 25.1, table 1). The analytical error of these measurements is too large to support an age difference with respect to *Ranikothalia*-bearing facies, but it is possible that the lower part of the Pochote section is older (Selandian?) than the basal limestones that onlap on underlying eroded formations at Cerro Espiritu Santo. On the other hand, the abundant occurrence of thick-shelled *Ranikothalia* is always associated with higher energy pack- to grainstone facies (see below). Much of the lower subunit of the Barra Honda Formation (Mora 1981) may correspond to rapid accumulation of coralgal micrites transported out of a restricted, very shallow platform by ebb-tidal currents into the near off-shore area (text-fig. 4, model), where accommodation space was available. The presence of Upper Cretaceous lithoclasts in the lower half of the Pochote section (text-fig. 4 B) indicates that the carbonate shoal was mounted on a tectonically uplifted and eroded high that was still exposed to erosion during the early stages of carbonate production.

Towards the north (Cerro Espiritu Santo, text-fig. 4, section A), sandy beach facies with bored cobbles of Barra Honda mud- and wackestones show the relative younger age of the transgressive progradation of the platform onto the eroded structural high during a relative sealevel rise, which could have been eustatic (Haq and Al-Qahtani 2005) and/or related to initial tectonic subsidence. Above the beach facies, lensy (dense) facies of cross-laminated pack- and grainstones contain algal oncoids composed of corallinaceans, such as *Sporolithon* and *Polystrata alba*, geniculate coralline algae, ooids and abundant small fragments of the microproblematicum *Distichoplax biserialis* (Dietrich). Locally, *Neodiscocyclina* sp. and thick-shelled *Ranikothalia* sp., considered here as *Ranikothalia catenula antillea,* and *R. c. tobleri* are abundant. This is a higher energy facies, which is more typical for the upper part of the Barra Honda Formation (Mora 1981). A lower energy facies with abundant micritic matrix contains fine grained bioclastic hash made of geniculate corallines and *Distichoplax biserialis.* Thin-shelled *Ranikotalia c. catenula and R. c. soldadensis,* probable calm water forms, are associated with these microfacies. Facies patterns are, however, small-scaled, patchy and show no clear paleogeographic onshore-offshore trend (Jaccard et al. 2001). In the northern hills, a variety of microfacies are juxtaposed, including outcrops with a clear open marine influence containing *Morozovella velascoensis* (Jaccard et al. 2001, plate 2-2). Small coralgal shoals with oncoid-oolite-LBF facies associations may have alternated with calm water lagoonal, miliolid-gastropod facies (model, Text-fig. 4) containing the pseudoquinqueloculid *Sigmoilopsis* sp. North of Puerto Níspero (coord. 401.1/244.3), Aguilar and Denyer (2001) described an isolated coral pach reef with m-sized coral colonies in living position of the new species *Euphyllia donatoi* Aguilar and Denyer 2001, unique in the whole Tempisque Basin. Such patch reefs were certainly located close to the open sea (text-fig. 4, model), that may have occurred towards the southeast, where the platform edge prograded over open marine environments (e.g. text-fig. 5, section B, Pochote).

The Barra Honda Formation is regionally overlain by the deep-water forearc turbidites of the Descartes Formation (Zapotal Member). The transition from shallow to deep water conditions has only been observed in a single outcrop in the "Teresita" quarry near Nicoya described above. It suggests rapid drowning of most of the Barra Honda platform due to a combination of factors, such as: (1) a relative sealevel rise due to tectonic subsidence and probably an eustatic component, (2) but more importantly, a paleoclimatic change around the Paleocene/Eocene boundary resulting in intensified weathering, runoff and eutrophication of the forearc area by dissolved organic matter and detrital input. A biosiliceous sedimentation episode is well known around this boundary (Buenavista Formation, Baumgartner et al. 1984). Renewed arc volcanic activity (Alvarado et al. 2007) and intense weathering during the Early Eocene Climatic Optimum (EECO) is evidenced by the red siliceous mudstones and distal turbidites of the Zapotal Member. An exception may be the early-middle Eocene limestones around Laguna Jicote discussed above. They represent echinoderm-rich heterozoan carbonate shoals that may have survived into the EECO on the highest part of the structural high of the N-Tempisque area.

Geological setting of the Herradura and Quepos areas

Herradura

The Herradura promontory (text-fig. 1.) hosts basaltic basements of at least two different origins. The southwest corner of Herradura has a CLIP geochemical signature (Hauff et al. 2000a), 40Ar/39Ar ages from basalts yielded 83.2 ± 1.8 Ma (Campanian, Sinton, Duncan and Denyer 1997) and 86.0 ± 2.0 Ma (Santonian, Hauff et al. 2000a). These basalts are topped by Campanian radiolarites and early Maastrichian pelagic limestones (Arias 2003). This corner of Herradura has often been considered part of the Nicoya Complex, based on its basalt geochemistry (e.g. Denyer, Baumgartner and Gazel 2006). However, it is definitely younger and could represent the true western edge of the CLIP (Buchs et al. 2009). It is overlain by the "Tulin Formation" (Malavassi 1967) a vast complex including Maastrichtian to Lower Eocene basalts, intrusive olivine cumulates and gabbros, epiclastic volcanics and pyroclastic breccias. It was dated by planktonic foraminifera and LBF

TABLE 2
$^{87}Sr/^{86}Sr$ ratios, errors and numerical ages obtained by Jaccard and Münster (2001) from samples of the Paleocene and Lower Eocene Barra Honda Formation. Numbers in brackets indicate micropaleontological constraints, Minimum and Maximum age* are after the LOWESS lookup table (McArthur, Howrath and Bailley 2001), not including the analytical error (2?).

Sample	$^{87}Sr/^{86}Sr$ corr	2σ	Minimum Age (+ 2σ)	Maximum Age (+ 2σ)	Minimum age*	Mean Age	Maximum age*	Locality / Age	Coordinates	Lithology/ sampled bioclast
4,1B	0,707746	3.96E-05	44.7	53.8	48.97	49.98	50.82	Laguna Jicote / early - mid. Eocene	381.8/266.2	LBF wackestone/ echinoderm fragm.
23.8	0,707729	5,66E-05	[34,3]	59,76	54,46	55,16	55,69	Pochote / Late Palaeocene	395.6/236.6	red algal wackest. matrix
6.8	0,707747	5,84E-05	[54]	62,36	55,61	56,10	56,68	Espiritú Santo / Late Palaeocene	388.1/263.1	red algal wackest. *Polystrata alba*
6.7A	0,707768	8,92E-05	[54]	[65]	56,65	57,32	58,14	Espiritú Santo / Late Palaeocene	388.1/263.1	red algal wackest. *Polystrata alba*
23.2IB	0,707781	3,10E-05	55,76	63,05	57,43	58,25	59,16	Pochote / Late Palaeocene	395.6/236.6	detrital packstone bioclastic matrix
17.2	0,707782	3,46E-05	55,66	63,66	57,57	58,40	59,34	Cerro Quebrada Honda/ Late Palaeocene	389.7/243.6	rhodolith rudstone
17.1B	0,707783	1,93E-05	56.44	61.83	57,57	58,40	59,34	Cerro Quebrada Honda/ Late Palaeocene	389.7/243.6	red algal wackest. bioclastic matrix
25.1	0,707798	1,84E-05	57.35	63.66	58,75	59,82	61,39	Cerro Copal / Late Palaeocene	396.3/239.6	red algal wackest. *Polystrata alba*
17.1A	0,707829	3,66E-05	58.3	[65]	64,14	64,64	64,91	Cerro Quebrada Honda/ Late Palaeocene	389.7/243.6	red algal wackest. *Polystrata alba*

found in sparse interbedded sediment lenses (Arias 2003). Since Malavassi (1967) several authors considered the Herradura basalts as an oceanic island, which is confirmed by the OIB geochemical characteristics of its basalts (Arias 2003, Denyer, Baumgartner and Gazel 2006). Rare Upper Cretaceous LBF and rudist fragments suggest that the oceanic island had a shallow-water area at least since the Maastrichtian. It may have lasted until the collision of the terrane with the western edge of the CLIP during early to middle Eocene, when it came into the reach of forearc turbidites.

In the Herradura area there is, until now, only one locality known, where Upper Paleocene shallow-water limestones crop out (Bolz and Calvo 2003). They are located in the middle reaches of the Rio Cañas, about 12 km north of the town Quepos (N 9°32'52", W 84°07'50"). According to Bolz and Calvo (2003), using data from Becker (1991) shallow-water limestones overlie basalt without a clearly visible contact. We studied samples collected by O. Arias from this locality (OA63-66) that were taken from "limestone breccias" and that have clear resedimented fabrics. Individual samples show different grain sizes, which is probably the result of hydrodynamic sorting in turbidites. Many bioclasts are abraded to well rounded. Neither the map of Arias (2003) nor that of Denyer and Alvarado (2007) show basalts in that area. As a consequence, the geologic setting of this outcrop has to be restudied.

Quepos promontory

Basement. The Quepos promontory (text-fig. 6) shows excellent outcrops of an Upper Cretaceous – Lower Paleocene basaltic basement, attributed to an oceanic island, that originated between 65.0± 0.4 Ma and 59.4 ± 1.8 Ma according to Ar^{39}/Ar^{40} radioisotopes (Sinton, Duncan and Denyer 1997; Hauff et al. 2000a, b; Hoernle et al. 2002). This age range has been recently extended to 70.6 ± 1.2 Ma by Trela et al. (2015). These authors are the first to use the term *Quepos Terrane*, which they attibuted to Galapagos plume tail activity.

Pink pelagic limestones interbedded between lava flows have been dated as Maastrichtian (Bolz and Calvo 2003) to Danian (Azéma et al. 1979). An OIB, intra-plate Galápagos origin is now generally accepted for the formation of the Quepos basement, based on petrological evidence and trace element data (Hauff et al. 1997, 2000a, b). Volcanic agglomerates observable at Punta Quepos (Fig 6) provide evidence of the emergence of the predominantly submarine volcanic edifice above sealevel (Baumgartner et al. 1984, Hauff et al. 2000a). The usually pillow forming lava flows of Quepos are dominated by a transitional tholeitic to alkaline rocks with incompatible trace element patterns indicative of an OIB source with a clear Galápagos isotopic signature (Hauff et al. 2000a, b; Geldmacher et al. 2003, Trela et al 2015). Arias (2003) pointed out the similarities between the Quepos basement and the basement rocks included in the "Tulin Formation".

*Sedimentary rock*s. Sediments cropping out in the Quepos promontory can be conceptually grouped into 3 distinct series: (1) the allochthonous Maastrichtian to lower Eocene seamount sedimentary cover; (2) the autochthonous Paleocene–middle Eocene forearc sequence (Cabo Blanco Formation formally defined in Baumgartner et al. 1984, now called Ario Formation (Astorga 1987, unpublished), which is the "substratum" into which the top of the Quepos seamount was accreted; and (3) the upper Eocene overlap sequence that seals the accretion event (Punta Serrucho Formation, Baumgartner et al. 1984). In the outcrops, the original seamount cover is completely dismembered and occurs as m- to several 100 m-sized blocks in the Punta Quepos Chaotic Formation (Baumgartner et al. 1984), which crops out in the coastal area of the Quepos Promontory (6igure 6). This formation contains (1) blocks of the seamount basement (e.g. the famous picrites and various basalts), (2) blocks of the seamount sedimentary cover, and (3) blocks of the tectonically and/or gravitationally reworked forearc turbidite-mudstone sequence. The matrix of the Chaotic formation is composed of siliceous-calcareous hemipelagic mudstones and minor silt to fine sandstones which seem to be largely reworked during the collision from the still unconsolidated forearc sequence (Cabo Blanco Formation).

Seamount sedimentary cover. The seamount sedimentary cover can be reconstructed from the blocks in the Punta Quepos Chaotic Formation. These include:

Isolated clasts of Campanian-Maastrichtian shallow-water limestone, dated by *Pseudorbitoides* sp. and *Sulcoperculina* sp. (Henningsen 1966, Azéma et al. 1979).

Pink pelagic limestones of Maastrichtian to lower Paleocene age cited above. They were dated by Azéma et al. (1979) as middle to late Danian (P1b-P1c). Bolz and Calvo (2003) described pyroclastic sediments including tephra layers from a small cove West of Puerto Escondido (M-P in text-fig. 6.) associated with Danian pelagic sediments.

Masses and individual blocks of upper Paleocene shallow-water breccias containing *Ranikothalia catenula* group, *Neodiscocyclina* spp. and undetermined rotaliid foraminifera (Azéma et al. 1979, Schmidt-Effing 1979). The *Ranikothalia catenula* group is discussed in detail in this paper.

Up to several 100 m sized blocks of pelagic, often siliceous, thin bedded limestone that was dated by Azéma et al. (1979) in a locality behind the wharf of Puerto Quepos as upper Danian to early Selandian (sample CR377: *Morozovella angulata* (White 1928): P2/3b) to lower Selandian -Thanetian (sample CR379: *Morozovella velascoensis* group, and probably *M. velascoensis acuta* Toulmin 1941: P4/P5). Schmidt-Effing (1979) described late Early Eocene radiolarians from the same limestones near Quepos: *Theocotyle (Theocotyle) alpha* Foreman 1973*, Theocosphaerella* cf. *agdaraensis* (Mamedov 1969), *Lithochytris archaea* Riedel and Sanfilippo 1970 and *Theocotyle cryptocephala* (Ehrenberg 1873).

Blocks of shallow-water-derived limestones dated by Azéma et al. (1979) in outcrops just NE of Punta Cathedral, between Playa Espadilla Sur and Playa Manuel Antonio. Here, *Eulinderina guayabalensis* (Nuttall 1930) among a rich LBF assemblage constrains the age of the sample to the early Middle Eocene.

The autochthonous forearc sequence. The Cabo Blanco Formation, (Baumgartner et al. 1984, Mora and Baumgartner 1984) exists as a relatively undeformed sequence 1-2 km inland, toward the east of the Chaotic Formation (text-fig. 6.) in fresh exposures of strata with 5-20 cm thick, greenish, hemipelagic, siliceous and/or calcareous mudstones layers rich in radiolaria and planktonic foraminifera alternate with fine grained turbidites containing arc derived lithoclasts and feldspars. Extracted radiolaria indicate a Late Paleocene-Early Eocene age (Lundberg 1982). Reworked fragments of LBF may indicate that the formation reaches the Middle Eocene (Baumgartner et al. 1984). The same lithologies can be observed in the Chaotic Formation either as coherent blocks of distal turbidites with hemipelagic calcareous/siliceous mudstone and interbedded 5-20 cm thick graded volcanic sandstones of an intermediate arc origin, or as an abundant matrix of siliceous/calcareous mudstone including disseminated lenses of sandstone, basalt/picrite and chert pebbles reworked from the seamount material.

The overlap sequence. The Punta Serrucho Formation (Baumgartner et al. 1984) rests unconformably with a very irregular contact on the Chaotic Formation. It starts with shallow, very proximal fan-delta type sediments exposed at Punta Catedral (text-fig. 6.), formed by over 100 m of coarse channelized conglomerates and cross-bedded fine conglomerates and sandstones. This sequence is overlain by an over 450 m thick, spectacularly outcropping section of first proximal and then more distal turbidites, rich in redeposited shallow-water material (LBF). The following taxa are present at Playa Playita (text-fig. 6.): *Asterocyclina asterisca* (Guppy 1866), *Fabiania cubensis* (Cushman & Bermudez 1936), *Gypsina* sp., *Lepidocyclina (Neolepidina) chaperi* Lemoine & R. Douville 1904, *L. (N.) macdonaldi* Cushman 1918, *L. (N.) pustulosa* H. Douville 1917, *Nummulites floridensis* Heilprin 1885 (= *Operculinoides soldadensis* Vaughan & Cole 1941), *N. striatoreticulatus* L. Rutten 1928, *N. willcoxi* Heilprin 1883, and *Pseudophragmina flintensis(Cushman 1920).* This assemblage is clearly of Late Eocene age, also recognized by Malavassi (1961a) near the mouth of the Rio Naranjo (text-fig. 6.).

Discussion: Sedimentation and accretion history

The Quepos seamount seems to have originated over the Galapagos hotspot in Late Cretaceous time and was the site of deposition of condensed oceanic sediments, while volcanic activity continued. The oldest sediments found as isolated blocks between lava flows may be so far undated pre-Campanian radiolarites (Schmidt-Effing 1979), followed by Maastrichtian to Danian pelagic limestones. At least since the Maastrichtian, the seamount reached into the photic zone and hosted small, shallow-water shoals on which the Upper Paleocene *Ranikothalia*-bearing limestones, discussed here, were deposited. Volcanic agglomerates indicate also a subaerial exposure of the island. Tephra layers associated with Danian planktonic foraminifera were interpreted by Bolz and Calvo as originated from the Middle American volcanic arc, and hence, interpreted as proof of a forearc origin of the Quepos basement. However, these brown, finely laminated tephra layers containing altered pyroxenes resemble much those decribed by Schindlbeck et al. (2015) from Miocene pelagic sediments at Site U1381, drilled on the Cocos Ridge. These have a basaltic bulk composition and display typical Galapagos trace element characteristics. Pending geochemical work, the Quepos tephra may reveal that plinian volcanism could have been active, along with the production of subaerial agglomerates during the Danian on the Quepos volcanic island.

Later, pelagic, siliceous limestones accumulated on the slopes of the island, after the volcanic activity ceased in the Selandian and until the late Ypresian, while reworked shallow-water material indicates the discontinuous presence of short-lived shallow-water carbonate environments, from the late Paleocene to the early middle Eocene.

By Middle/early Late Eocene times the seamount approached the Middle American Trench and started to dig into the forearc sediments of the hanging wall of the decollement zone. The top of the seamount intrusive and volcanic suite and the overlying sediments became sheared off and incorporated into the upper plate, while the base and the underlying oceanic crust were subducted.

During the process of collision of the seamount top with the largely unconsolidated forearc slope apron, the seamount sequence became dismembered and mixed with the forearc sequence. Most of this material was then subject to gravitational mass wasting and ended up down slope on basement fragments of the seamount. The whole event caused rapid tectonic uplift of

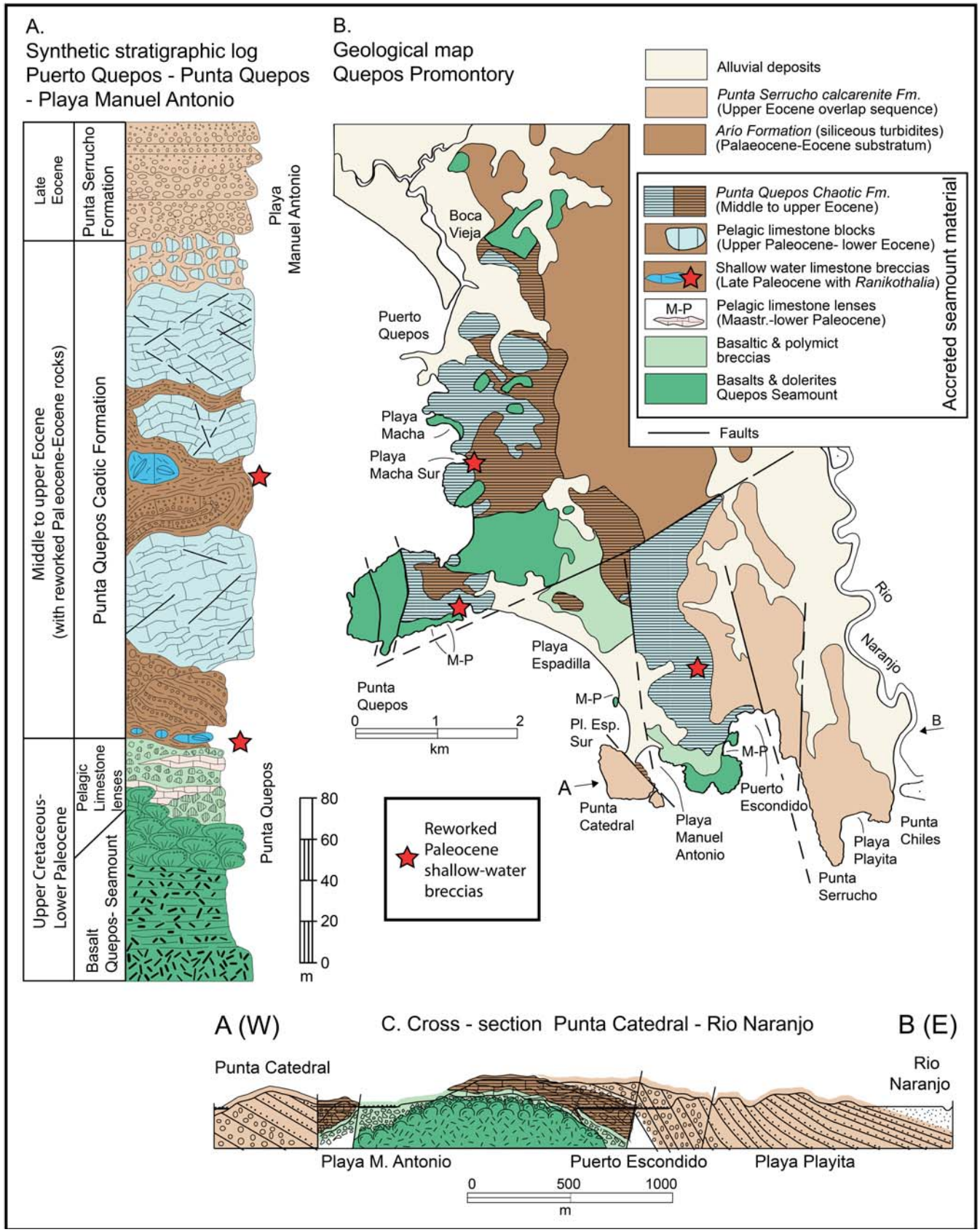

TEXT-FIGURE 6
Stratigraphic section of the Punta Quepos area with location of studied samples. B. Geological map and cross-section of the Quepos Promontory. After Baumgartner and Mora (1984), Baumgartner et al. (1984).

the collisional area. By Late Eocene, the accreted complex reached into the wave base and high-energy channelized conglomerates and cross-bedded sandstones accumulated in a shallow offshore environment. Soon after, tectonic relaxation resulted in subsidence allowing the deposition of a thick turbiditic overlap sequence.

According to Ranero and Von Huene (2000), the modern Mid American Trench is characterized as an erosive convergent margin based on the interpretation of seismic lines and the observation of seamounts leaving big scars in the forearc sediments. It is certain that the subducting seamount base scoops down into subduction an unknown amount of forearc sediments. However, the tectonic uplift into the wave zone of the Quepos complex suggests a short-lived compressive regime with rapid tectonic uplift, followed by relaxation and rapid subsidence during the Late Eocene. The fact that the Quepos Terrane and the much larger Herradura block ("Tulin Formation") are outcropping today, shows that the MAT (Middle America Trench) was rather accretionary than erosive during the Paleogene (see discussion in Buchs et al. 2009).

Travel path of the Quepos terrane. The youngest radioisotopic age of the Quepos volcanic suite is 59.4 ± 1.8 Ma (Selandian/Thanetian, Hoernle et al. 2002), which is a bit younger than the interflow Danian sediments. If we assume that accretion took place near the Lutetian/Bartonian boundary (41.2 Ma) the travel time from the Galapagos area to the MAT would have been 18.2 ± 1.8 Ma. Assuming that the Quepos seamount had travelled along a straight line parallel to the Cocos ridge, in the present day plate setting over a distance of about 1200 km, the long term convergence rate during the Paleogene would have been about 6-7.3 cm/year, which is very reasonable, but somewhat below the modern convergence rates (Mann 2007).

Geological setting of the Osa – Burica peninsulas

The Golfo Dulce – Osa – Burica area in southern Costa Rica (text-fig. 1) represents a complex puzzle of basement blocks and the Osa-Caño Acretionary Prism, now called Osa Mélange, that forms most of the outer Osa Peninsula (Obando 1986, Baumgartner 1986, Di Marco et al. 1994, Di Marco 1994). The first map representing the various basement units was published by Buchs and Baumgartner (2007). Refined subdivision and interpretation of the different basement complexes was presented in Buchs et al. (2009, 2010), based on field observations of the tectonostratigraphy, micropaleontological and geochemical analyses. Differences in basalt geochemistry and petrology as well as differences in the overlying Upper Cretaceous-Paleogene sediments indicate the presence of several discrete accreted blocks, that are exotic with respect to the trailing edge of the CLIP. In the Golfito area basaltic basement outcrops and associated pelagic and volcanoclastic sediments represent a proto-arc that was active in the late Campanian-Paleocene (Buchs et al. 2010). The Osa Igneous Complex (OIC, Buchs et al. 2009) crops out in the Burica peninsula, along the N-shore of the Golfo Dulce, and in the Osa isthmus (text-fig. 1). The OIC includes an assemblage of oceanic sequences essentially composed of pillowed and massive basalts with subordinate and thin interbeds of pelagic and volcaniclastic sediments (Berrangé and Thorpe 1988; Meschede and Frisch 1994; Di Marco et al. 1995; Hauff et al. 2000b; Buchs et al. 2009). The complex was subdivided into an Inner and Outer OIC based on the presence of a tectonic boundary outlined by strongly deformed limestones and basalts, and on contrasting lithologies across the boundary, with clear evidence for several accreted volcanic edifices in the Outer OIC (Buchs et al. 2009).

Inner Osa Igneous Complex

Biostratigraphic and $^{40}Ar/^{39}Ar$ data indicate a Late Cretaceous (Coniacian-Santonian, ~85 Ma) age of formation for the Inner OIC. This complex was formerly interpreted as an exposure of the CLIP (Hauff et al. 2000). New tectonostratigraphic data suggest that the Inner Osa Igneous Complex originated in the Pacific before being accreted to the CLIP margin during the Paleocene (Buchs et al. 2009, 2016). Protoarc dykes have not been encountered in the Inner Osa Igneous Complex, whereas they occur in the Golfito arc basement and in the Azuero Plateau, an autochthonous oceanic plateau part of the Azuero Marginal Complex (Buchs et al. 2010). It is the Inner OIC that is covered unconformably by an Upper Paleocene to Eocene, mostly deep water sequence, considered here as an overlap sequence. It contains abundant reworked Upper Paleocene to Upper Eocene shallow-water limestones, discussed further in this chapter. Biostratigraphic and $^{40}Ar/^{39}Ar$ data indicate a Late Cretaceous (Coniacian-Santonian, ~85 Ma) to Middle Eocene (~41 Ma) age of formation for the composite outer OIC (Di Marco, Baumgartner and Channell 1995; Hauff et al. 2000b; Hoernle et al. 2002; Buchs et al. 2009).

Osa Mélange

The Osa Melange was recognized and differentiated from the Nicoya Complex by Baumgartner (1986) and Baumgartner et al. (1989), who postulated the presence of an Eocene accretionary prism cropping out on the outer Osa Peninsula and Caño Island (Mora, Baumgartner and Hottinger 1989). The Osa Mélange contains mainly forearc-derived turbiditic and mass-flow trench fill and slope deposits that form the matrix of a mixture produced by gravitational emplacement, with a variety of igneous and sedimentary blocks (Di Marco 1994, Di Marco et al. 1994, Buchs et al. 2009). The matrix, dated by rich radiolarian assemblages, planktonic foraminifera and redeposited shallow-water LBF ranges in age from the Middle/Late Eocene (Agujitas, Marenco, San Pedrillo, Rio Tigre) to the middle Miocene (Cabo Matapalo). In some places (Punta La Chancha and Playa Carbonera) stratigraphic sequences can be reconstructed and the matrix can be considered as broken formation (Hsü 1973). The blocks include 10-100 m sized fragments of seamounts with associated pelagic limestones and or radiolarites of Campanian/Maastrichtian to Paleocene age. A variety of other igneous blocks include vesicular basalts, gabbros, rhyodacites, etc., some of which are probably derived from the hanging wall by mass wasting due to the collision of incoming seamounts. The trench fill sequences are stacked in lenticular bodies of several 100 m size that are separated today by subvertical shear-zones in which tectonic mélanges have developed. At a smaller scale, hydrofracturing, extensive calcite cement fabrics (up to 50% of carbonate rocks) and sedimentary intrusions of the less lithified lithologies indicate high fluid pressures and fluid activity during accretion. Temperatures may have reached values in the order of 150° C (Meschede et al. 2009), but no metamorphic rocks are known from the Osa Mélange. Di Marco (1994) and Di Marco, Baumgartner and Channell (1995) subdivided the Mélange into three tectono-stratigraphic units, from NE to SW: (1) the San Pedrillo Unit, (2) the Cabo Matapalo Unit, and (3) the Punta Salsipuedes Unit.

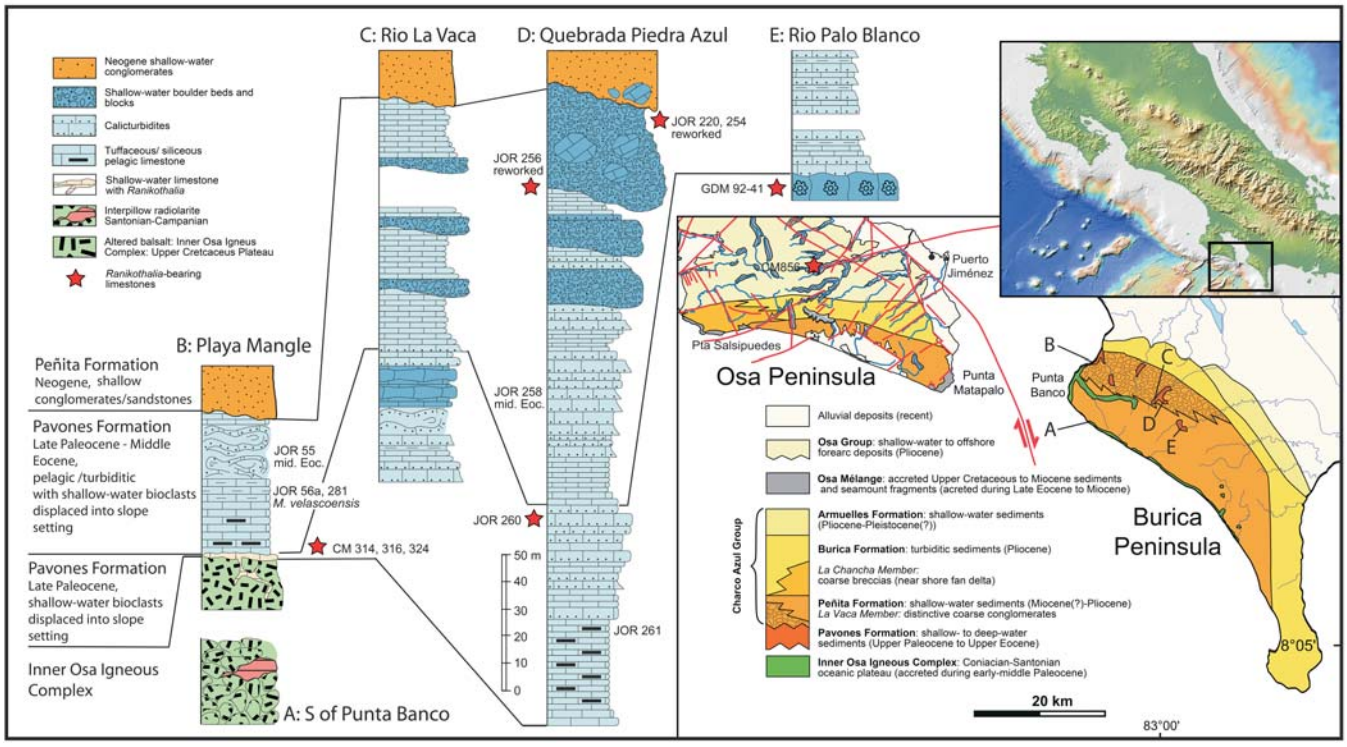

TEXT-FIGURE 7
A. Simplified geological map of the southern Osa and Burica peninsulas after Di Marco, Baumgartner and Channell (1995), Coates et al. (1992), Buchs et al. (2009). B. Stratigraphic logs of Paleogene carbonates outcropping in the Burica Peninsula, modified after Di Marco, Baumgartner and Channell (1995). Sample locations are indicated by red stars.

San Pedrillo Unit (text-fig. 7) It consists of a deformed matrix of detrital and siliceous sediments enclosing variable amounts of blocks of igneous rocks, pelagic sediments and resedimented shallow- water carbonates (Di Marco, Baumgartner and Channell 1995). The siliceous fraction of the matrix was dated as Middle Eocene on the basis of radiolarian assemblages (Azéma et al. 1983). The igneous blocks have been interpreted as remnants of accreted seamounts by most authors (e.g. Di Marco, Baumgartner and Channell 1995). According to Di Marco (1994), the San Pedrillo Unit is well exposed along the northwestern shore of the Osa Peninsula, from Bahia Drake to Punta Llorona (text-fig. 7). The Rio Rincon, Rio Cedral, and Rio Tigre also have good exposures of this unit. The matrix includes blocks of dark graywacke (often siliceous), red radiolarian chert and mudstone (Bahia Drake, Rio Cedral), and shallow-water redeposited limestones (Bahia Drake). The radiolarian chert and mudstone occur in sequences a few meters thick (Bahia Drake, Rio Cedral) to hundreds of meters thick (Rio Rincon) as dismembered interbeds in a matrix of volcaniclastic graywacke. Shallow-water carbonates are often included in the graywacke matrix as centimetric to metric clasts or blocks that represent broken debris flow units, or as calciturbidites, supposed to have originated from the inner wall of the trench. Blocks of OIB-basalt and associated sediments (basaltic breccias, red radiolarian cherts/mudstones, red siliceous limestones) are found in variable amounts in the San Pedrillo Unit. These blocks are interpreted as fragments of seamounts originally located on the subducting oceanic plate and eventually incorporated into the trench-fill sediments by offscraping and dismembering of the top of the incoming oceanic crust. Between Bahia Drake and San Pedrillo (text-fig. 7), the ophiolitic component is locally very important and represents up to 80 to 90% of the volume of rocks. However, the basaltic bodies are always within a volcaniclastic sedimentary matrix. The age of the matrix is Middle to Late Eocene based on radiolarians (Azéma et al. 1983, Diserens 2002) and redeposited LBF (Buchs et al. 2009).

The only occurrence so far of *Ranikothalia*-bearing Upper Paleocene limestone, reported here for the first time, is from the upper reaches of the "Brazo Derecho del Rio Tigre", 7.8 km WSW upstream from Dos Brazos del Rio Tigre, at 8°31'07.24"N, 83°26'39.30"W, see also Di Marco 1994, figure 42, herein: Sample CM 856 (text-fig. 7). It consists of a large block (>20m in diameter) of limestone breccia with shallow-water LBF-rhodolith clasts and black chert and volcanic sandstone clasts in a greywacke matrix (pebbly mudstone). It is interpreted as a debris flow redeposited from the sedimentary cover of the Inner Osa Igneous Complex (see below) that was already accreted to the upper wall.

Paleogene overlap sequence of the Burica Peninsula: Pavones Formation.

The Burica Peninsula is a northwest-southeast-oriented promontory shaped by the Panama Fracture Zone (text-fig. 7). Structurally, the Burica Peninsula is a tilted fault block of a CLIP-type oceanic plateau, unconformaby overlain by Paleogene sediments, the Pavones Formation. Another unconformity separates the Paleogene form thick Neogene (Pliocene-Pleistocene) forearc sequences. The Neogene sequences

and the recent structure have been studied by Corrigan, Mann and Ingle (1990). According to Buchs et al. (2009) the Inner Osa Igneous Complex continues into the Burica Peninsula, because of identical geochemical characteristics and similar fossil and radioisotopic ages. Coastal outcrops at Punta Banco and along the SW-coast of the peninsula present large outcrops of dolerites, massive and pillow basalts, dated in one place near Banco (text-fig. 7 A) as Santonian-Campanian by radiolaria extracted from an interpillow radiolarite (Di Marco et al, 1994, Diserens 2002). Important deformation prior to the onset of Paleogene sedimentation is evidenced by overturned pillow lavas just S of the mouth of Rio Claro (8° 23' 33" N, 83°06' 21" W, text-fig. 7, Obando 1986).

The Paleogene sediments were first described in detail by Obando (1986). He defined the Pavones Formation, which is composed of: (1) A pelagic to hemipelagic-turbiditc background sedimentation rich in planktonic foraminifera in the calcareous intervals and rich in radiolaria in siliceous beds. The detrital fraction shows lithic volcanic clasts, plagioclase and amphiboles and is certainly arc-derived. (2) Redeposited shallow-water carbonates occur in calciturbidites, and in up to 20 m thick boulder beds alterating with calciturbidites and hemipelagic beds, that may represent very proximal debris flows or even rockfall (scarcity of matrix) derived from a carbonate shoal in a tectonically active setting.

At Playa Mangle (300 m SW of mouth of Quebrada Mangle, 8°24'13" N, 83°07'44"W, text-fig. 7, B, *Ranikothalia*-bearing shallow-water carbonates occur as infill in fissures penetrating several meters into an altered surface of massive basalt (plate 7, fig. 1). A discontinuous limestone bed, rich in resedimented shallow-water bioclasts mixed with planktonic foraminifers, covers the basalt surface (text-fig. 7). Upsection, we measured a 30-m-thick sequence of siliceous pelagic limestones interbedded with tuffaceous mudstones (plate 7, fig. 1) and with limestone turbidites in the upper part. *Morozovella velascoensis* and other planktonic foraminifers that characterize the late Paleocene/earliest Eocene were identified both in the basal resedimented limestones and in the bedded pelagic limestones. Several Paleogene sections in rivers inland from Playa Mangle show similar sections, with a general increase in reworked shallow-water material towards the East. In the Quebrada Piedra Azul (text-fig. 7), we measured a section of over 60 m composed of coarsening-upward limestone turbidites and breccias, overlain by a boulder bed, at least 20 m thick, containing middle Eocene larger foraminifers and rhodoliths. This limestone sequence is underlain by the same siliceous pelagic facies that form the top of the Playa Mangle sequence. However, the basaltic basement does not crop out in Quebrada Piedra Azul.

In the headwaters of Rio Palo Blanco, Panama (N 8°20'08", W 83°01'35", text-fig. 7, E) we observed large blocks of massive, *Ranikothalia*-rich shallow-water limestones (plate 1, fig. 6) that occur near the base of the unconformable Neogene sediments. Even without good outcrops, these blocks suggest the presence of a late Paleocene carbonate shoal in the immediate vicinity. White outcrops visible on Google Earth about 2 km N of the Rio Palo Blanco, at a place called "Los Plancitos" (*Fide* Google Earth 2015, 8°20'50" W, 83°01'40", next to the Costa Rican border) suggest large outcrops of coherent massive limestone. In the Rio Palo Blanco we also discovered a >50 m thick sequence of siliceous limestones with interbedded turbidite and mass-flow deposits containing shallow-marine material as young as Late Eocene.

Discussion: sedimentation history and accretion of the Inner Osa Igneous Complex (IOIC).

The upper Paleocene-upper Eocene sections described above are unique to the Burica Peninsula. They suggest uplift of part of the IOIC and the formation of an isolated carbonate shoal since the Late Paleocene, which lasted (probably with interruptions) until the Late Eocene. Very proximal slope breccias (Quebrada Piedra Azul) and more distal carbonate turbidites demonstrate resedimentation of the platform carbonates into deeper water environments on the nearby slopes of a tectonically active, "outer high" hosting the carbonate shoal. The pelagic – hemipelagic deeper water sediments are rich in radiolarians and planktonic foraminifera, reflecting high fertility conditions, which are common during the Late-Paleocene-Early Eocene along the Middle American Pacific margin (see the Buenavista Formation in N-Costa Rica above). A fine-grained arc-derived component is present in distal turbidites. It shows that the Inner Osa Igneous Complex had reached the forearc area by late Paleocene, but was probably bypassed by the coarsest arc-derived material (Baumgartner et al. 1989).

Overturned pillow basalts found along the coast, just S of the mouth of Rio Claro (8° 23' 33" N, 83°06' 21" W, text-fig. 7., Obando 1986), 3 km from Playa Mangle, indicate that the basaltic basement underwent important deformation prior to the deposition of the upper Paleocene-Eocene sequence, which is only gently folded. The absence of a latest Cretaceous-early Paleocene sedimentary record and deep alteration of basalts prior to the onset of the upper Paleocene sedimentation suggest emergence of the Burica basement as a consequence of the (probably early Paleocene) accretion of the Inner Osa igneous Complex to the western edge of the CLIP (Buchs et al. 2009, 2016). Subsequent drowning of the trench-ward portion of the IOIC is documented by the downslope gravitational emplacement of shallow-water material into a sheltered, high fertility forearc environment. Trench-ward tilting and subsidence could be explained by tectonic erosion along the decollement of the deeper parts of the accreted plateau (Buchs et al. 2016).

Biostratigraphy, test motphology and paleo-environments of the *Ranikothalia catenula* group

Biostratigraphic historical

1932 - Cushman and Jarvis erected the new species *Operculina catenula* "from Upper Cretaceous of pit at Lizard Springs near Guayaguayare" (10°11'34"N, 61°05'16"W, 7.5 km NW of the centre of Guayaguayare Bay, sample Maerki 102b III, Lower Lizard Springs Formation, *Morozovellla velacoensis* Zone , P5, loc. 21, in Caudri 1996). This LBF was described along with many new taxa of small benthic foraminifera, now known as a lower bathyal to abyssal assemblage (Kaminski et al. 1988). Hence, the holotype of *R. catenula* is clearly displaced or reworked in a hypothetical mass flow deposit. The Lizard Springs Formation was subdivided by Cushman and Renz (1946) on the basis of distinct smaller benthic foraminifera into a lower and an upper unit, both assumed to be of Maastrichtian to Danian age. Bolli (1957) attributed a Paleocene age to the lower and an Early Eocene age to the upper unit. Initially, it was not clear whether the holotype had been collected in the lower (Paleocene) or upper (Lower Eocene) Lizard Springs Forma-

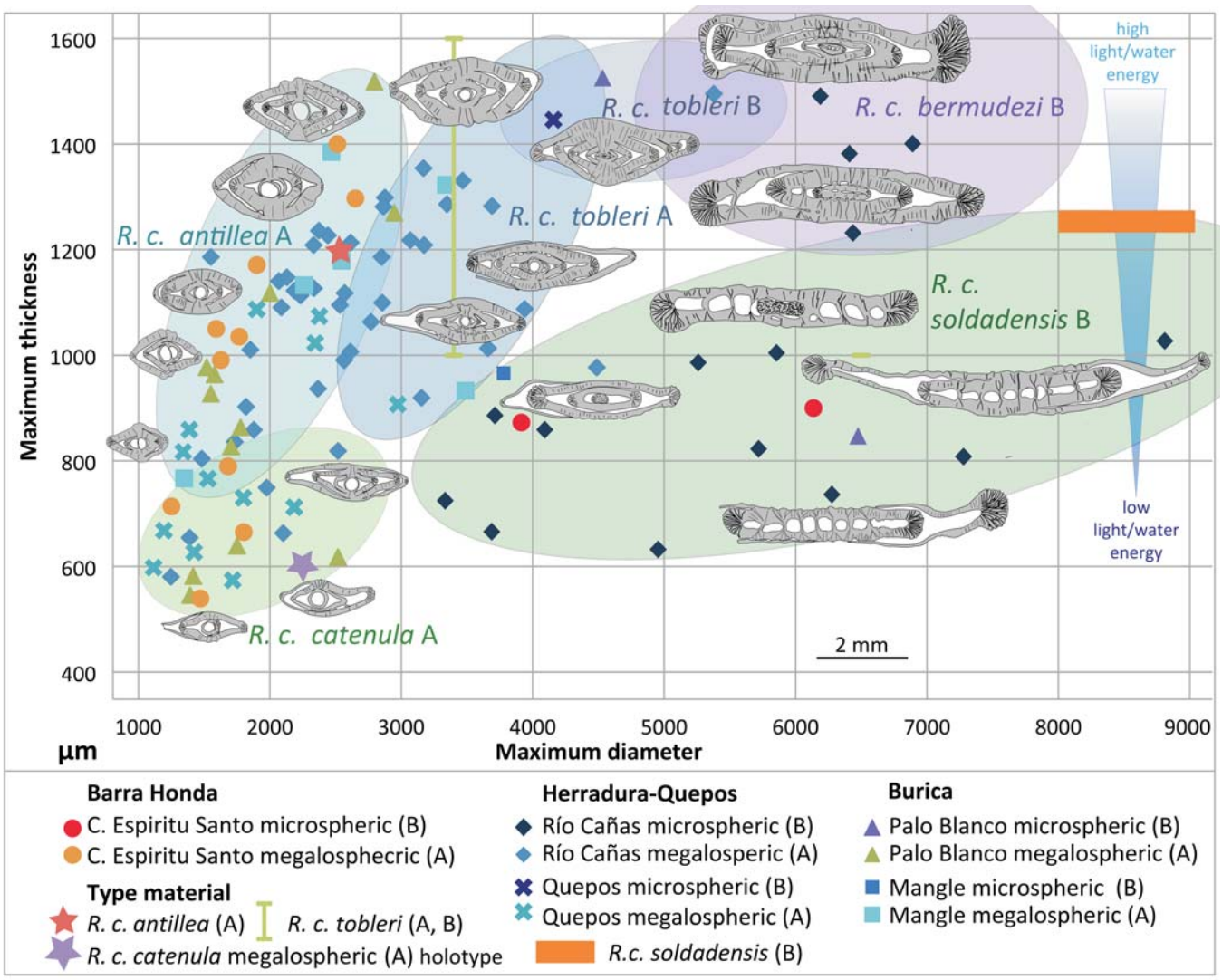

TEXT-FIGURE 8
Diameter *vs.* thickness of studied specimens of the *Ranikothalia catenula* group, based on axial sections observed in thin sections from all localities. Drawings of typical specimens are placed approximately at their position in the graph. Scale for all drawings: 2 mm (lower right). Note the approximate and overlapping fields of the subspecies. In general, flat, delicate forms are thought to be typical of low light and low hydrodynamic energy, whereas thick-shelled, inflated-lenticular forms probably dwelled in high energy and intense light conditions.

tion. Bolli (1957, p. XX) described the surface outcrops of the formation as "small slides not suitable for comprehensive stratigraphic studies". Caudri (1996, p. 1144) writes: "The locality from which the rich larger foraminiferal fauna was collected could at later surveys not been found again. It is assumed that the larger foraminifera were washed in from a contemporary reef ».

1946 - Cushman and Renz list the following LBF from the Lizard Springs type locality (Maerki sample): *Discocyclina (Discocyclina) aguerreverei* Caudri, *Discocyclina (Discocyclina) caudriae* Vaughan, *Discocyclina (Discocyclina) grimsdalei* Vaughan and Cole, *Discocyclina (?Discocyclina) meandrica* (Caudri), *Lepidorbitoides* cf. *planasi* Rutten, *Miscellanea antillea* (Hanzawa), *Miscellanea catenula* (Cushman and Jarvis), *Miscellanea* cf. *soldadensis* Vaughan and Cole, *Miscellanea tobleri* Vaughan and Cole; *Pseudophragmia* (*Athecocyclina*) *soldadensis* Vaughan and Cole, and *Pseudophragmina* (*Proporocyclina*) cf. *tobleri* Vaughan and Cole. In this list all morphotypes but *R. bermidezi,* included here with the *Ranikothalia catenula* group are present.

1957 - Sachs studied a large suite of topotypes of *Ranikothalia bermudezi* (Palmer) in which he demonstrated by measurements and illustrations of external views and thin sections the variation which occurs among specimens. Moreover, he showed that a number of species erected by Hanzawa (1937), Barker (1939), Cizancourt (1948; 1951), Vaughan and Cole (1941), Vaughan (1945), and Cole and Herrick (1953) are synonyms of *R. bermudezi*

1959 - Cole defines the "*Operculina catenula* Fauna" by the association of *O. catenula* with *Actinosiphon semmesi* Vaughan, *Discocyclina (Discocyclina) barkeri* Vaughan and Cole, *D. (D.)*

cristensis (Vaughan), *D. (D.) weaveri* Vaughan, and *Pseudophragmina* (*Athecocyclina*) *stephensoni* (Vaughan). Cole considered this association as typical of the Upper Paleocene without excluding its reach into the Lower Eocene.

1960 - Butterlin and Bonet reply with a discovery of abundant and well preserved *O. catenula* associated with *Coskinolina elongata* Cole 1842 and *Borelis floridanus* Cole 1941 in a conformable sequence ranging form the late Paleocene to the middle Eocene in Southern Campeche (Mexico). Since *C. elongata* is known from the Lower-Middle Eocene of Florida and Trinidad, the authors conclude that *O. catenula* ranges though the Lower Eocene.

1969a - Cole illustrates axial and equatorial sections of topotypic material of *Camerina catenula* from Lizard Springs, Trinidad. He also includes *Operculinoides bermudezi* (Palmer) in synonymy with *C. catenula.*

1969 - Butterlin and Monod describe *Rainkothalia* species ranging through the entire Lower Eocene from the Tauris of Turkey.

1972 - Blondeau states that *Ranikothalia*-faunas of French Guyana, Venezuela and the Antilles are of Paleocene age, whereas those of Haiti and Yucatan (according to Butterlin and Bonet 1960) range clearly into the Lower Eocene.

1975 - Kugler and Caudri report on the *Ranikothalia* Limestone from Bed 2 of Soldado rock. Beds 1 and 2 represent a Paleocene shallow-water limestone block set between beds 3 and 4 which are Late Eocene in age and contain reworked *Ranikothalia*. They conclude on a Paleocene age based on Bolli (1952) and Brönnimann (1952) who correlated the planktonic foraminifera of Bed 2 with those of the lower Lizard Springs Formation of Trinidad, which probably is the type level of *R. catenula.*

1975 - Caudri agrees with Cole (1959,1969a) to put *R. antillea* and *R tobleri* in synonymy with *R. catenula*, but keeps the names of what she calls "forms" on species level.

1981 - Butterlin establishes the *Ranikothalia bermudezi* Zone with a Paleocene to Early Eocene range (P3-P9). He also agrees with the idea that there is only one American species of *Ranikothalia*, with a large variability both in A and B forms, since there is no difference in stratigraphic range of the different species described so far.

1990 - (p. 749) Caudri writes: "I am in favour of calling the Caribbean species *Ranikothalia catenula* (Cushman and Jarvis), still listing its three morphological varieties "*antillea*", "*tobleri*" and "*soldadensis*", as I have done in my paper on Soldado Rock (Caudri 1975)".

1993 - Robinson and Wright restrict *R. catenula* to the Late Paleocene based on independent dating by nannofossils (NP5-7, according to Jiang and Robinson 1987), which corresponds to the late Selandian–early Thanetian or to top of P3 to upper part of P4 of Berggren et al. (1995).

1996 - Caudri (published posthumously, after her passing away on February 2, 1991) draws an overview of the worldwide distribution of *Ranikothalia*, typical for the Late Paleocene. In Trinidad Cole's "*Operculina catenula*" assemblage is composed of: "*Ranikothalia antillea, tobleri* and *soldadensis*, *Neodiscocyclina barkeri (*Vaughan & Cole 1941*), N. caudriae* (Vaughan 1944), *N. grimsdalei* (Vaughan and Cole 1941), *N. aguerreverei* (Caudri 1944)*, N. fonslacertensis* (Vaughan 1945) and *N. mestieri* (Vaughan 1945), *Athecocyclina soldadensis* (Vaughan and Cole 1941), *Hexagonocyclina inflata* (Caudri 1944), *H. meandrica* (Caudri 1944), and *Actinosiphon barbadensis* Vaughan 1929. For other localities, *Discocyclina weaveri* Vaughan 1929, *Athecocyclina stephensoni* Vaughan 1929) *Hexagonocyclina cristensis* (Vaughan 1929) and *Actinocyclina semmesi (*Vaughan 1929) should be included". Caudri cites the few observations of *Ranikothalia* reaching into the Eocene, amongst them: "Butterlin traced its occurrence from the Late Paleocene to high in the Early Eocene (zones of *Morozovella aragonensis* (P8) and *Acarinina pentacamerata (Subbotina)* (P9)". Besides that, she warns to be careful, as many of the Eocene occurrences could be reworked, even if well preserved, such as the assemblage in the Middle Eocene Murphy's beds of Barbados.

1998 - Serra-Kiel et al. define the Shallow Benthic foraminiferal Zone SBZ 3 "early Thanetian sensu Schaub 1981" (planktonic foraminifera zone P4) by the biostratigraphic range of *R. bermudezi* (Palmer) amongst others. There is no reference section for SBZ3 given in the American Realm. As reference for the characterisation of taxa the reader is referred to Hottinger 1977b, plate 17, figures 2-6, which represent equatorial sections of *R. sindensis (Davies 1927)* form the middle Paleocene of the Pyrenees. It should be noted that Hottinger (1977b, p. 50) considers *R. bermudezi* (Palmer) as a synonym of *R. sindensis*.

1998 - Tosquella et al. revise the SBZ 3 zone characterized, among other species by the range of *R. sindensis*. Corresponding now to the Late Selandian and most of the Thanetian (upper P4a to lower part of P4c of Berggren et al. 1995). *R. bermudezi* disappears from the SBZ zonation.

2003 Mello e Sousa et al. define a biozone LF1, which is dominated by *R. bermudezi*. Without calibration to other microfossils, they follow Butterlin (1981) in extending the *R. bermudezi* zone, defined by the total range of this group from the late Paleocene to the early Eocene (planktonic foraminifera zones P3 to P9).

2009 - Schreibner and Speijer, based on sections in Egypt, correlate the SB-Zones to the newly defined GSSP of the Paleocene/Eocene boundary by means of stable carbon isotopes. SBZ 3 remains late Selandian to late Thanetian, whereas SBZ 4 occupies now the remainder of the Thanetian up to the Carbon Isotopic excursion, i.e. the newly defined P/E-boundary, and the beginning of the Paleocene/Eocene Thermal Maximum. This limit, according to these authors, coincides with the Larger Foraminifera turnover and the base of the "Ilerdian" (Hottinger and Schaub 1960). *Ranikothalia* spp. are mentioned as characteristic of SBZ 4. However, in one section (section F), *Ranikothalia* sp. occurs above the P/E boundary, which is reflected by a stippled line ranging into SBZ5-6 of this genus in their figure 9.

2010 - Haynes et al. establish the new genus *Caudrina* with *Miscellanea soldadensis* (Vaughan and Cole) as type species (see systematic part below). *Caudrina* essentiallly includes *R. soldadensis* by virtue of its more evolute final whorl. *Chordoperculinoides* Arni is represented according to these authors by only one Western Hemisphere species, *R. bermudezi*, and *R. sahni* of the Eastern Hemisphere. According to these authors, *Caudrina* and *Chordoperculinoides* are said to be restricted to

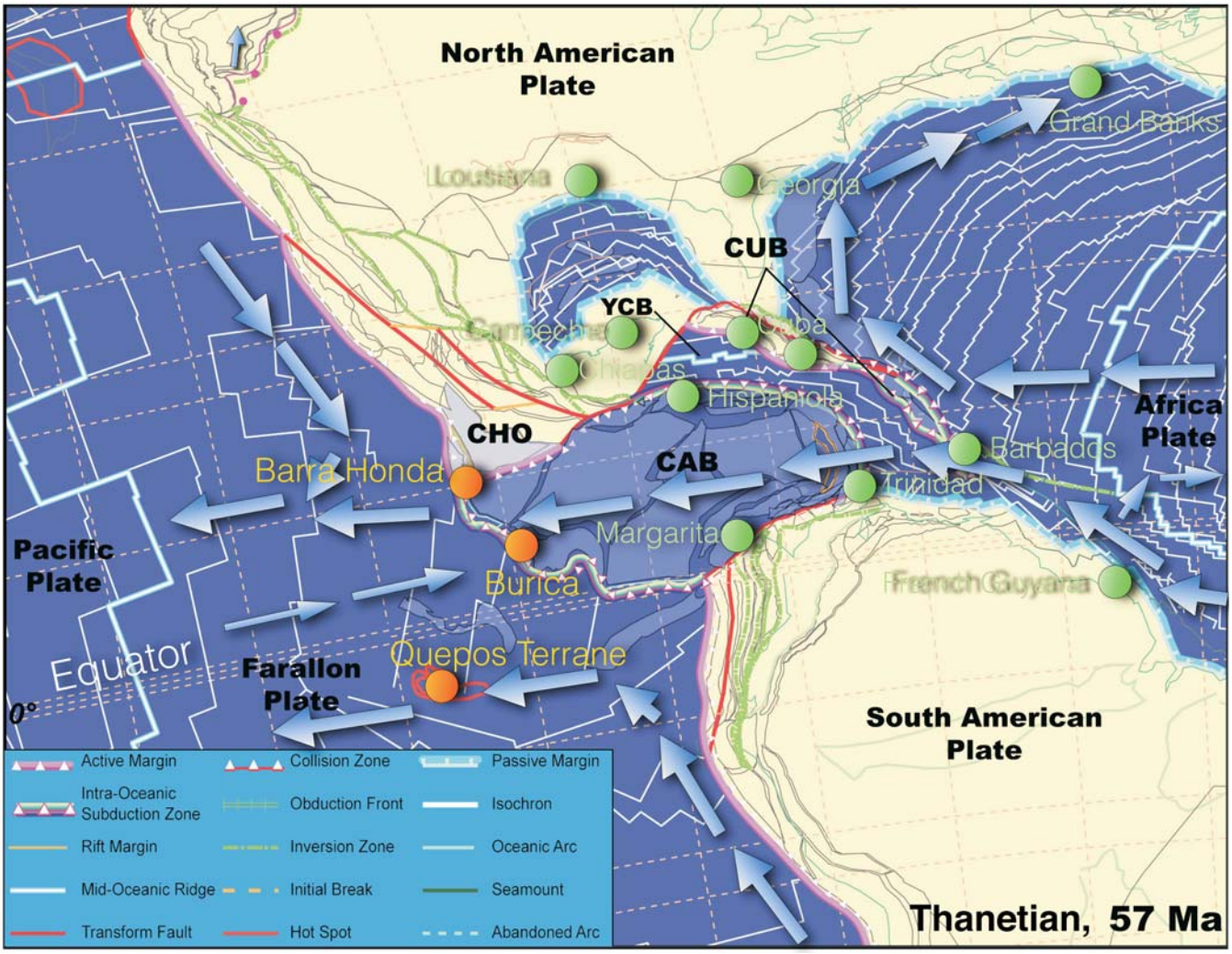

TEXT-FIGURE 9
Plate tectonic reconstruction of the Caribbean region after Flores (2009) at 57 Ma, Thanetian (Late Paleocene). The paleogeographic position of *Ranikothalia*-bearing carbonate occurrences described herein are marked with orange dots, Occurrences form the literaure are marked with green dots. Blue arrows show hypothetical oceanic surface current patterns based on modern oceanographic concepts. CAB: Caribbean Basin, CHO: Chortis Block (of which the Mesquito Composite Oceanic Terrane is colored in light mauve), CUB: Cuba, YcB: Yucatan Basin. Oceanic plateaus (in part the Caribbean Large Igenous Provionve, CLIP) are colored in lighter blue.

The CLIP occupies now most of the inter-American seaway. The Chortis Block rotates counter-clockwise and provokes northward, shallow subduction of parts of the CLIP and its newly formed proto-arc. Uplift of the Manzanillo Terrane, now part of Chortis, could have been the consequence of this subduction and could have triggered the Barra Honda Platform. At the Galapagos hotspot seamounts, such as the Quepos and Herradura Terranes formed since the latest Cretaceous in the wake of plume tail activity. Upper Paleocene fringing shoals or atolls are documented in the Quepos/Herradura seamounts. The South American Caribbean margin is at equatorial latitudes allowing an important branch of the Atlantic equatorial current to connect with the Central Pacific equatorial current system. This connection could have been a migration route for LBF via the Caribbean margin of South America into the Pacific realm. The East Pacific seamounts may have served as "stepping stones".

the late Thanetian (upper SBZ3 to SBZ5 in their figure 2), but *Chordoperculinoides* shows a stippled line ranging up including SBZ7, whereas the genus *Ranikothalia*, that for them only includes *R. nuttalli*, ranges up to the lower half of SBZ7. Hence, according to Haynes et al. (2010), the *R. catenula* group as defined herein would be restricted to the Thanetian, without any biostratigraphic argument.

2013 - Vicedo et al. describe allegedly Paleocene *Ranikothalia bermudezi* from the Sierra de Chiapas (Mexico) along with *Taberina*. The measures for megalospheric forms (max diameter: 1.4-2.1 mm, max thickness: 0.9-1.1 mm) fit well in our scatter plot of measurements of the *R. catenula* group from Costa Rica and W-Panama (text-fig. 8). *R. bermudezi* (=*R. sindensis*?) is said to be restricted to the Thanetian by making reference to SBZ 3 of Serra-Kiel et al. (1998)

2014 - Vicedo et al. describe *Ranikothalia* from Campeche (Mexico) as *R. soldadensis,* which is taken as characteristic of SBZ 3? to SBZ 4 (Thanetian), without further discussion. The measures and illustrations given (max, diameter: 2.5-3 mm, max. thickness: 0.6-0.9 mm) fit to the smaller forms of our ma-

terial. For these authors, *Ranikothalia soldadensis* differs from *R. bermudezi* by its flatter morphology, tighter spiral and smaller test size. However, the measures given for megalospheric forms of *R. soldadensis* are larger than those given for *R. bermudezi* in the 2013 paper (see above). We suspect a confusion of the two "species". Additionally, the authors suggest that the assemblages with *R. bermudezi* from Chiapas are younger than those with *R. soldadensis* form Campeche, without any supporting evidence.

Biostratigraphic discussion

From the historical review above it becomes clear that the various species of *Ranikothalia* described from the American Realm have approximately the same, rather poorly defined stratigraphic range. Neither from previous studies, nor from our material we can conclude on a biostratigraphic relevance of the various morphotypes regrouped by us in the *R. catenula* group. A major obstacle in achieving higher biostratigraphic resolution, even for the whole group, is the fact that much of the studied *Ranikothalia* occurrences, including the type material, come from shallow-water material that was redeposited into a deep-water environment. This circumstance may have the advantage of providing biostratigraphic control by planktonic foraminifera and nannofossils. On the other hand, redeposited material is isolated from its original stratigraphic and paleogeographic/paleoecologic context. The planktonic assemblage gives a minimum age of the time of emplacement of the shallow-water material, which may be reworked from older strata. Additionally, redeposited assemblages may have suffered from hydrodynamic sorting, biasing the composition of a sample. Despite of all these inconveniences, redeposited material is often well-preserved, embedded in a clay-rich matrix allowing isolation of specimens. Apart from the large, long-lived carbonate shelves set on continental margins, such as Yucatan or Florida, the tectonically active Caribbean Realm was the site of small short-lived, isolated carbonate shoals that originated on tectonically uplifted oceanic basements or on volcanic edifices. Accommodation space for carbonate buildup was limited on many of these shoals; this may explain why much more redeposited rather than *in situ* platform material has been found.

Nevertheless, we can conclude from the historical review above that *R. catenula* group ranges certainly through the Thanetian. It may appear in the Selandian and extend into part of the Ypresian. In contrast with many other statements, Butterlin and Bonet (1960) and Butterlin (1981) insist that the *R. catenula* group ranges though the enitre Ypresian (Lower Eocene) in Yucatan and Haiti, based on co-occurrences with species typical for the Lower-Middle Eocene. No calibration by planktonic foraminifera is available, so far for these occurrences. On the other hand, a possible diachroneity of the last occurrences of *R.* gr. *catenula* could be explained by the survival of this group in subtropical, highly oligotrophic refuges, while it went extinct in the tropical areas due to hot and eutrophic contitions during the Paleocene-Eocene thermal maximum.

The occurrences in Costa Rica and W-Panama discussed herein are often directly related with the occurrence of *Morozovella velascoensis*, a species easily recognizable in thin section of pelagic interbeds that accompany shallow-water resediments in Herradura-Quepos and Burica. *M. velascoensis* is also present in the Barra Honda Limestone in facies that formed under an open marine influence (Jaccard et al. 2001). The range of this species was given by Berggren et al. (1995) as 60.0 – 54.7 Ma, which included most of the Selandian and the Thanetian, according to the Berggren et al. (1995) time scale. More recently, according to the new definition of the P/E boundary, corresponding to the Carbon Isotopic Excursion, the Benthic Foraminiferal Extinction Event, and the beginning of the Paleocene/Eocene Thermal Maximum, the range of *M. velascoensis* had to be reassessed. Considering that the P/E boundary is now placed at 55.5 Ma (Aubry et al. 2007) or at 56.0 Ma (IUGS/ICS International Chronostratigraphic Chart 2016/04) in early chron C24r, *M. velascoensis* goes extinct about 200 Ka to 1 Ma after the isotopically defined P/E boundary (Pak and Miller 1992, Kelly, Bralower and Zachos (1998), Molina, Arenillas and Prado1999; Arenillas, Molina and Schmitz 1999.

Both by the co-occurrence with *M. velascoensis* and the Sr-isotope data presented in this paper, we can confirm a late Selandian-Thanetian, possibly earliest Ypresian range of *R. catenula* group. The Sr-ratios cluster, however, around 58 Ma, which is in the early Thanetian according to the time scale used for the calibration of the Sr-curve (see above).

A sharp, but conformable change from Barra Honda platform carbonates to red, siliceous, hemipelagic-turbiditic facies suggests the demise and tectonic drowning of the platform at the P/E-boundary. On the other hand, the carbonate resediments in Herradura, Quepos and Burica seem to record a (perhaps intermittent) continuation of carbonate shoal conditions on oceanic islands/outer highs until the Middle/Late Eocene.

Test morphology of the Costa Rican material

A morphometric study on 200 specimens of *Ranikothalia* spp. that co-occur in all studied samples, both form *in situ* carbonate shoals, and from assemblages resediemnted in deeper water. Resedimented assemblages have the advantage to represent a pal-ecological cross-section form shallowest to deepest environments. In addition, the specimens displaced into deeper water escape intense microboring and early diagenesis and consequently may show in cathodoluminescence excellent preservation of microstructures (see plates).

Morphologic continuum. Our study reveals a morphologic continuum between megalospheric (A) forms and microspheric (B) forms (text-fig. 8) of morphotypes previously described as several different species. We redefine here the *R. catenula* group including several, formetly described American species at subspecies level. In agreement with many previous workers (Caudri 1974, 1990, Sachs 1957, Hotttinger 1977b, Vicedo et al. 2014) we conceive that these co-occurring morphotypes correspond to the same biological species. The separation of this group into 2 generta according to Haynes et al. (2010) seems highly hypothetical to us, since we observe transitional forms in many samples between the "sub-evolute" microspheric forms *"Caudrina" soldadensis* (*Ranikothalia catenula soldadensis* herein) and the "involute" "*Chordoperculinoides*" *bermudezi* (*R. c. bermudezi* herein). In addition, no quantifiable differences in the size of perforations nor of the size of radial canals in the marginal chord have been observed by us, that would justify a distinction at a generic level.

Neither in previous studies nor in our material we can find biostratigraphic evidence of differing ranges of the various morphotypes regrouped by us in the *R. catenula* group. In particular, we cannot confirm the stratigraphic succession suggested by Vicedo et al. (2014), from flatter (*R. soldadensis*) to

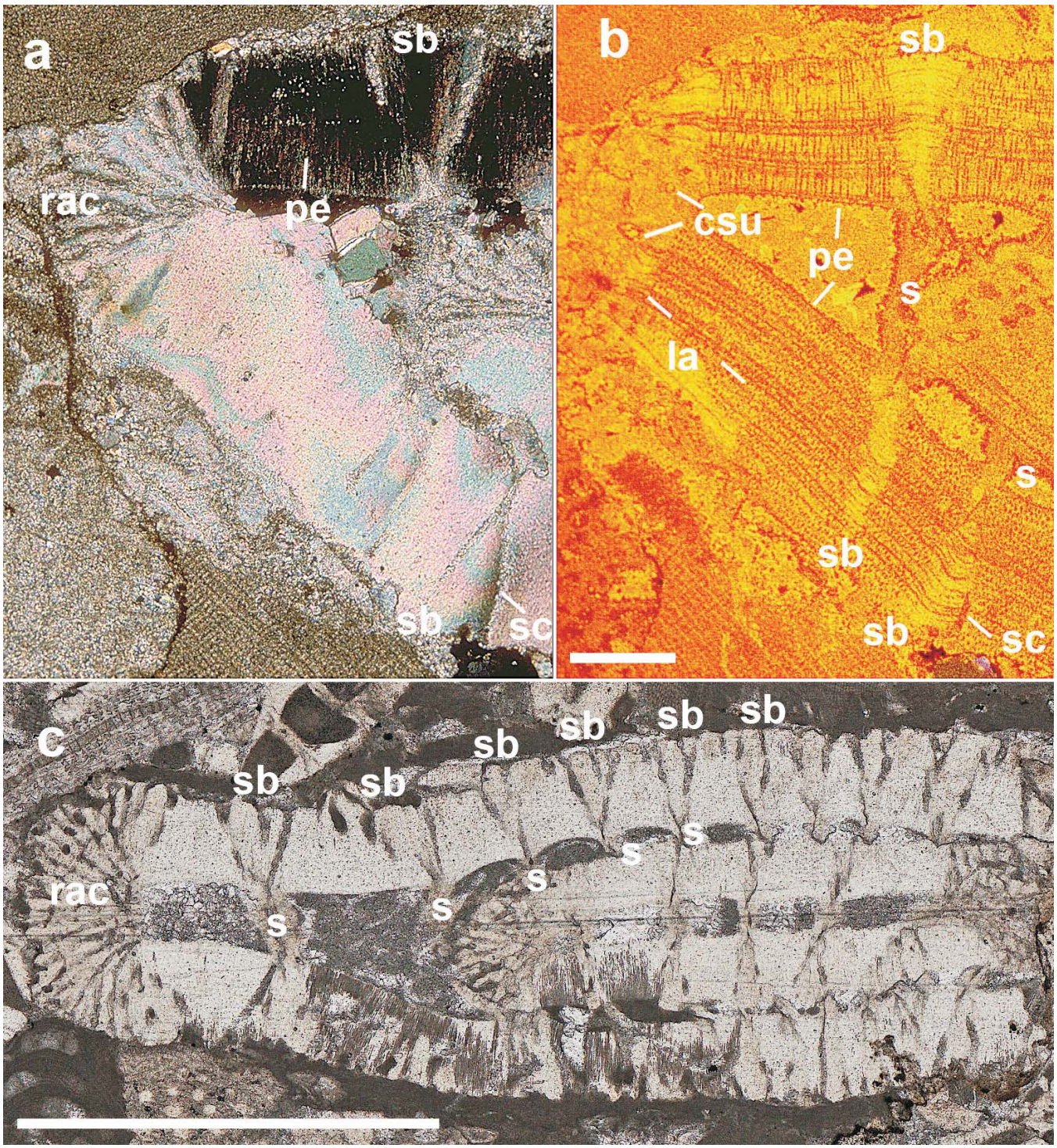

TEXT-FIGURE 10
a, b. Oblique axial section of *Ranikothalia catenula antillea*. Sample CM 324.2, Playa Mangle, scale = 100 µm. a. polarized light, b. CL. The well preserved internal structure of the test is visualized by darker earliest diagenetic cements filling the perforation (pe) and in interlamellar linings (la). Note the imperforate pillar-like structure beneath the sutural bands (sb) connecting with septae (s). Note change of orientation of calcite fibres around the sutural band in polarized light. Sutural canals (sc) are rarely visible. Coarse radial canals (rac) and sulcal canals (csu) are visible in the marginal chord. c. *Ranikothalia catenula soldadensis*, sample OA65, Scale =1 mm. Note funnel-shaped structures around sutural bands: some may be sutural canals, some may be enhanced by bio-corrosion creating an irregular surface of the test.

more robust (*R. bermudezi*) forms, since these morphotypes co-occur with transitional forms in many of our samples.

Shape and shell thickness distribution. The variability of morphotypes of the *Ranikothalia catenula* group can be interpreted in terms of hydrodynamic energy and light availability in their habitat, in applying the observations made on living LBF. This interpretation matches the hydrodynamic energy deduced from the microfacies and the abundance of photosynthetic algae in our thin sections. The presence of flat lenticular delicate A-forms *R. c. catenula* together with delicate B-form *R. c. soldadensis* in the upper Barra Honda Limestone and in resediments from open oceanic shoals suggests that these forms may have lived both in shallow protected and deeper off-shore calm water areas. Their presence is therefore not necessarily an indicator for the deeper euphotic zone. On the other hand, the most robust B-form *R.c. bermudezi* is absent from the Barra Honda Limestone, but occurs in resediments from open oceanic shoals. This form may be a good indicator of shallow, high energy paleoenvironments. The thick-shelled, small, inflated-lenticular, A-forms *R. c. antillea* together with *R. c. tobleri* dominate in numbers in almost all thin sections. This abundance may be the result of hydrodynamic sorting in classical turbidites, due to their small size but high shape entropy (Hofmann 1994; Briguglio and Hohenegger 2009, 2011), but also could be the result of wave action in high-energy shallow-water *in situ* deposits. The scarcity of the most robust B-form *R. c. bermudezi* in resediments may indicate different hydrodynamic sorting, since its larger size and high shape entropy and hence, high settling velocity, restricts its occurrence to debris flows, rather than classical turbidites.

Paleoenvironmental interpretation *Ranikothalia catenula* group: *in situ* habitats and resedimentation.

Populations of *Ranikothalia* gr. *catenula* occur both in *in situ* shallow-water deposits of the Barra Honda Platform and the Río Palo Blanco (Burica) outcrops, as well as resedimented in deep-water environments on basaltic basements of accreted oceanic seamounts/plateaus.

Studies on living, symbiont-bearing perforate hyaline LBF provide important keys to the paleo- environmental interpretation of fossil LBF populations. Living LBF exhibit a strong correlation between their morphology and environmental parameters (Hallock Röttker and Wetmore 1991; Hottinger 1997b, 2000). Recent LBF host photosynthetic symbionts (Hallock 1985) that are advantageous in warm, oligotrophic waters, where light is abundant and nutrients are scarce, and occur as particulate organic matter (Hallock 1981). Hydrodynamic energy and light availability may both result in an optimisation of shell morphology for each species in each habitat (Hallock, Röttker and Wetmore 1991).The decrease of light intensity with increasing water depth is a function of water transparency, in turn depending on the particulate nutrient flux, and the trophic level (Hallock 1987, 1988). As a consequence, LBF build more robust shells in high energy (shallow) environments, whereas in deeper, calm water environments thin-walled, flat shells, with an increased surface-to-volume ratio, dominate (Hallock 1981; Hallock, Röttker and Wetmore 1991; Hottinger 1977b, 2000; Bernoulli et al. 2010). Microstructures in the test wall serve to increase strength and to focus light to get maximum profit from their symbionts (Hallock, Röttker and Wetmore 1991; Hottinger 1997a). Species that live in shallow-water have to deal with higher hydrodynamic energy and illumination levels. These species are more robust, thick-shelled, or are capable of strongly attaching to the substrate (Hohenegger 2004).

Hallock (1987, 1988) presented a model in which the depth-dependent community structure of symbiont-bearing benthic foraminifera is a function of nutrient flux determining the depth of the euphotic zone. Light penetration through the water column is limited by turbidity, which is a function of plankton density and fluvial influx of particulate and dissolved organic matter and suspended sediment. Hottinger (1977b, 1983) showed that the distribution of LBF in the Gulf of Aqaba is determined by sediment structure, light intensity, water energy and food availability.

Hohenegger (1994) and Hohenegger et al. (1999) studied the occurrence of 21 species of larger foraminifera near Okinawa (Ryukyu Islands, Japan) in terms of light intensity, water movement and substrate type. They found that each species showed its own characteristic distribution with respect to these parameters. Many of the above mentioned studies were carried out in highly oligotrophic seas, where living LBF are recorded up to 120 m depth (Reiss and Hottinger 1984; Hallock,1984; Hohenegger 2000). On the other hand, Renema (2002) reported data on living LBF from several localities of Indonesia, from regions which are characterized by a monsoonal climate with a seasonally changing suspension load from river input, resulting in a variable trophic level and an over all much shallower euphotic zone. The vertical morphological zones of Hallock (1987) are compressed and typical deep-water specialists may be absent.

The Costa Rican deposits discussed in this paper were located during the Late Paleocene at slightly lower paleolatitudes than today (Di Marco et al. 1994). Nevertheless, they were certainly affected by seasonally high rainfall under the inter-tropical convergence zone. The Barra Honda Platform formed in a fore-arc setting (see "Geologic setting, age and facies of the Barra Honda Formation" above) which, *a priori*, was rich in detrital input both from air-borne ash fall and from terrestrial and submarine erosion of a hypothetical volcanic arc. However, during the Late Paleocene-earliest Eocene we observe a gap in arc-derived detrital input (see above) resulting in siliceous/calcareous pelagic sediments in deep water areas and in the pure Barra Honda Limestone, attesting for a low detrital input in the uplifted forearc area.

During the Late Paleocene, the oceanic islands documented in the accreted terranes of Quepos and Herradura were located several 100 km offshore on their way from the Galapagos hot spot towards the Middle American Trench. Apart from occasional tephra layers (see "geological setting") and the local (mostly mechanical) reworking of the basaltic basement (see above) no suspended detrital input can be observed in the rocks.

By the Late Paleocene, the Inner Osa Igneous Complex, represented by the Burica basalts, was accreted and uplifted. The Palo Blanco (Burica) limestones considered as *in situ* are free of clays, but show well-rounded lithoclasts of basalt reworked from the underlying basement. Soon after the formation of the *Ranikothalia*-bearing limestones, the area was under the influence of fine grained, probably air-borne, arc-derived material documented in the tuffaceous siliceous limestones that overlie the limestones a Playa Mangle and contain resedimented limestone breccias in the other localities of the Pavones Formation (text-fig. 7).

In summary, all localities shared relatively clear water conditions during the Late Paleocene. However, contemporaneous siliceous pelagic deposits in deeper areas (Sandino Basin, Andjic, Baumgartner-Mora and Baumgartner 2016, Pavones Formation, Burica) may be diagnostic of offshore upwelling conditions along the Mid-American margin.

In the following we compare the carbonate microfacies and the geological setting of the studied localities with the abundance and distribution of robust inflated-lenticular vs, delicate flat morphotypes of *Ranikothalia.* The Barra Honda Platform is overall, and especially in its thick, massive lower part (Mora 1981), dominated by restricted, probably very shallow, perhaps seasonally hypersaline, carbonate mud- producing environments. Non-fossilized green algae and red algae, such as *Polystrata alba,* present in almost any sample of Barra Honda, and geniculate corralines, as well as *Distichophax biserialis* (a green alga?) must have dominated. This facies contains herbivorous gastropods and some porcellanacous foraminifera such as miliolids and *Sigmoilopsis* sp. In this part of the column LBF are very scarce: Small discocyclidids, such as *Neodiscocyclina barkeri* were reported by Di Marco et al. (1994), and Jaccard et al. (2001).

In the areas of the Cerro Espiritu Santo and Cerros Guayacan (text-fig. 3.) the Barra Honda facies are transgressive over older Formations (see above) and present higher energy, well-washed pack and grainstones with macroscopic cross-lamination. *Neodiscocyclina*- and *Ranikothalia*-grainstones occur, along with levels of rhodoids baffling finer grained bioclasts (plate 4, fig. 17). In these high-energy facies, thick-shelled, inflated-lenticular *Ranikothalia catenula antillea* are abundant. Fragments of thick marginal chords, most probably belonging to the delicate *R. c. soldadensis* may be reworked from adjacent calm-water bioclastic facies, which contain other delicate morphotypes of the *Ranikothalia catenula* group, such as *R. c. catenula,* and small rotaliids. These findings imply that delicate morphotypes of the *R. catenula* group may also occur in shallower, more restricted calm-water environments. In Barra Honda, we have not found the sturdiest morphotype *R. c. bermudezi*, present only in the oceanic seamount/plateau settings (see below).

The rocks cropping out in the headwaters of Río Palo Blanco, Burica, Peninsula, Panama are probably the source area of all the resedimented material that occurs in several sections of the Pavones Formation (Burica, text-fig. 7). Both at outcrop scale (plate 1, fig. 6) and in thin section, the facies is a probably *in situ* rhodoid rudstone to bafflestone whith some coarse sand sized, detrital (reworked basement) matrix. It contains both delicate *R. c. catenula* and *R. c. soldadensis* along with robust *R. c. antillea*, *tobleri* and rare *bermudezi* (Plate 6, figs. 12-15). Both flat, delicate and lenticular *Neodiscocyclina* sp. are present. No delicate *Distichophax biserialis*, *Polystrata alba* nor geniculate corralines are present. This facies is interpreted as a moderate to high-energy open marine oceanic carbonate shoal located on a tectonically uplifted portion of the Inner Osa Igneous Complex. It became established as the consequence of accretion/collision of this complex on the trailing edge of the CLIP (Buchs et al. 2010, 2016).

The localities of Rio Cañas (Herradura), Quepos, Rio Tigre (Osa) and several localities of the Pavones Fromation of the Burica Peninsula (text-fig. 7) all show resedimented limestones either as hydrodynamically sorted (often graded) calciturbidites, or as coarse breccias representing dismembered debris flows. The high variability of microfacies of adjacent samples from the same locality suggests reworking of lithoclasts or even multiple reworking of breccias in the Quepos Chaotic Formation (see above). Shallow-water lithologies are often mixed or interbedded with contemporaneous pelagic material yielding planktonic foraminifera, such as *Morozovella velascoensis*. The most abundant LBF in calciturbidites are small robust *R. c. antillea* and *tobleri* followed by similar-sized and -shaped *Neodiscocyclina* sp. In coarser beds (e.g. Rio Cañas, Playa Macha Sur, Quepos), large *R. c. bermudezi* and mostly fragmented *R. c. soldadensis* are mixed in. We interpret the source environment of these redeposits as insular, open marine carbonate shoals where storms or earthquakes may have triggered downslope gravitational transport of poorly cemented and isolated bioclasts from both shallower, high energy and deeper, low energy environments. The source environments lacked significant amounts of micrite, *Polystrata alba* and other bioclasts that would indicate restricted conditions, as observed for Barra Honda.

CONCLUSIONS

Paleocene – earliest Eocene *Ranikothalia*-bearing shallow-water limestones occur in 3 distinct paleogeographic settings in Southern Central America (Costa Rica, W-Panama).

1. Barra Honda Limestone. This formation is, according to $^{87}Sr/^{86}Sr$-ratios and biostratigraphy of mid Selandian to late Thanetian (? earliest Ypresian) age. The Late Paleocene tectonic uplift of the Manzanillo Terrane, a splinter of the CLIP that accreted to the Chrortis Block (text-fig. 9) in Coniacian-Santonian times (Andjic, Baumgartner-Mora and Baumgartner, submitted), is thought to be the consequence of an attempted N-dipping, shallow subduction of parts of the CLIP and its newly formed Middle American proto-arc. Tectonic uplift and temporary extinction of the arc during the mid Selandian allowed the formation of the very pure Barra Honda Limestone encroaching on a tectonic high that was still exposed to erosion during the early stages of carbonate production, as documented by Upper Cretaceous lithoclasts. The lower subunit of the Barra Honda Formation (Mora 1981) may correspond to rapid accumulation of coralgal micrites, that were transported out of a restricted, very shallow platform by ebb-tidal currents into the near off-shore area (text-fig. 4, model), where accommodation space was available. The upper, well-bedded subunit onlaps transgressively with higher energy facies on older formations. Here, *Neodiscocyclina* spp. and *Ranikothalia catenula* group are locally abundant. In a small scaled facies pattern open marine facies with *Morozovella velascoensis* interfinger with the topmost part. Renewed tectonic subsidence, resumed arc activity, eustatic sea-level rise and hot/humid climate resulted in eutrophication and rapid drowning during the PETM event. This event may be expressed by the sharp change from the Barra Honda limestone to red, deep water cherty and then turbiditic sediments of the lower Zapotal Member, reminiscent of the pelagic Late Thanetian-Early Ypresian Buenavista Formation of the Santa Elena Peninsula. (Andjic, Baumgartner-Mora and Baumgartner 2016).

2. Herradura – Quepos carbonate shoals on oceanic seamounts. The Herradura and Quepos terranes may represent the earliest seamounts formed about 1200 km to the SW of of their present position (text-fig. 9). by the Galapagos hotspot plume tail activity. Pelagic, latest Cretaceous to Danian interflow sedi-

ments were overlain by subaerial volcanic breccias and tephra associated with Late Paleocene-earliest Eocene shallow-water limestones rich in *Ranikothalia catenula* group, *Neodiscocyclina* spp. and coralline algae. Short-lived, discotinuous carbonate shoals may have existed until the early Middle Eocene. The shallow-water material is essentially preserved as resedimented breccias and turbidites associated with deeper water, seamount slope facies and possibly by outcrops of *in situ* shallow-water deposits encroaching directly on balsalt (Rio Cañas). By late Middle/early Late Eocene the Quepos Seamount approached the Middle American Trench, where the top of the seamount intrusive - volcanic suite and the overlying sediments became sheared off and incorporated into the upper plate. The seamount sequence became dismembered and mixed with the forearc sequence, and graviationally displaced trench-wards by mass wasting.

3. Inner Osa Igneous Complex – Burica Peninsula – carbonate shoal on an accreted oceanic plateau. The headwaters of the Rio Palo Blanco (Burica Peninsula, Panama) probably host the only *in situ* Late Paleocene shallow rhodoid rudstones of the area. All other localities (text-fig. 7) reveal redeposited shallow-water material in turbidites and debris flow breccias, which are overlain or interbedded with siliceous pelagic lime- and mudstones containing arc-derived fine (probably air- borne) volcaniclastic material. The absence of a Latest Cretaceous-early Paleocene sedimentary record and deep alteration of basalts prior to the onset of the upper Paleocene sedimentation suggest emergence of the Burica basement as a consequence of the (probably early Paleocene) accretion of the Inner Osa igneous Complex to the western edge of the CLIP (Buchs et al. 2009, 2016).

Test morphology of the Ranikothalia catenula group. A morphometric study on 200 specimens of *Ranikothalia* spp. that co-occur in all studied samples reveals a morphologic *continuum* between megalospheric (A) forms and microspheric (B) forms (text-fig. 8) of morphotypes previously described as several different species.

In agreement with many previous authors, we conceive that these co-occurring morphotypes belong to the same biological species. The separation of this group into 2 genera according to Haynes et al. (2010) seems highly hypothetical to us, since we observe transitional forms in many samples between the "sub-evolute" microspheric and the "involute" forms. In addition, no quantifiable differences in the size of perforations or on the size of radial canals in the marginal chord have been observed by us, that would justify a distinction at a generic level.

Neither from previous studies nor from our material we can extract biostratigraphic evidence for different ranges of the various morphotypes regrouped by us in the *R. catenula* group. In particular, we cannot confirm the stratigraphic succession from flatter (*R. soldadensis*) to more robust (*R. bermudezi*) forms, since these morphotypes co-occur with transitional forms in many of our samples.

Shape and shell thickness distribution. The morphotypes of the *Ranikothalia catenula* group can be interpreted in terms of hydrodynamic energy and light availability in their habitat, in applying the observations made on living LBF. The presence of flat lenticular delicate A-forms *R. c. catenula* together with delicate B-form *R. c. soldadensis* in the upper Barra Honda Limestone and in resediments from open oceanic shoals suggests that these forms may have lived both in shallow protected and deeper off-shore calm water areas. Their presence is therefore not necessarily an indicator for the deeper euphotic zone. On the other hand, the most robust B-form *R.c. bermudezi* is absent from the Barra Honda Limestone, but occurs in resediments from open oceanic shoals. This form may be a good indicator of shallow, high energy paleoenvironments. The thick-shelled, small, inflated-lenticular, A-forms *R. c. antillea* together with *R. c. tobleri* dominate in numbers in almost all thin sections. This abundance may be the result of hydrodynamic sorting in classical turbidites, due to their small size but high shape entropy (Hofmann 1994; Briguglio and Hohenegger 2009, 2011), but also could be the result of wave action in high-energy shallow-water *in situ* deposits. The scarcity of the most robust B-form *R. c. bermudezi* in resediments indicates different hydrodynamic sorting, since its larger size and high shape entropy and hence, high settling velocity, restricts its occurrence in debris flows, rather than classical turbidites.

Paleobiogeographic implications of *Ranikothalia* gr. *catenula* occurrences on ancient Pacific seamounts

The paleogeographic position of the *Ranikothalia* occurrences described herein lies far more to the south-west than that of the American localities known so far and may have extended over 1000 km into the Paleocene Pacific (text -fig. 9). This implies a westward migration of *Ranikothalia* populations, most easily explained by LBF that survived attached to floating seaweed or wood (Adams 1967). The South American Caribbean margin was at equatorial latitudes allowing an important branch of the Atlantic equatorial current to connect with the Pacific equatorial current system, without significant obstruction of the young Middle American arc (text-fig. 9). This connection could have been an important migration route of LBF from the Eastern Hemisphere via the Caribbean margin of South America (occurrences in Trinidad and Venezuela) into the Pacific realm. The Middle American island arc (e.g. Barra Honda, Burica) and the East Pacific seamounts (e.g. Quepos) may have served as "stepping stones".

On the other hand, migration from eastern N-America to Europe via the North Atlantic gyre (Ly and Anglada 1991) seems to be documented by the occurrence of LBF as far north as the Newfoundland Grand Banks. Urquhart et al. (2007) reported the presence of LB, including *Ranikothalia* with Caribbean affinities at Site 1276 (Cores 210-1276A-13R through 9R) which are reworked into Lower-Middle Eocene sediments. These authors suppose shallow-water carbonate platforms to have existed on the southeastern Grand Banks, Newfoundland Seamounts, or southern Flemish Cap during the latest Paleocene and early Eocene. They relate these occurrences with high sea level and global warmth, shifting paleobiogeographic boundaries much further north by a proto-Gulf Stream probably crossing the offshore Newfoundland region.

SYSTEMATIC PALEONTOLOGY

The main purpose of this chapter is to analyse populations of *Ranikothalia* sp. both in *in situ* shallow-water deposits of the Barra Honda Platform and the Río Palo Blanco outcrops, as well as from resedimented limestones found in the context of accreted oceanic seamounts/plateaus. The Barra Honda Platforms contains LBF both in calm-water micritic bioclastic limestones and in higher energy coralgal pack-and grainstones. Delicate morphotypes of *Ranikothalia* occur in the calm-water facies and commonly as fragments in redeposited material. Ro-

bust, thick-walled forms occur in the well- washed higher energy *in situ* microfacies, as well as in often hydrodynamically sorted redeposited calciturbidites and debris flows of Herradura, Quepos, Osa and Burica Peninsulas. Redeposited material may represent a mixture of calm-water (restricted or off shore) and high energy assemblages. During the Late Paleocene, resedimentation is penecontemporaneous, since the redeposited material is usually accompanied by planktonic foraminifera indicating a Thanetian (to earliest Ypresian) age. On the other hand, clearly reworked lithoclast containing Paleocene assemblages occur in Lower to Middle Eocene debris flows in the Burica Peninsula (text-fig. 7). We have measured principally axial sections of about 150 specimens in thin sections oriented perpendicular to bedding from all localities (text-fig. 8). Except for the calm-water microfacies of Barra Honda, all samples show a similar range of morphotypes plotted with different symbols in text-figure 8. There is a morphologic *continuum* between thin-shelled flat and thick-shelled rounded-lenticular macrospheric forms on one hand and the range of much larger flat thin-shelled to sturdy microspheric forms, that are all considered to belong to the same species group here called *Ranikothalia catenula* group. However, detailed morphotypic description in conjunction with facies analysis may reveal that shape and shell thickness of the *Ranikothalia catenula* group is controlled by paleo-environmental conditions. Therefore, we subdivide the observed *continuum* of sizes and thickness/diameter ratios into macro- and microspheric morphotypes and relate them to some of the previously described species, which we treat here at a subspecies level. It is beyond the purpose of this chapter to review the relationships between *Ranikothalia* spp. of the Western and the Eastern Hemispheres. Much more work on topotypic material for each realm, and the physical stratigraphic superposition of morphotypes recovered from continuous sections will be necessary to compare the two realms and to establish a more detailed worldwide biochronology and paleo-ecology for *Ranikothalia*.

Orthophragminids, essentially *Neodiscocyclina* sp., co-occur in the higher energy and the redeposited material. They are listed here without further detail. A more in-depth study of this group is necessary.

Order FORAMINIFERIDA Eichwald 1830
Suborder ROTALIINA Delage and Horouard 1896
Superfamily NUMMULITACEA de Blainville 1825
Family NUMMULITIDAE de Blainville 1825

Genus ***Ranikothalia*** Caudri 1944, emend. Hottinger 1977a, **emend.**
Type species: *Nummulites nuttalli* Davies 1927.

Ranikothalia n. gen. - CAUDRI 1944, p. 10.
Ranikothalia (*Nummulitoides*) n. subgen. – ABRARD 1955, p. 489.
Nummulites (*Chordoperculinoides*) n. subgen. – ARNI 1965b, p. 26.
Sindulites n. gen. – EAMES 1968, p. 435.
Ranikothalia Caudri – HOTTINGER 1977a, p. 10. – BUTTERLIN 1981, p. 30. – CAUDRI 1996, p. 1181.
Caudrina n. gen. – HAYNES et al. 2010, p. 37.

Generic diagnosis: Caudri (1944, p. 17): "-... the following characteristics which can be even much more readily recognized in most sections because they are independent from the state of preservation: 1. The bluntly rounded chamber tops in equatorial section. 2. The thickness of the coarsely gutted supplementary skeleton as compared with the majority of other Nummulitids."

Hottinger 1977a (compilation and translation by the authors): "Chambers planispiral, involute or evolute, as with subfamiliy, coarsely perforate. Supplementary stolons simple, comparatively rare, disposed irregularly on unfolded, thick septa. Coarsely calibrated canal system. Meshes of marginal canal network relatively short and coarse. Plexus connecting interseptal with marginal canals radially directed. This structure creates the rounded shape of chambers towards the margin, seen in equatorial section. Sutural canals simple and vertical, opening out in alternating rows at the margin of the imperforate sutural band."

Intraseptal canals have evident bifurcations radial prolongations into the well-developed marginal chord. In axial section, these coarse radial canals form a fan-like structure that diverges from the apex of the chamber. Canals ramify distally to form a coarse irregular meshwork (Blondeau 1972), seen especially in large chords with a bulbous section of adult microspheric forms. The prominent (inflated) marginal chord develops during the growth of one whorl. It may, therefore, be invisible on one apex of axial sections cutting recently grown chambers. Once it becomes recovered by the next whorl it stops growing and is preserved.

Remarks: The generic definition of *Ranikothalia* is herein emended, because Caudri (1944) did not provide a detailed description and differential diagnosis of generic criteria for this genus. In the following, Cole (1960, 1969a) regarded *Ranikothalia* as a synonym of *Camerina*. Hottinger (1977a) analysed the canal system of operculinid LBF and came to the conclusion that the species attributed to *Ranikothalia* shared common and unique features of their canal system, that is intermediate in complexity between that of Late Cretaceous Sulcoperculinidae and that of Tertiary *Operculina* species. We have compiled the generic characteristics of the canal system from Hottinger (1977) and added criteria observed by Blondeau (1972) and our own criteria observable in CL observation of polished thin sections.

In accordance with Hottinger (1977a) and Caudri (1990 1996) we regard the subgenera *Nummulitoides* Abrard (1956) and *Chordoperculinoides* Arni (1965) as synonyms of *Ranikothalia*. Haynes et al. (2010) reject Hottinger's generic criteria based on the canal system, because "of their limited use to micropaleontologists dealing with fossil material". Instead, Haynes et al. (2010) erect the new genus *Caudrina* to accommodate quasi-evolute to sub-evolute forms, whereas *Ranikothalia* and *Chordoperculinoides* are considered by them as involute forms, distinguished from each other only by the coarseness of the vertical canals/perforation. According to this classification, *Caudrina* (*C. soldadensis*) and *Ranikothalia* (*R. nutalli*) would be monospecific and *Chordoperculinoides* would be represented by two species (*C. bermudezi* and *C. sahnii*). Additionally, an evolutionary descent from *Ranikothalia* to *Chordoperculinoides* during the late Selandian/early Thanetian (P4a) is suggested without any supporting evidence.

In contrast to such a classification we can state:

1. The degree of involute vs. evolute growth is related to ontogeny: only the largest, discoidal forms (*R. catenula soldadensis*) representing full-grown, microspheric forms (Caudri 1996), may become sub-evolute in their late ontogenetic stages. All other forms of the *Ranikothalia catenula* group (see below) are involute.

2. The criteria used for the differentiation of the above genera are, at best, specific or even intraspecific, distinguishing megalospheric from microspheric forms. Sachs (1957: p. 107-113) studied a large suite of topotypes of *Ranikothalia bermudezi* (Palmer), in which he demonstrated by measurements and series of illustrations of extenal views and thin sections, the variation that occurs among specimens of one population. Moreover, he was able to show conclusively that a number of species proposed by Hanzawa (1937, *R. antillea*), Barker (1939), de Cizancourt (1948; 1951), Vaughan and Cole (1941, *R. tobleri, R. soldadensis*), Vaughan (1945), and Cole and Herrick (1953, *R. georgianus*) are synonyms of *Ranikothalia bermudezi*. However, at that time Sachs could not analyse *Ranikothalia catenula* Cushman and Jarvis, because topotypic material was not available. After Cole (1969a) published several axial and equatorial sections of topotypic material, we prefer to use the name *catenula* for this group, since this specific name has priority. Some other arguments to do so will be discussed under the species group.

3. Until now there are no biostratigraphic data available in the Western Hemisphere that would allow the establishment of a sequence of first and last appearances of several species of *Ranikothalia*.

Ranikothalia catenula (Cushman and Jarvis) group
Plates 2 - 7

Here we give the principal synonymy of original and subsequent descriptions that reflect our concept of this group. A more detailed differential synonymy will be given under each morphotype treated here as subspecies.

Operculina catenula nov. sp. CUSHMAN and JARVIS 1932, p. 42, pl. 2, fig. 13. Herein: pl. 2., figs. 1-2.
Operculina bermudezi nov. sp. PALMER 1934, p.2 38, pl. 12, figs. 3, 6–9. Herein: pl. 1, figs, 16-20.
Pellatispirella antillea nov. sp. HANZAWA 1937, p. 116, pl. 20, figs 8-10, pl. 21, fig. 1. Herein: pl. 1, fug. 9.
Miscellanea tobleri nov. sp. VAUGHAN and COLE 1941, p. 35, pl. 4, figs. 5-7, pl. 7, fig. 1 (same specimen as pl. 4, fig. 5, herein: pl. 2, figs. 10-12.
Miscellanea antillea (Hanzawa) VAUGHAN and COLE 1941, p. 33, pl. 4, figs. 1-2, pl. 6, figs. 3, 3a. – VAUGHAN 1945, p. 27, pl.3, figs. 1-10, pl. 4., fig.1.
Miscellanea sp. cf. *M. antillea* (Hanzawa) VAUGHAN and COLE 1941, p. 33, pl. 4, figs. 3-4.
Miscellanea soldadensis nov. sp.. VAUGHAN and COLE 1941, p. 36, pl. 4, figs. 8-9. – VAUGHAN 1945, p. 29, pl. 5, figs. 2-5.
Miscellanea sp. VAUGHAN 1945 p. 29, pl. 4, figs. 2-5, (3-4, tangential sections microspheric form, 5, *R. catenula*)
Nummulites (*Operculinoides*) *bermudezi* (Palmer) DE CIZANCOURT 1948, p. 27, pl. 1, figs. 1-5. Herein: pl 2, figs.7-9.
Nummulites (*Operculinoides*) *catenula* (Cushman and Jarvis) DE CIZANCOURT 1948, p. 25, pl. 3, figs.17- 24, herein: Pl. 2, figs. 1-6.
Ranikothalia antillea (Hanzawa) CAUDRI 1944, p. 372, pl. 30, figs. 4-5, pl. 32, figs. 15, pl. 33, figs. 19-21, pl. 34, figs. 23, 25. – CAUDRI 1975, p. 539, pl. 1, figs. 5-7, pl. 2, figs. 2-3, 5, pl. 6, figs. 4-6. – CAUDRI 1996, p. 1183, pl. 5, figs. 1-2.
Ranikothalia tobleri (Vaughan and Cole) CAUDRI 1944, p. 372, pl.3 4, fig. 22,
Ranikothalia soldadensis (Vaughan and Cole) CAUDRI 1944, p. 372, pl. 33, fig. 19, pl. 34, fig. 26. – CAUDRI 1975, p. 539; pl. 1, figs. 1, 4; pl. 2, figs. 1, 6, 8; pl. 6, figs. 1, 3; pl. 7, figs. 1-5; p. l.8, figs. 1-3. – VICEDO et al. 2014, p. 58, figs. 14 A-H.

PLATE 1
All images by Claudia Baumgartner-Mora and Peter O. Baumgartner

1-2 Top of the Barra Honda Formation, at "Teresita" limestone quarry, 4 km E of the town center of Nicoya, Costa Rica. Fig. 1. The topmost cherty, white Barra Honda limestones (Upper Paleocene) are overlain by a 30-60 cm thick tuffaceous (glauconitic?) layer, followed by the base of the red, cherty Zapotal Member (Lower Eocene). This sharp contact may represent the Paleocene/Eocene boundary (see text). Scale bar = 30 cm. Fig. 2. Alternations of white and grey (tuffaceous) limestone of the uppermost Barra Honda Formation exposed in the quarry. Hammer measures 45 cm.

3 Aerial view of the Cerro Barra Honda (lower centre, looking towards SE) and other hills with their typical flat-toped karst morphology. In the background the Cerro Jesus, made of basaltic basement of the Manzanillo Terrane.

4 Polymict breccia of the Punta Quepos Chaotic Formation, N end of Playa Espadilla, Quepos. Sheared angular boulders of *Ranikothalia*-bearing limestone breccias set in a dark green siliceous mudstone matrix along with volcanic sandstone boulders (dismembered turbidites). Scale bar = 10 cm.

5 Siliceous pelagic limestones interbedded with arc-derived tuff layers, Pavones Formation (Late Paleocene), Playa Mangle, Burica Peninsula. These limestones are located upsection from the basal contact with the basaltic basement and pockets of *Ranikothalia*-bearing limestone breccias (pl. 7, fig. 1).

6 Rhodoid rudstone, uppermost headwaters of Río Palo Blanco, Burica Peninsula, Panama. Basaltic basement clasts (left) are encrusted by Melobesiae. This rock represents most probably an in situ carbonate shoal. Hammer grip measures 15 cm.

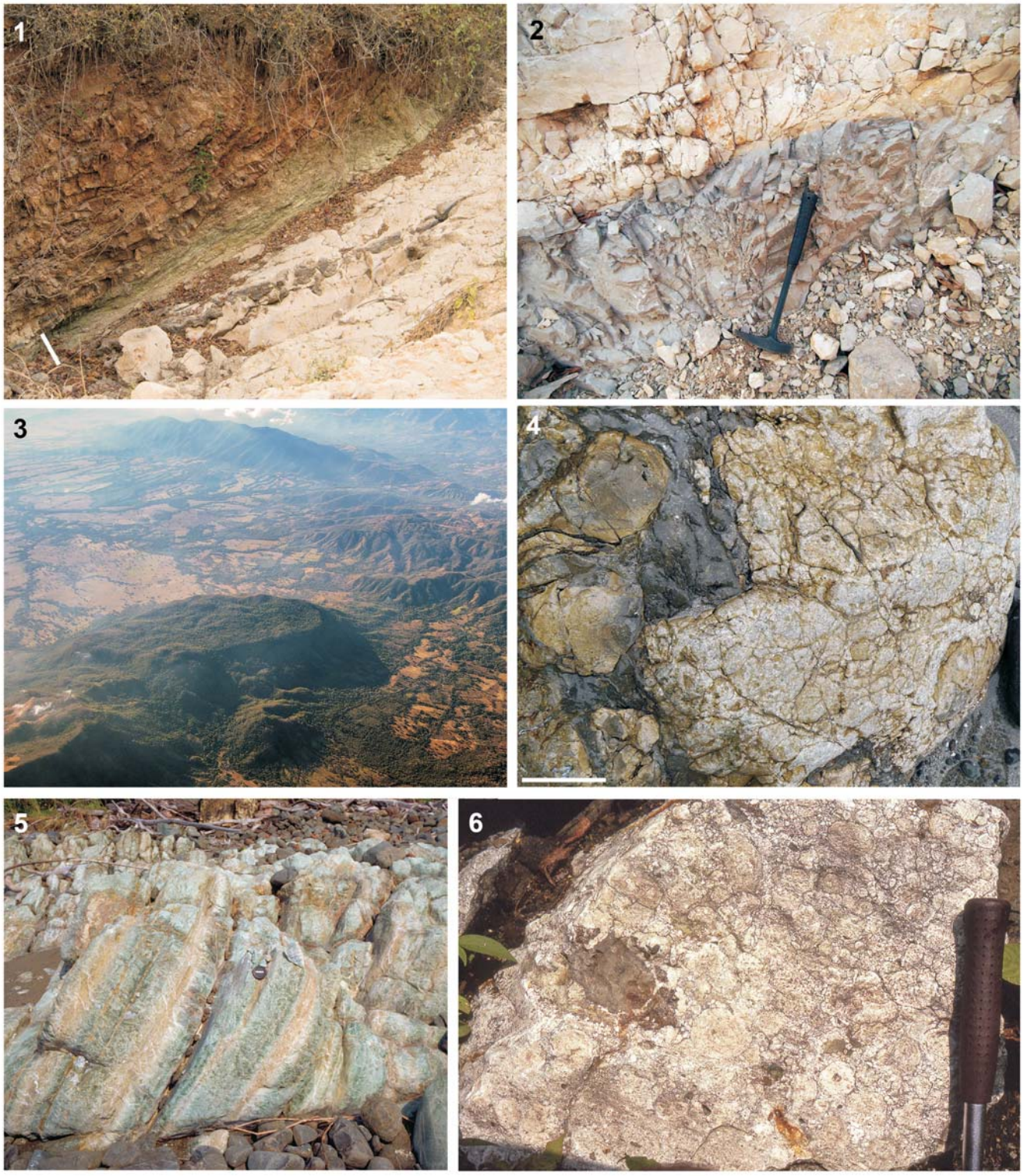
1
2
3
4
5
6

Operculinoides georgianus nov. sp. COLE and DERRICK 1953, 52-54, pI. 4, figs. 1-21; pI. 5, figs. 1-3.
Operculinoides bermudezi (Palmer) SACHS 1956, p. 107. pl. 14, figs. 1-27.
Camerina catenula (Cushman and Jarvis) COLE 1960, p. 192-193, pl. 25, fig. 3, 6, pl. 26, fig. 1, pl. 25, fig. 6, pl. 26, fig. 1 from Maerki's sample 102b III, pit at Lizard Springs, Trinidad. – COLE 1969a, p.78, pl. 17, fig. 1-4, 6, 8, topotypes from Maerki's sample 102b III, pit at Lizard Springs, Trinidad.
Ranikothaila bermudezi (Palmer) BUTTERLIN 1981, pl. 9, figs. 1-3. – SERRA-KIEL. et al. 2007, p. 377, pl. 3, figs. 5-7. – VICEDO et al. 2013, p. 179, figs. 8, 1-5, figs. 15, A-F.
Ranikothalia catenula (Cushman and Jarvis) ROBINSON and WRIGHT 1993, p. 329, figs. 28.1-7.

Description: The following description is adapted from Sachs (1957, p. XX):

Megalospheric forms – "Test involute lenticular, dimensions in our material from 1.15 to 5.4 mm. in diameter, 0.6 to 1.5 mm in thickness, with a diameter/thickness ratio of 1.3 to 3.6. The more compressed individuals have the greater diameter (text-fig. 8.). The periphery is variably rounded and occasionally slightly inflated. The axial periphery is marked by an elevated boss, which in corroded specimens appears to be made of a cluster of knobs which surround a larger central mass. Straight or slightly recurved sutures, which are sometimes beaded in weathered specimens, radiate from the umbonal cluster to the periphery. The surface between the sutures is smooth and finely perforate. Equatorial sections show 1.75 to 3.5 whorls with a total of 22 to 55 chambers in all whorls and 10 to 30 chambers in the final whorl. The chambers of the final whorl are higher than wide. The spiral wall is double, composed of a thick outer wall traversed by coarse radial canals, and a thin, denser inner wall. These walls are separated by a spiral canal approximately 5µm in diameter. The septa are straight or slightly recurved with double walls resulting from infolding and prolongation of the inner shell layer (PIate 7, figs. 15-20). As a result of this infolding, the spiral canal is bent inward with the inner shell layer to form a radial extension 5 to 10 µm in diameter running down the middle of each septum. The inner wall lines cover the entire chamber except in the zone of the marginal cord where the proximal chamber wall is formed by the outer margin of the preceding spiral wall. At this point, the infolding and prolongation of the inner layer forming the septa fall short of the base of the chamber by approximately 40 µm, thus forming the slitlike aperture directly above the marginal chord. The embryonic apparatus is bilocular, either with both chambers subspherical or with the second slightly compressed, separated by a straight or nearly straight wall.

Axial sections show the regions on both sides of the embryonic apparatus to be occupied by axial plugs, which are separated into wedge-shaped segments by a series of radiating canals. The peripheral marginal cord is generally well developed, and is composed of numerous radiating wedge-shaped masses separated by coarse canals which extend from the outer surface to a point approximately 3/4 of the distance to the inner surface. The development of the marginal chord appers to be dependent upon the size of the individual, as larger specimens have better developed cords than do smaller ones. The development of the marginal cord seems to occur during the formation of successive chambers of an entire whorl until it becomes covered by the next whorl. This explains why axial sections have often a poorly developed marginal cord on one extremity. The wall of the test between the marginal cord and axial plug is pierced by numerous fine straight radiating pores which appear to open on both the exterior and interior surfaces of the wall."

Microspheric forms - The test is more or less compressed lenticular to flat discoidal with an axial boss. The margin is distinctly more inflated and more broadly rounded than in megalospheric forms, reflecting the highly developed marginal cord in the last, and especially the outermost whorls. In some cases, the devel-

---

PLATE 2

Type material of American *Ranikothalia* spp. From the literature, except Fig. 15 re-photographed from the collection of the Naturhistorisches Museum Basel (NHMB). Scale bar = 2 mm for all figures.

1-2 "*Operculina catenula*" (= *Ranikothalia catenula catenula*) Cushman and Jarvis 1932, p. 42, pl. 12, fig. 13 a, b, holotype.

3-8 "*Operculina catenula*" Cole, 1969, pl. 17, Figs. 1-4, 6, 8, topotypes. Figs. 3, 5. = *Ranikothalia catenula antillea*, Figs. 4, 6-8. = *Ranikothalia catenula catenula.*

9 "*Pellatispirella*" *antillea* (= *Ranikothalia catenula antillea*) Hanzawa, 1937, p. 116, pl. 20, fig.8, holotype.

10-12 "*Miscellanea*" *tobleri* (= *Ranikothalia catenula tobleri*) Vaughan and Cole 1941, p. 35 pl. 4, figs. 5-7, cotypes.

13-14 "*Miscellanea*" *soldadoensis* (= *Ranikothalia catenula soldadensis*) Vaughan and Cole, p. 36, pl. 4, figs. 8-9, holotype.

15 *Rantikothalia soldadensis (= Ranikothalia catenula soldadensis*) (Vaughan and Cole) Caudri, 1975, pl. 7 fig. 1, axial section of B-form, rock thin section from sample Rz. 248, erratic limestone block originated from the Paleocene, Soldado Rock, Trinidad, West Indies. figured in Caudri 1975. Pl. 7, figs. 1-4. Re-photographed from NMB no. C 31227.

16-20 "*Operculina*" *bermudezi* (= *Ranikothalia catenula bermudezi*) Palmer, p. 238, pl. 12, figs. 3, 6–9, cotypes. Fig. 16 is probably *Ranikothalia catenula soldadensis* in our terminology.

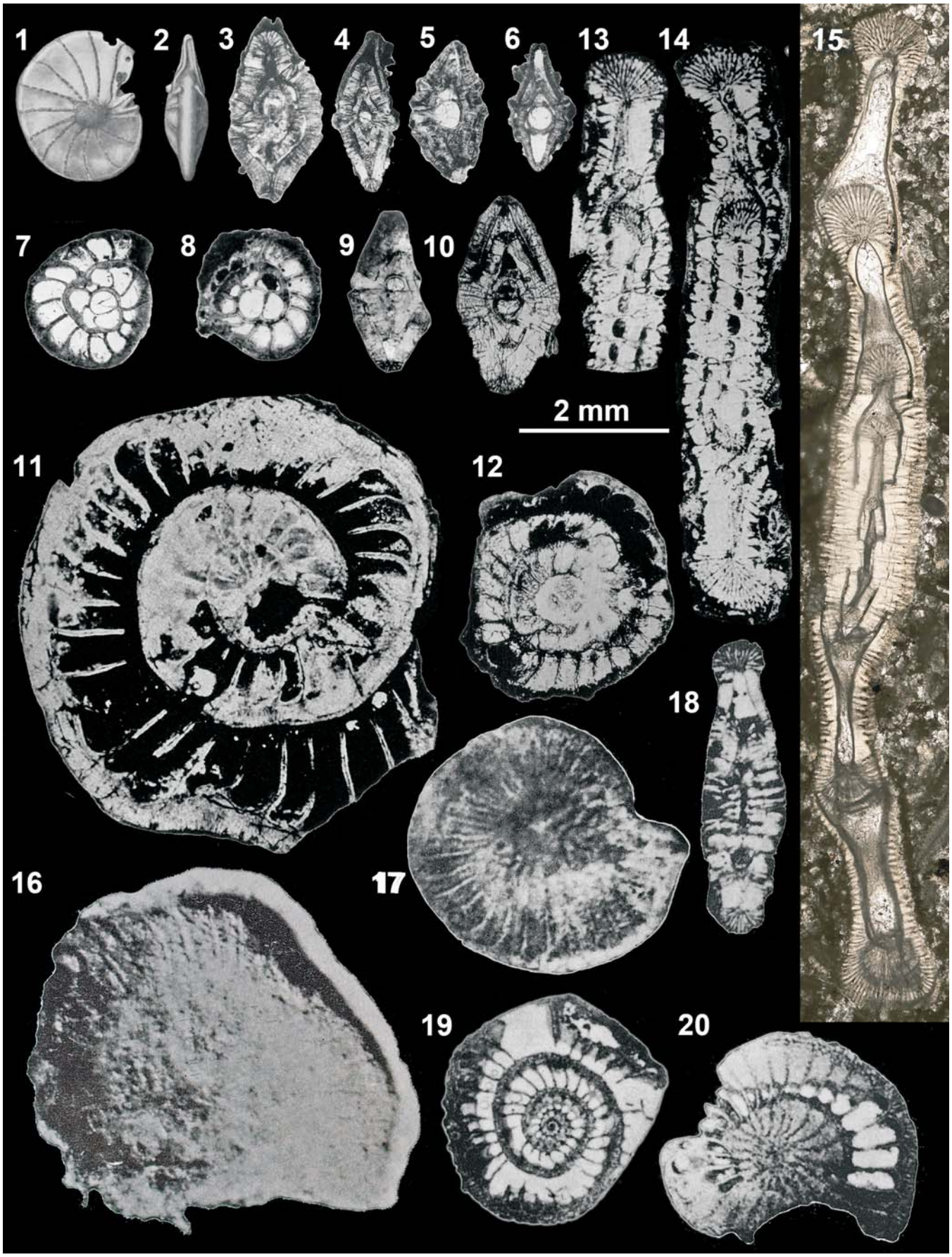
1
2
3
4
5
6
13
14
15
7
8
9
10
2 mm
11
12
18
16
17
19
20

opment of this feature is such that its trace may be seen externally as it revolves around the margins of the inner whorls (plate 2, fig. 9). Dimensions of microspheric specimens in our material range from 3.3 to 8.8 mm. in diameter and from 0.6 to 1.5 mm in thickness, with a diameter/thickness ratio of 3 to 8.6. The lower values of diameter and diameter/thickness correspond to measurements of subaxial rather than strictly axial sections. A maximum diameter of 12 mm has been reported by Palmer (1934, p. 239). In equatorial section, 3.5 to 5 whorls are present with a total of 40 to 65 chambers in all whorls and 20 to 30 chambers in the final whorl. Axial sections show the highly developed marginal cord, composed of wedges of shell material separated by coarse radial canals opening to the exterior. These canals extend inward to a point approximately 1/6 of the distance from the inner margin of the spiral wall where they are met by numerous fine radial canals. These fine canals penetrate the entire thickness of the lateral wall in the region between the marginal cord and the axial plug in the same manner as in the megalospheric generation.

Remarks: The status of several species of the Caribbean representatives of the genus *Ranikothalia* has been a subject of a long debate. Sachs (1957) presented biometrical data to show that there is a gradual transition between several previously described species, which were therefore considered as synonymous. These taxa are *Operculina bermudezi* (Palmer 1934), *Pellatispirella antillea* (Hanzawa 1937), *Miscellanea tobleri* (Vaughan and Cole 1941), *Miscellanea soldadensis* (Vaughan and Cole 1941) and *Operculinoides georgianus* (Cole and Herrick 1953). Additional species described by de Cizancourt (1948) under the genus *Nummulites* from the Paleogene of Barbados could be synonymous. Drooger (1960) also was in favour of this large synonymy, like Robinson and Wright (1993), who considered *Operculina catenula* (Cushman and Jarvis), *Pellatispirella antillea* (Hanzawa,), and *Miscellanea tobleri* (Vaughan and Cole) as synonymous. Caudri (1996) writes: "I am in favour of calling the Caribbean species *Ranikothalia catenula* (Cushman and Jarvis), still listing its three morphological varieties "*antillea*", "*tobleri*" and "*soldadensis*", as I have done in my paper on Soldado Rock (Caudri 1975) ". Hitherto, this interpretation of the fossil record has been generally accepted, since all of the above mentioned taxa have recently been considered synonyms of *Ranikothalia bermudezi* (Palmer) by Vicedo et al. (2013) or of *R. soldadensis* (Vaughan and Cole) by Vicedo et al. (2014). We have discussed the alleged differences between these species put forward by these authors under "biostratigraphy" above.

While the small lenticular, more or less robust macrospheric forms attributed variably to *R. catenula, R, antillea* or *R. tobleri* are present in many assemblages described in the literature, it is important to note that Sachs (1957), in his revision of topotypes of *R. bermudezi* (Palmer) does not illustrate large flat, discoidal microspheric forms close to the holotype of *R. soldadensis* (Vaughan and Cole), although this species appears in his synonymy. On the other hand, Caudri (1975, 1996) does not mention, nor illustrate large lenticular microspheric morphotypes that would be close to the holotype of *R. bermudezi* (Palmer). Hence, we have to deal with several macrospheric and microspheric morphotypes that show clear differences in their

---

PLATE 3

Published material of American *Ranikothalia* spp. re-photographed from the collection of the Naturhistorisches Museum Basel (NHMB). Scale bar = 2 mm for all figures except Figs. 4 and 9 = 4 mm.

1-6 *R. catenula* group (Cushman and Jarvis), tagged as "*Nummulites* (*Operculinoides*) *catenula*" in the de Cizancourt collection. Figs. 1-2. *Ranikothalia catenula antillea*, Fig 1. External view (unpublished). Fig. 2. Same specimen, equatorial section obtained by spliting. A-form from sample Senn S. 34c, NHMB, no. C 29533, figured in de Cizancourt 1948, pl. 2, fig. 18. Fig. 3. *Ranikothalia catenula tobleri* B-form from sample Senn S. 34c, NMB, no. C 29535, figured in de Cizancourt 1948, pl. 2, fig. 23. Fig. 4. *R. catenula bernudezi*, B-form, from sample Senn S. 101, NMB, no. C 29538, figured in de Cizancourt 1948, pl. 2, fig. 22. Fig. 5. *R. catenula tobleri*, B-form, from sample Senn S. 34c NMB, no. C 29536, figured in de Cizancourt 1948, pl. 2, fig. 21. Fig.6, *R. catenula antillea*, A-form, from sample Senn S. 34c NMB, no. C 29535, figured in de Cizancourt 1948, pl. 2, fig. 19.

7-9 *R. catenula soldadensis* (Palmer) tagged as "*Nummulites* (*Operculinoides*) *bermudezi*" in the de Cisancourt collection. Fig. 7. B-form from sample Senn S. 80, NMB, no. C 29503. Figured in de Cizancourt 1948, pl. 1, fig. 5. Fig. 8. B-form from sample Senn S. 110, NMB, no. C 29499, figured in de Cizancourt 1948, pl.1, fig.1. Fig. 9. B-form from sample Senn S. 101, NMB, no. C 29500 figured in de Cizancourt 1948, pl. 1, fig. 2.

10-15 *R. catenula antillea*, A-forms. Figs. 10-12. Sample H.G. Kugler K. 2951. Figs. 13-15. Sample H.G. Kugler K.2951, NMB, no. C 31140. Fig. 13. Illustrated in Caudri 1975 pl.6, fig. 6. Figs. 14-15 unpublished.

16 *R. catenula soldadensis*, coll. Kugler, K. 2951 B, NMB, no C 31168, figured in Caudri 1975, pl. 8, fig. 1-2.

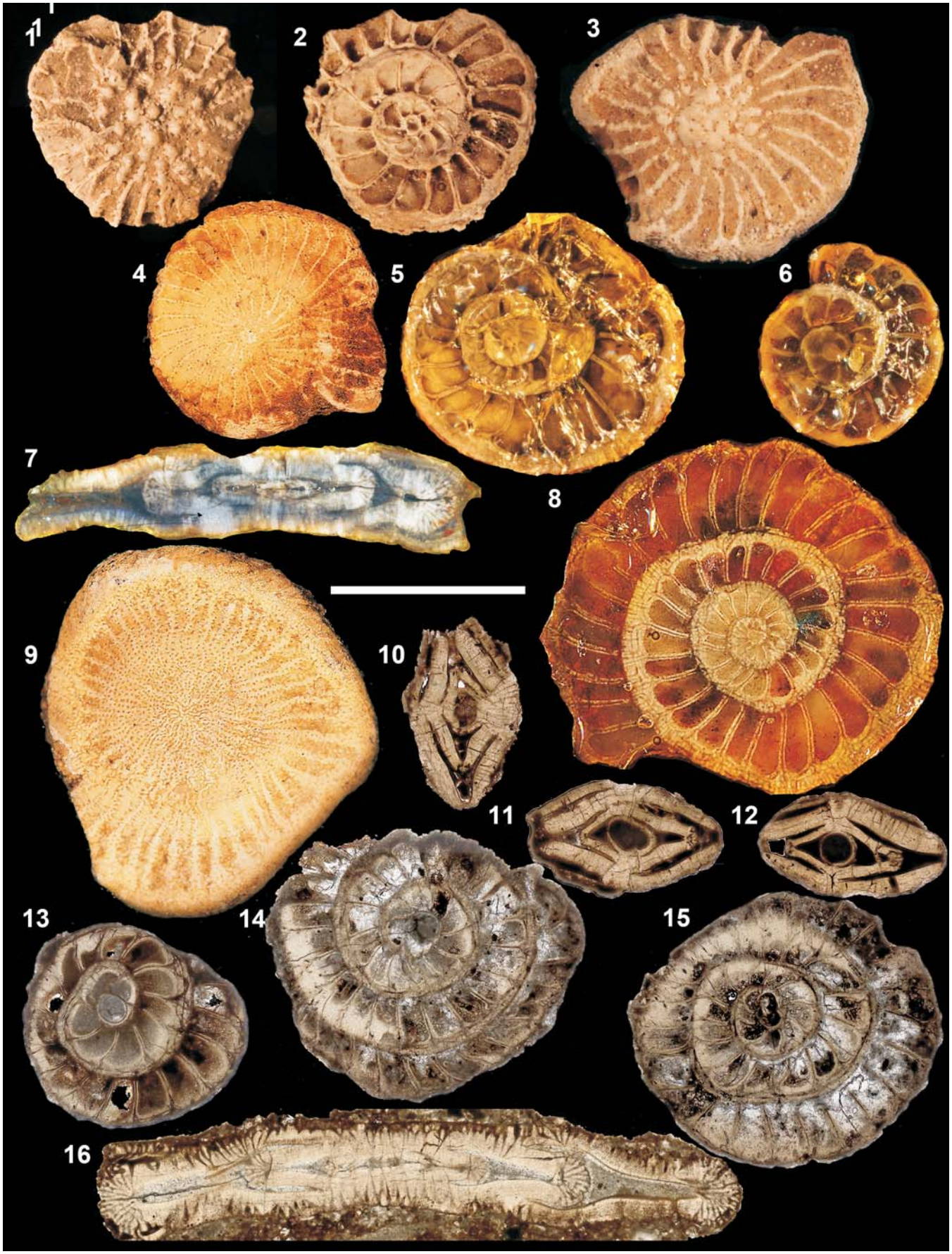
1
2
3
4
5
6
7
8
9
10
11
12
13
14
15
16

early ontogenetic stages, which may be controlled by the paleo-environment (see remarks under the respective subspecies), and therefore, lacking from some assemblages.

The range of morphotypes shown by Sachs (1957, Plate 14) from Cuba corresponds to what we find in our assemblages, with some modifications: In addition, we found morphotypes matching *Ranikothalia catenula soldadenis* in all samples. We did not find typical morphotypes matching *R. c. bermudezi* in the calm-shallow-water Barra Honda limestone. These findings will be commented under remarks of the respective subspecies. Our morphometric analysis (text-fig. 8) is based on over 100 axial sections of macrospheric and about 50 axial sections of microspheric forms from all studied localities, of which most macrospheric forms show the embryonic apparatus, whereas the microspheric forms are mostly subaxial sections. Unfortunately, we have only few equatorial sections of macrospheric forms (plates 4-7). We find a morphologic *continuum* similar to that of Sachs (1957). We conceive, that this series of morphotypes could belong to the same biological species (see also Caudri 1975, p. 539), treated here as *Ranikothalia catenula* group. In accordance with Caudri (1990) all these forms should be included by priority with *R. catenula* (Cushman and Jarvis 1932). This is possible, since Cole (1960, 1969) illustrated both axial and equatorial sections of topotypic material of *R. catenula* (see plate 2, figs. 3-8 herein).

Synonymies under this group contain only the original species descriptions and some references to work that shares the species group concept proposed here. In our material the most abundant morphotypes are the small, more or less robust, more or less thickly lenticular macrospheric forms that form a morphological *continuum* fitting between the original descriptions of *R. c. catenula, R. c. antillea* and *R. c. tobleri* (text-fig. 8, plates 4-5, 7). The large flat discoidal microspheric forms with strongly inflated marginal chord are less abundant but often preserved as fragments of the typical marginal chord (plate 4, figs. 3-4), they are here grouped under *R. catenula soldadensis*. Large, thick shelled, lenticular microspheric morphotypes are rare in our material, their proportions come close to the holotype of *R. bermudezi,* though some are somewhat smaller. They are grouped here as *R. catenula bermudezi.*

Geographic distribution: Belize, Costa Rica, W-Panama (Tempisque, Herradura, Quepos, Osa, Burica) Cuba, Dominican Republic, Haiti, Mexico (Campeche, Chiapas,), Trinidad (Soldado Rock, Paradise Gate, Lizard Springs, Venezuela (Los Morros).

Chronostratigraphic range: Costa Rica, W-Panama: Late Paleocene-?earliest Eocene (mid Selandian – Thanetian, ?earliest Ypresian), Mexico: to Ypresian (according to Buttelin 1981).

PLATE 4

LBF and microfacies of the Barra Honda Limestone, Tempisque Basin, Costa Rica. Scale bar = 2 mm, except Figs. 9-12, 15 = l00 µm. Figs. 1-3, 4, 5-8, 11, 13, 14, 16, 17. transmitted light thin section scans. 4a, 10, cathodoluminescence microscopy, 9, 15, transmitted light microscopy,11, SEM. The following samples are from Cerro Espiritu Santo, N-Tempisque: Figs. 2, 6-7, 14: Sample 1534-03. Fig. 3: Sample Santo 02. Fig. 1, 4-5, 8, 11, 13, 16 – 17: Sample 1533-01.

1 Part of axial section of *Ranikothalia catenula soldadensis* B-form. Note the lateral compression of the last whorls.

2 Subaxial section of a juvenile *R. catenula soldadensis* (or transitional form to *R. c. bermudezi*?) with a newly formed chamber at bottom. Note absence of coarse marginal chord in the first whorl.

3,5 Axial and subequatorial sections of *R. c. antillea* A-form and a marginal chord fragment of *R. c. soldadensis* (Fig. 3, lower right). *Distichoplax biserialis* and geniculate corraline algae in the matrix.

4-4a *R. catenula soldadensis*, fragment of inflated marginal chord in axial section. Note thick branching radial canals originating at the apex of the chamber lumen and several peripheral marginal canals filled with brighter cements in CL. Scale bar = 0.5 mm.

6-7 *R. catenula catenula*, A-form. Note flat lenticular shape and thin shell.

8,16 Axial sections of *R. catenula antillea*, corroded specimens.

9-10 *Morozovella velascoensis*, Fig. 9. Sample 8-2D (Jaccard et al. 2001), Cerro Alto Viejo, N-Tempisque. Fig. 10. Sample CM1532.

11-13 Fragments of *Distichoplax biserialis*, a common *microproblematicum* (red or green alga?). Fig. 12 is a polished and slightly etched surface under the SEM, Sample JM6, Cerro Guayacán.

14 *Neodiscocyclina grimsdalei*, microspheric form scale bar =0.5 mm.

15 *Polystrata alba*, Sample 23.8 (Jaccard et al. 2001).

17 Melobesian-*Polystrata* bafflestone, Espiritu Santo, Sample CM1533. Po.: *Polystrata alba*, Sp.: *Sporolithon*, m.c.: intraclast of a stained microbial crust, several oblique sections of *R. catenula antillea*, abundant bioclasts of geniculate coralline algae and *Distichoplax biserialis*.

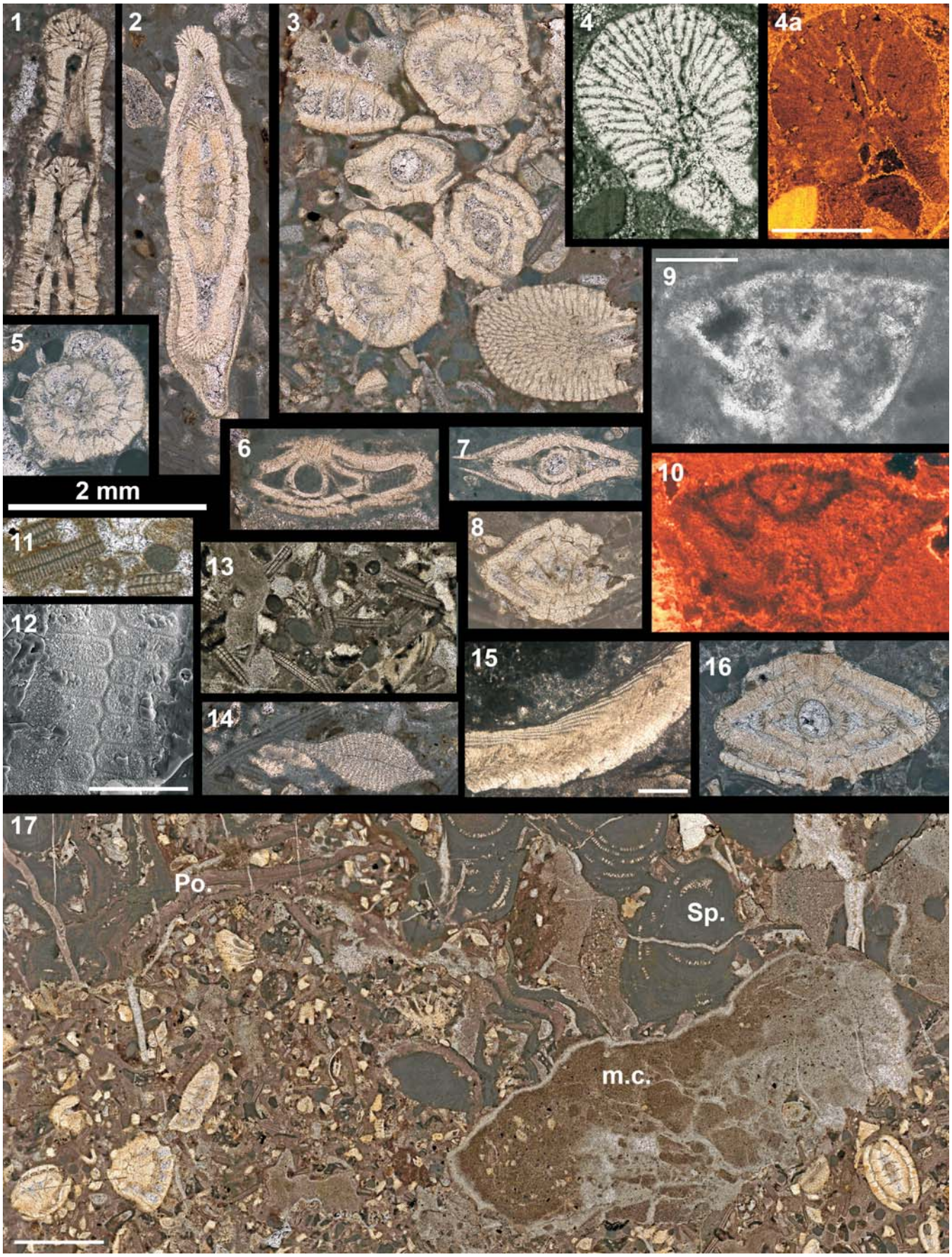
1
2
3
4
4a
5
9
6
7
2 mm
10
8
11
13
12
15
16
14
17
Po.
Sp.
m.c.

Ranikothalia catenula catenula (Cushman and Jarvis) 1932
Plate 2, figures 1-2, 4. 6-8. Plate 4, figures 6-7. Plate 6, figures 4, 14. Plate 7, figure 8.

Operculina catenula nov. sp. - CUSHMAN and JARVIS 1932, p. 42, pl. 12, fig. 13.
Miscellanea antillea (Hanzawa) VAUGHAN 1945, p. 27, pl. 4, fig. 5
Operculinoides georgianus nov. sp. - COLE et HERRICK, pars 1953, p. 52, pl. 1, figs. 1-7, 10-12, 14-21 Non fig. 8-9.
Ranikothalia tobleri (Hanzawa) – CAUDRI, pars 1996, p. 1183, pl. 9, fig. 5.

Diagnosis: Macrospheric involute form. Test small, thin-walled, flat lenticular, with 2.5-3 whorls, large spherical proloculus. Diameter 1.1 - 2.5 mm, thickness 0.5 – 0.8 mm, diameter/thickness ratio: mostly 2.4-4.0.

Differential diagnosis: This subspecies is in morphologic continuity with *R. catenula antillea* (as defined below), which is thicker and rounder lenticular (*bord obtus*) and thick-walled, and with *R. catenula tobleri*, which is larger and has more whorls.

Original description: (Cushman and Jarvis 1932, p. 42, based on an uncut specimen): "Test broadly complanate, periphery rounded, greatest thickness in the umbonal region; chambers distinct, about 15 in the last formed coil, of rather uniform shape and increasing somewhat in length as added; sutures distinct, limbate, raised, ornamented by numerous beadlike protuberances which are slightly elongate in the line of the suture, sutures ending in the umbonal region in a distinct boss which itself is somewhat beaded; wall between the sutures smooth. Diameter, 2.25 mm; thickness, 0.6 mm."

Diameter/thickness ratio is 3.75.

Remarks: This is the smallest and most fragile morphotype, which is present in calm water wackestones of the Barra Honda Platform. It is rare in the redeposited limestones of the oceanic islands. It could represent a calm water macrospheric form.

Ranikothalia catenula antillea (Hanzawa 1937)
Plate 2, figures 3-5, 9
Plate 3, figures 1-2, 6, 10-15
Plate 4, figures 3, 5, 8, 16-17
Plate 5, figures 1-2, 9-10
Plate 6, figures 2, 8-9, 13
Plate 7, figures 2-3, 4, 6-7, 10-12, 16-20

Pellatispirella antillea nov. sp. HANZAWA 1937, p. 116, pl. 20, figs. 8-10; pl. 21, fig.1.
Miscellanea antillea (Hanzawa) VAUGHAN and COLE 1941, p. 33, pl. 4, figs. 1-4, pl. 6, figs. 3, 3a. – VAUGHAN 1945, p. 27, pl. 3, figs.1-10, pl. 4, fig. 1. – COLE and BERMUDEZ 1947, p. 195, pl. 15, figs. 1-10.
Ranikothalia antillea (Hanzawa) CAUDRI 1944, p. 372, pl. 30, figs. 4-5, pl. 32, fig. 15, pl. 33, fig. 21, pl. 34, figs. 23, 25. – CAUDRI 1948, pl. 74, fig. 3. – CAUDRI 1975, p.539, pl. 1, fig. 5-7, pl. 2, figs. 2, 3, 5, pl. 6, figs.4-6. – CAUDRI 1996 p. 1183, pl. 5, figs. 1-2., pl. 9, fig. 8
Nummulites (Nummulites) senni nov.sp. DE CIZANCOURT 1948, p. 19, pl. x, figs. 13-17.
Operculinoides georgianus nov. sp. COLE and HERRICK 1953, p. 52 pl. 1, fig. 13.
Operculinoides bermudezi (D.K. Palmer) SACHS 1957, p. 107, pl. 14, figs. 13-17, 20.
Operculina catenula Cushman and Jarvis BUTTERLIN 1960, pl. 2, figs. 1-5.
Camerina catenula (Cushman and Jarvis) - COLE 1969a, p. 78, pl. 17, figs. 1-4, 6, 8.

PLATE 5

Transmitted light thin section scans of LBF, and microfacies of Upper Paleocene redeposited carbonates from Quepos (CM806, Playa Macha Sur,) and Río Cañas (OA), Herradura. Scale bar for all figures = 2 mm, except Fig. 19, = 250 µm.

1-2 Axial sections of *Ranikothalia catenula antillea*, A-form, abraded margin. Sample OA 65.2

3,6 Axial sections of *R. catenula bermudezi*, massive, high energy, B-form. Fig. 3. Sample OA 64BB, Fig. 6. Sample OA 64-15.

4 Subaxial section of *R. catenula soldadensis*, delicate B-form, probably deeper/lower energy form. Sample OA 65CC,

5 *R. catenula tobleri*, tightly coiled, probably shallow/high energy, B-form. Sample CM 806.

7-8,11 Axial sections of *R. catenula tobleri* (?) A-forms. Sample CM 806.

9-10 Equatorial sections of *R. c. antillea*. Sample OA 65-02.

12 *Neodiscocyclina* sp. Sample OA 63.

13 *Neodiscocyclina barkeri*, Sample CM 806.

14-15 *Neodiscocyclina* sp. Fig. 14. oblique section, Fig. 15. partial equatorial section. Sample CM 806.

16 *Neodiscocyclina barkeri*, Sample QC15.2, Quebrada Camaronera, Quepos.

17 *Neodiscocyclina weaveri*, Sample CM 806.

18 Size-sorted and oriented *R. catenula* group, *Neodiscocyclina* sp. and geniculate corallines in a redeposited calcarenite, Sample QC15.2.

19 Pelagic lithoclast in redeposited limestone breccia with *Morozovella velascoensis* (top right) and globigerinids. Sample Esp 084, N-end of Playa Espadilla, Quepos.


1
2
3
4
5
6
7
8
9
10
11
12
13
14
15
16
17
18
19
2 mm

Ranikothalia catenula (Cushman and Jarvis) ROBINSON and WRIGHT 1993, p. 329, pl. 28, figs.1-7.
Ranikothaila bermudezi (Palmer) SERRA-KIEL, J. et al. *pars* 2007 pl. 3, figs.5, 6, non pl.3. fig.7. – VICEDO et al. pars 2013 p.179, figs 8, 1-4, non 5.
Chordoperculinoides bermudezi (Palmer) HAYNES et al., *pars* 2010 p. 40, pl. 2, figs.1–4, non 5-6.
Ranikothalia soldadensis (Vaughan and Cole) VICEDO et al. pars 2014 p. 58, figs. 14 C-H non A-B, figs. 15 A-E, non F, figs. 16 A-C, non D-I.

Diagnosis: Macrospheric involute form. Test small, thick-walled, inflated lenticular, with 2.5-3 whorls, large spherical proloculus. Diameter 1.1 - 2.5 mm, thickness 0.8 - 1.2 mm, diameter/thickness ratio: mostly 1.8-2.3. Smaller forms tend to be thicker.

Differential diagnosis: This subspecies is in morphologic continuity with *R. catenula catenula* (as defined above), which is flatter and thin-walled, and with *R. catenula tobleri*, which is slightly larger and flatter, and has more whorls.

Original description (Hanzawa 1937, p. 116): "Test, thick, lenticular, attaining 2.5 mm in diameter and 1.2 mm in thickness, but usually 2 mm in diameter and 1.2 mm in thickness; involute, consist of two and half or sometimes three whorls; several conical plugs developed on both sides of the umbilical regions; proloculum spherical or ellipsoidal, 230 to 290 µm or 230 x 320 µm in diameter, surrounded by a thick wall 15 to 30 µm thick; spiral laminae of the first and second whorls thick, attaining 228 µm in thickness, that of the last whorl thinner, 75 µm thick; whorls divided into chambers by radial, straight double septa; number of chambers 7 to 8 in the first whorl, 14 to 15 in the second whorl, and 7 to 20 in the last whorl; spiral laminae in general finely perforated in places by thick vertical pores (7 µm in diameter), which usually open on both the upper and lower surface of the spiral laminae, but sometimes closed near the bottom of the ordinary finely perforated walls so as to make a double-layered lamina, as in *P. matleyi* (Vaughan); straight vertical canals well developed in umbonal region around compact conical plugs; marginal cord showing characteristic features as already mentioned; apertures multiple along the base of the septa The specimens examined are all megalospheric."

Remarks: *R. catenula antillea* is a small, thickly rounded lenticular, thick-walled morphotype, very abundant in our material, especially in allochthonous assemblages, probably due to hydrodynamic sorting sorting (Aigner 1985). It is also present in higher energy shallow facies of Barra Honda and Río Palo Verde (Panama). It could represent a shallow, higher energy-resistant form.

Ranikothalia catenula tobleri (Vaughan and Cole 1941)
Plate 2, figs. 10-12. Plate 3, figs.3, 5. Plate 5. figs. 5, 7-8, 11. Plate 6, figs. 3. 16. Plate 7, figs. 9, 13

PLATE 6

1 *Ranikothalia catenula soldadensis*, B-form, sample K 2951 B, coll. H. Kugler, re-photographed from NMB no. C 31170, illustrated in Caudri 1975, pl. 6, fig. 3, pl. 7, fig. 5. Scale bar=4 mm.

2-15 – Transmitted light thin section scans of LBF, and microfacies of Upper Paleocene redeposited carbonates from Río Cañas, Herradura (OA), Playa Mangle, Burica Peninsula, Costa Rica, and Río Palo Blanco, Burica Peninsula, Panama. Scale bar for all figures = 2 mm.

2 *R. catenula antillea*, A-form, axial section. Sample CM 324, Playa Mangle Burica.

3 *R. catenula tobleri*, A-form, axial section. Sample CM 324, Playa Mangle.

4 *R. catenula catenula*, A-form, axial section. Sample CM 324, Playa Mangle.

5 *Paleonummulites* sp. Sample CM 324.9, Playa Mangle.

6-7 *R. catenula*, parts of equatorial sections showing interseptal to marginal canal system and arched chamber periphery. Sample CM 324.9, Playa Mangle, Burica.

8-9 *R. catenula antillea*, tangential equatorial sections showing slightly curved separate and coarse interseptal – marginal canal system. Sample CM 324, Playa Mangle, Burica.

10 *R. catenula soldadensis*, full grown delicate, deeper/calm water B-form. Sample OA65CC, Río Cañas, Herradura

11 Two peri-axial sections of *R. catenula soldadensis*, B-form and axial sections fo R. catenula antillea, A-forms in bioclastic packstone with rhodophycean fragments, Neodiscocyclina and other fragment sample OA65CC, Río Cañas, Herradura.

12-15 – Sample CM 924.1, Rio Palo Blanco, Panama.

12 *R. catenula bermudezi* B-form. Note thick test and saucer-shaped broadly rounded outline probably a shallow/high energy form.

13 Axial section of *R. catenula soldadensis*, B-form and oblique section of *R. catenula*, A-form.

14 Subaxial section of *Discocylina weaveri*, and axial section of *R. catenula catenula*, A-form.

15 Axial section of thick *R. catenula tobleri*.

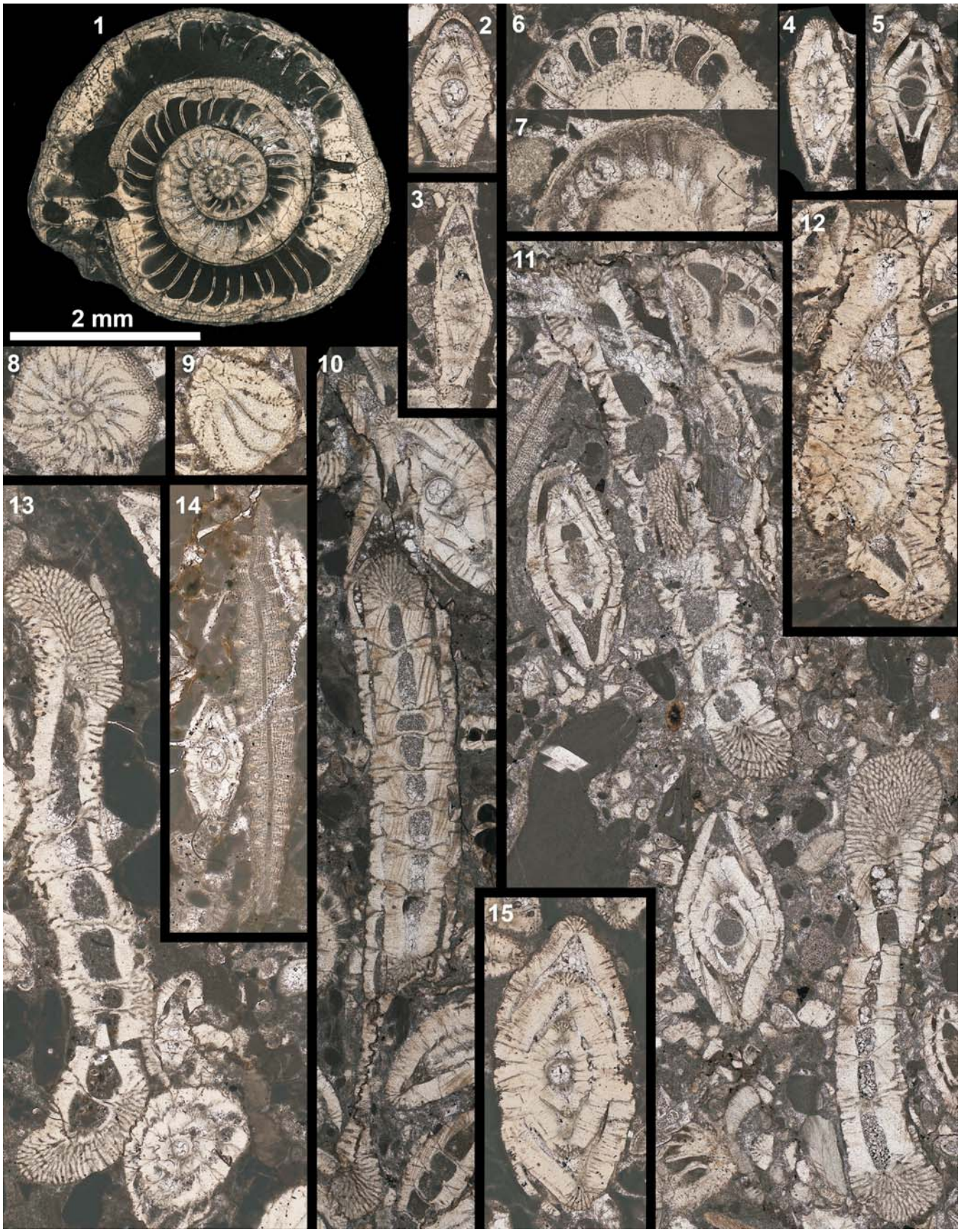
1
2 mm
2
3
4
5
6
7
8
9
10
11
12
13
14
15

Miscellanea tobleri n. sp. VAUGHAN and COLE 1941 p. 35, pl.4, fig. 5-7, pl. 7, fig. 1(same specimen as pl.4, fig. 5.
Ranikothalia tobleri (Vaughan and Cole) CAUDRI 1975, pl. 1, fig. 2-3, pl. 2, fig. 4, 7. pl6. Fig. 2. – CAUDRI 1975, Pl. 1, fig. 2-3, pl. 2, fig. 4, 7. Pl6. Fig. 2 – CAUDRI, pars 1996, p. 1183, pl.5, fig 1-2, pl. 9, fig. 2, 4, non 5.
Camerina catenula (Cushman and Jarvis) COLE 1960, p.192-193, pl. 25, fig. 6.
Operculina catenula (Cushman & Jarvis) BUTTERLIN and BONET, pars 1960, p. 11., pl. 2, fig. 5.
Ranikothalia cf. *antillea* (Hanzawa) SCHMIDT-EFFING ?1979, fig. 32.
Ranikothaila bermudezi (Palmer) BUTTERLIN, pars 1981, pl.9, fig. 2. non fig. 1.
Ranikothalia soldadensis (Vaughan and Cole) VICEDO et al. pars 2014, p. 58, figs. 15 F.

Diagnosis: Macrospheric and small microspheric involute forms. Macrospheric forms small, thick- walled, flat lenticular or rhomboid in axial section, with 3.5-4 whorls, large spherical proloculus. Diameter 2.7 – 4.9 mm, thickness 1 - 1.6 mm, diameter/thickness ratio: mostly 2-4. Microspheric forms thick-walled lenticular to rhomboid in axial section. At least 4 whorls. Diameter 4.5 – 6.3 mm, thickness 1.4 – 1-6 mm, diameter/thickness ratio: 2 – 4.

Differential diagnosis: This macrospheric forms are in morphologic continuity with *R. catenula antillea* (as defined above) which is smaller and thicker, and has less whorls. The microsperic form is transitional to small forms of *R. c. bermudezi*, which is marginally more rounded with a sturdier marginal chord and a broad central boss, which gives it a saucer-shaped form.

Remarks: This subspecies includes the largest macrospheric and the smallest microspheric forms, both are thick-shelled, probably adapted to higher water energy.

Ranikothalia catenula bermudezi *(*Palmer 1934)
Plate 2, figs. 16-20?, Plate 4, fig. 2, Plate 5 figs. 3, 6, Plate 6, fig. 12

Operculina bermudezi nov. sp. PALMER 1934, p. 238, pl. 12, figs 3, 6-9.

Miscellanea bermudezi (Palmer) COLE 1947, p. 235–236, pl. 3, fig. 12.
Nummulites (Operculinoides) bermudezi (Palmer) DE CIZANCOURT 1948, 27, pl. 1, fig 1–6.
Operculinoides bermudezi (Palmer) COLE 1953a, p. 35–37, pl. 1, figs 5–7; pl. 3, fig 2–12. – SACHS pars 1957, pl. 14, fig. 21, ?22.
Ranikothalia bermudezi (Palmer) NAGAPPA 1959, pl. 23, fig. 5-6. – BUTTERLIN and MONOD 1969, p. 595, pl. 2, fig. 1-2. – VICEDO et al. pars 2013, p. 179, fig. 8, 5.
Chordoperculinoides bermudezi (Palmer) HAYNES et al. pars 2010, p.40, pl. 2, fig. 5-6, non 1-4.

PLATE 7

1 Outcrop at Playa Mangle. Altered basalt penetrated by sedimentary dykes, overlain by pockets of resedimented Paleocene shallow limestone breccias, in turn overlain by greenish – reddish pelagic marls and siliceous pelagic limestones (after sand cover in the upper left corner, see Pl. 1, Fig. 4).

2-19 – Transmitted light thin section scans (fig. 4, 12), photomicrographs (figs. 6, 8, 10, 14, 16) and cathodoluminescence (CL) micrographs (figs. 2, 3, 5, 7, 9, 11, 13, 15, 17-19) of LBF, and microfacies of Upper Paleocene redeposited carbonates from Playa Mangle, Burica Peninsula and Playa Macha Sur, Quepos.

2 Oblique axial section of *Ranikothalia catenula antillea*, CL. The well preserved internal structure of test is visualized by a darker lining (early cements?) between the lamellae. The imperforate pillars connect to the surficial sutural bands. Sample CM 324.2, Playa Mangle, scale bar = 400 µm.

3,5-6, 9-11 *R. catenula antillea* A-form, Figs. 3, 5, 9, 11. CL. Note thick lenticular shape, thick walls, large proloculus. Figs. 5-6. Sample CM 324.4, Figs. 3, 9-10. Sample GDM 92-41, Río Palo Blanco, W-Panama, Scale bar in Fig. 3 = 1 mm. Fig. 11. Oblique section with micropore and lamellar systems visualized in CL.

4 Current-oriented and size-sorted *Ranikothalia* spp. Upper left: *R. catenula catenula* A-form, middle right: probably B-form. Sample CM 324.02, scale bar = 2 mm.

7 *R. catenula catenula*, A-form. Note flat lenticular form with thin walls. Probably a deeper/calmer water morphotype.

8,12 *R. catenula tobleri*, A-form, Fig. 8. polarized light, rhomboidal form with approximately 4 whorls, scale bar (Fig. 12) = 2 mm. Sample CM 324.03.

13-14 *Neodiscocyclina weaveri*, peri-axial section. Note dark intrinsic Cl (Fig. 13), surrounded by brightly luminescent corallinacean bioclasts. Sample GDM 92-41, Río Palo Blanco, W-Panama. Scale bar (Fig. 3) = 1 mm.

15-16 *R. catenula antillea*, detail of equatorial section showing plexus connecting interseptal canals to radial canals, Sample CM 316.01, Playa Mangle.Scale bar = 200µm.

17 *R. c. antillea*, thick-walled A-form, equatorial section, with only 2 whorls. Sample CM 314, Playa Mangle. Scale bar = 1 mm.

18-19 *R. c. antillea*, thick-walled A-form, equatorial section, with 2.5 whorls. Note well-preserved lamellar structure. Scale bar (Fig. 17) = 1 mm for Fig. 18, = 400 µm for Fig. 19. Sample CM 806, Playa Macha Sur, Quepos.

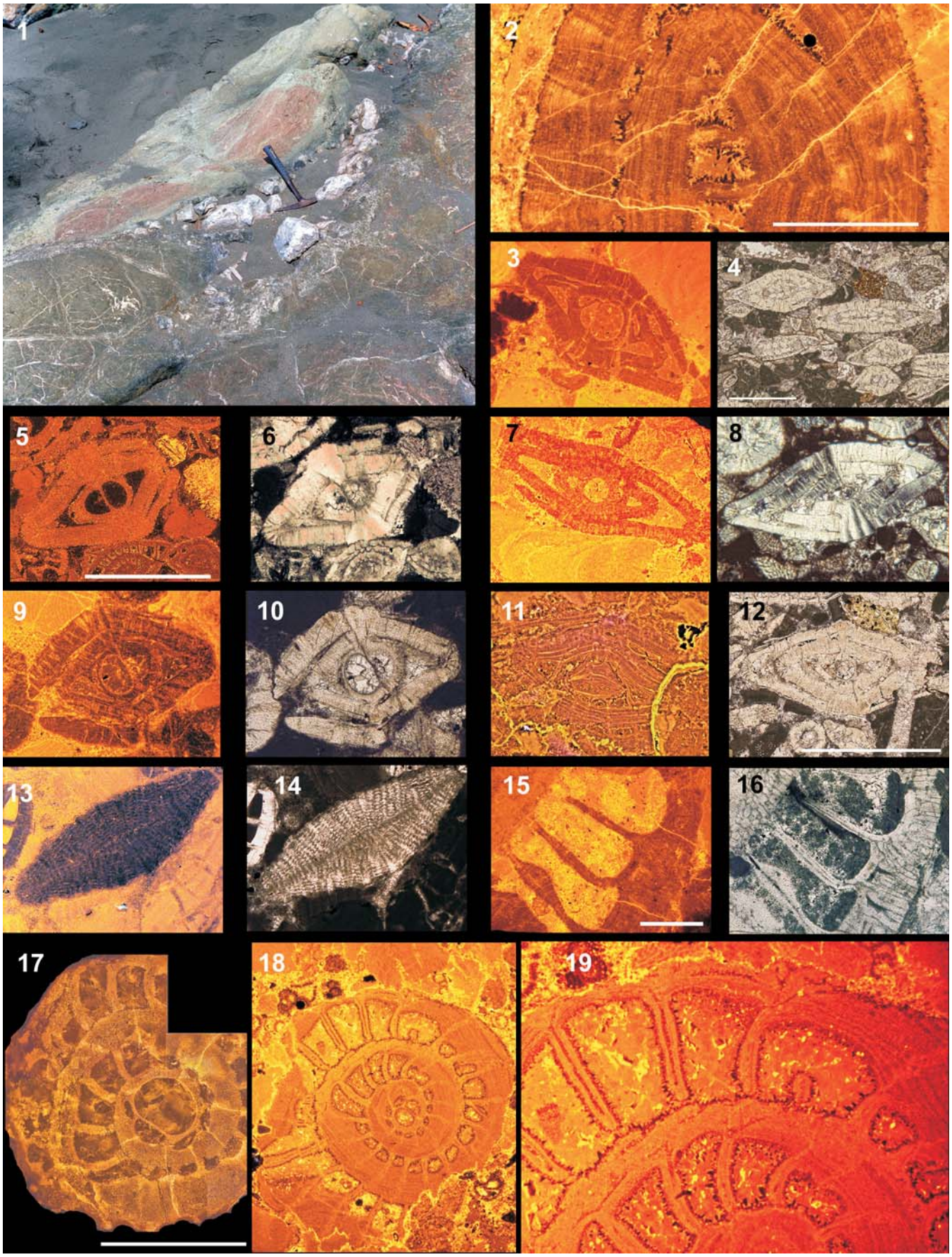
1
2
3
4
5
6
7
8
9
10
11
12
13
14
15
16
17
18
19

Diagnosis: Microspheric involute form. Test thick-walled, in axial section chamber lumen area is much smaller than test surface area. Outline bossed-lenticular, with sturdy inflated marginal chords. Slight or no lateral constriction between central bossed area and base of the marginal chord. Size variable, probably depending on habitat: Palmer (1934) average diameter: 5 mm, average thickness: 2 mm diameter up to 12 mm (may be *R. c. soldadensis*). Holotype (see Pl. 2, Fig. 18 herein): diameter: 4 mm, thickness: 1.13 mm. Very rare in our material: Diameter 4.4 -6.2 mm thickness 1.5 mm. Does not correspond to the evolute specimen of *R. sindensis* shown in Babazaded 2011.

Differential diagnosis: This subspecies is in morphologic continuity with *R. c. soldadensis*, which is distinguished by a flat discoidal shape, thinner test walls, delicate, sometimes subevolute second last and last whorls and marked lateral constrictions between the main body and the inflated marginal chord of the last whorls.

Original description: The following description is from Palmer (1934): "Test large, complanate, with prominent umbos and thickened, rounded periphery; smooth except for the tendency toward the development of papillae on the umbos and the spiral ridge marking the early margin. Worn specimens usually show the septa.

The horizontal section of an average-sized specimen (about 5 mm in diameter) shows 4 to 4.5 whorls with approximately 31 chambers in the final volution. The whorls increase regularly but gradually in width and the septa are very gently curved, almost radiate, with conspicuous intraseptal canals. In tangential horizontal section the branches of the intraseptal canals appear in two alternating rows along the suture line and the perforate structure of the test may be clearly seen. Furrows of the marginal chord are distinct. Aperture at base of septum. The vertical section shows the conspicuous development of the marginal chord and canals, the tendency toward the development of pillars in the umbonal region and the position of the aperture. Both megalospheric and microspheric forms have been found. The former is not common and in external characters may be distinguished only by its smaller size" (the megalospheric forms are here included in *R. c. tobleri*)

Remarks: This subspecies is rare in our material from the oceanic seamounts (Quepos, Herradura and Burica). It seems to be absent from the more restricted Barra Honda Limestone. It could represent a high energy/shallow morphotype as opposed to *R. c. soldadensis* which is larger, flatter and more delicate, probably restricted to deeper or calmer waters.

Ranikothalia catenula soldadensis (Vaughan and Cole 1941)
Plate 2, figs. 13-14, 15, ?16. Plate 3, figs. 7-9, 16. Plate 4, figs. 1-5. Plate 5, fig. 4. Plate 6, figs. 1, 10-11, 13.

Miscellanea soldadensis nov. sp. VAUGHAN and COLE 1941, p. 36, pl. 4, fig. 8-9. – VAUGHAN 1945, p.30, pl.5, fig.2-5.
Operculina catenula (Cushman and Jarvis) BUTTERLIN et BONET pars 1960, p. 11., pl. 2, fig. 4 ?fig. 3
Operculinoides georgianus nov. sp. COLE and HERRICK pars 1953, p. 52 pl. 2, fig. 1-2.
Ranikothalia soldadensis (Vaughan and Cole) BLONDEAU 1972, pl. 2, figs. 8-9. – CAUDRI 1975, p. 539; pl. 1, fig. 1,4; pl. 2, fig. 1, 6, 8; pl. 6, figs. 1,3; pl. 7; figs. 1-5, pl. 8, figs. 1-3. – Ranikothalia soldadensis (Vaughan and Cole) CAUDRI 1996, p. 1185, pl. 5, fig.4, pl. 9, fig. 1. – VICEDO et al. pars 2014, p. 58, figs. 14, A-B.
Ranikothalia cf. *soldadensis* (Vaughan and Cole) SCHMIDT-EFFING 1979, fig. 31.
Ranikothalia bermudezi (Palmer) BUTTERLIN pars 1981, pl. 9, fig. 1. non fig. 2-3.

Diagnosis: Microspheric form. Test thick-walled involute in early ontogeny, becoming thin-walled and sometimes subevolute in the last whorls. Overall shape discoidal, flat. Sometimes with small central boss. Significant lateral constrictions occur in the last whorls between the chamber wall built around the marginal chord of the previous whorl and the inflated chord of the last whorls (Pl.5 Fig.16-20). Size: Vaughan and Cole (1941): Diameter > 8 mm, thickness 1.25 mm. In our material: diameter 4.5 –8.8. mm (may include tangential sections not showing full diameter), thickness 0.8 – 1.4 mm. In resedimented

---

PLATE 8

Transmitted light thin section scans of orthophragminids and bryozoans from Playa Mangle, Burica Peninsula, Costa Rica. Scale bar = 1 mm. Sample CM 324.

1 Axial oblique sections of *Neodiscocyclina* sp. cf. *N. weaveri*. Sample CM 324.03.

2 Oblique section crossing the equatorial plane of *Neodiscocyclina* sp. cf. *N. barkeri*, showing the neanic equatorial chambers with a rectangular shape.

3-4 Tangential and longitudinal sections of bryozoan fragments.

5 Undulating equatorial patterns in *Neodiscocyclina* sp. cf. *N. bullbrooki*, the nepionic equatorial chambrs are completely recrystalized. Sample CM 324.09.

6 Partially equatorial section of *Neodiscocyclina weaveri*. Note the different dissolution in the border of the test. Sample CM 324.09.

7 Oblique section showing a reniform deuteroconch, the rossettes pattern is observed in the highest plane. Sample CM 324.09.

8 Fragment of equatorial section of orthophragminid. Sample CM 324.09.

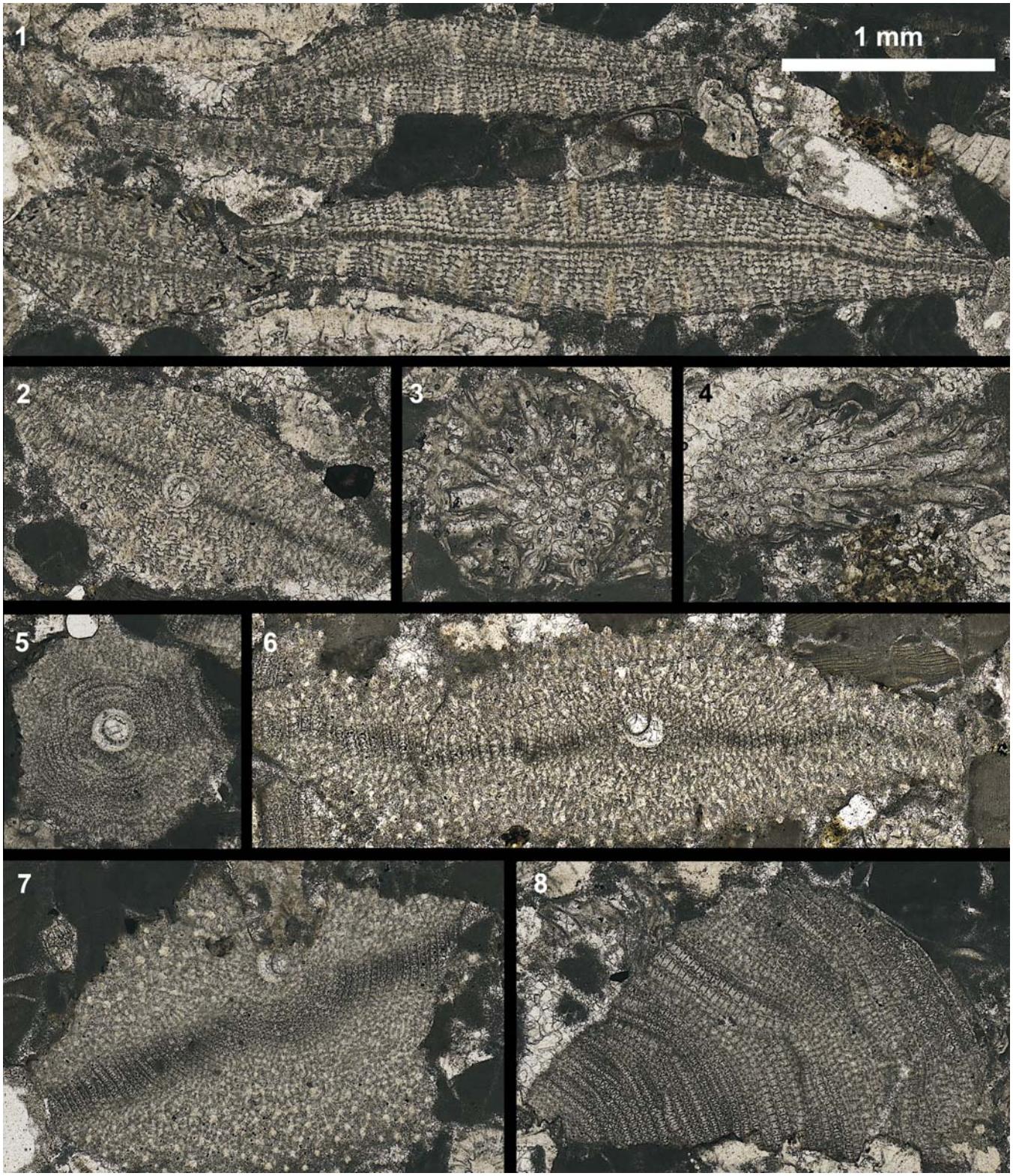
1
1 mm
2
3
4
5
6
7
8

limestones the inflated marginal chord is often present as fragments broken off at the delicate constrictions of the last whorls.

Differential diagnosis: Intermediate forms between this subspecies and *R. c. bermudezi* exist (Pl. 5, Fig. 3). This subspecies differs by its very flat discoidal shape and delicate, laterally constricted, sometimes subevolute last whorls.

Original description: Vaughan and Cole (1941) based on an axial section described this species as: "The test is discoidal, large more than 8 mm.in diameter, and 1.25 thick. It consists in more than two whorls of involute type. The chamber walls thick, 375 µm in thickness, usually finely perforated but in places penetrated by thick vertical canals, which, as their diameters increase toward the outer surface of the walls, are usually funnel-shaped in diameter vertical section, 30-75 µm in diameter. The marginal chords well developed and penetrated by vertical canals, 23 µm in diameter and marginal canals, 15 µm in diameter."

Remarks: This subspecies is the largest and most delicate of the *R. catenula* group. It could represent a deeper/calm water form which is rare in many samples of Soldado Rock (Caudri 1975, 1996), and seems to be absent from Palmer's sample from Cuba (see Sachs 1957, pl. 14), where the sturdy, high energy/shallow-water form *R.c. bermudezi* was described (compare also Sachs 1957, pl. 14. Figs, 21, 22).

Concluding remarks on Ranikothalia: The "thick" or "funnel shaped" vertical canals with a diameter of 30-75 µm" appear in the original descriptions, cited above, of *R. c. antillea*, *R. c. bermudezi* and *R. c. soldadensis*. They are believed to penetrate the chamber walls, in addition to the fine perforation. These structures appear in transmitted light (TL) microscopy as opaque zones and sometimes connect to a very dissected outer surface of the test (plate 2 fig. 16). On the surface of well-preserved specimens (plate2, figs. 4, 9) the sutural canals can be seen as stated in the generic definition of Hottinger (1977): "Sutural canals ... opening out in alternating rows at the margin of the imperforate sutural band". They have a diameter of about 20µm. In axial sections the sutural band is seen as an imperforate pillar-like structure, well visible under cathodoluminescence (CL, plate 7, fig. 2). In well preserved specimens, the fine perforations can be seen in CL thanks to the shallow excitation depth (<5µm), but the sutural canals are only occasionally visible (text-tig. 10). In transmitted light, thin sections may be too thick (30 µm) to resolve these fine structures. The dark to opaque fan-shaped patterns that appear in TL in most axial sections of *Ranikothalia,* not only at the sutures, are more likely to be the result of optical refraction between conically arranged calcite fibres of the imperforate sutural bands and parallel calcite fibres of the finely perforate wall (text-fig. 10). Any superposition of differently oriented calcite fibres may cause dark bands (like partially crossed Nicols) due to the high birefringency of calcite. Post mortem (bio-) corrosion and microboring of the perforate tests may enhance sutural canals and create the "funnel shaped" craters at the surface of large specimens (text-fig. 10c). These features cannot be used as diagnostic generiuc characters (e.g. "coarse vertical canals" in Haynes Racey and Whitacker 2010), since they are the result of calcite birefringency and post mortem modifications.

Superfamily ORBITOIDACEA
Family ORBITOCLYPEIDAE Brönnimann 1946
Genus *Neodiscocyclina* Caudri 1972
Type species: Discocyclina anconensis Barker 1932

Neodiscocyclina barkeri (Vaughan and Cole 1941)
Plate 5, figs. 13, 16?, Plate 8, fig. 2.

Discocyclina barkeri nov. sp. VAUGHAN and COLE 1941, pl. 18, fig. 4-7, pl. 21, figs. 1-2. – BUTTERLIN 1981, p. 49, pl. 26, fig. 5-7.
Discocyclina (*Discocyclina*) *barkeri* VAUGHAN 1945, p.18, pl. 6, fig.1-10.
Neodiscocyclina barkeri (Vaughan and Cole) CAUDRI 1975, p.550, pl. 3, fig. 7-9, pl. 14, fig. 1-4, 6- 10, pl. 23, fig. 1. – CAUDRI 1996, p.

PLATE 9

Transmitted light thin section scans of Upper Paleocene *Ranikothalia*- and *Neodiscocyclina*-bearing limestones from Costa Rica and Western Panama, Scale bar = 4 mm. For sample location, see table 1.

1, 2 – Barra Honda Limestone, Cerro Espiritu Santo, N-Tempisque (text-fig. 3)

1 Sample 1534-03, in situ low energy coralgal-LBF pack- to wackestone, delicate *Ranikothalia* gr. *catenula*, geniculate corallines, *Distichoplax biserialis*, small benthic foraminifera.

2 Sample Santo 02, in situ, rhodoid-*Polystrata* bafflestone. Polystrata alba is encrusting melobesian rhodoids (upper left and right), poorly preserved solenoporid alga in the center of a rhodoid (upper right). This facies contains predominantly small, robust *Ranikothalia catenula antillea* and fragments of *R. c. soldadensis*. Medium energy environment.

3 Sample CM 92-41, Rio Palo Blanco, Panama, *in situ*, well washed melobesian bafflestone to boundstone with LBF, mixed large discoidal and small thick lenticular forms: *R. catenula antillea*, *soldadensis, bermudezi* (rare), *Neodiscocyclina*, basalt lithoclasts from underlying basement. Probably an open marine shoal.

4 Sample QC 16, Quebrada Camaronera, Quepos. Melobesian-LBF rudstone. Contains almost exclusively *Neodiscocyclina* spp. Sample is from a limestone boulder in a debris flow of the Quepos Chaotic Formation.

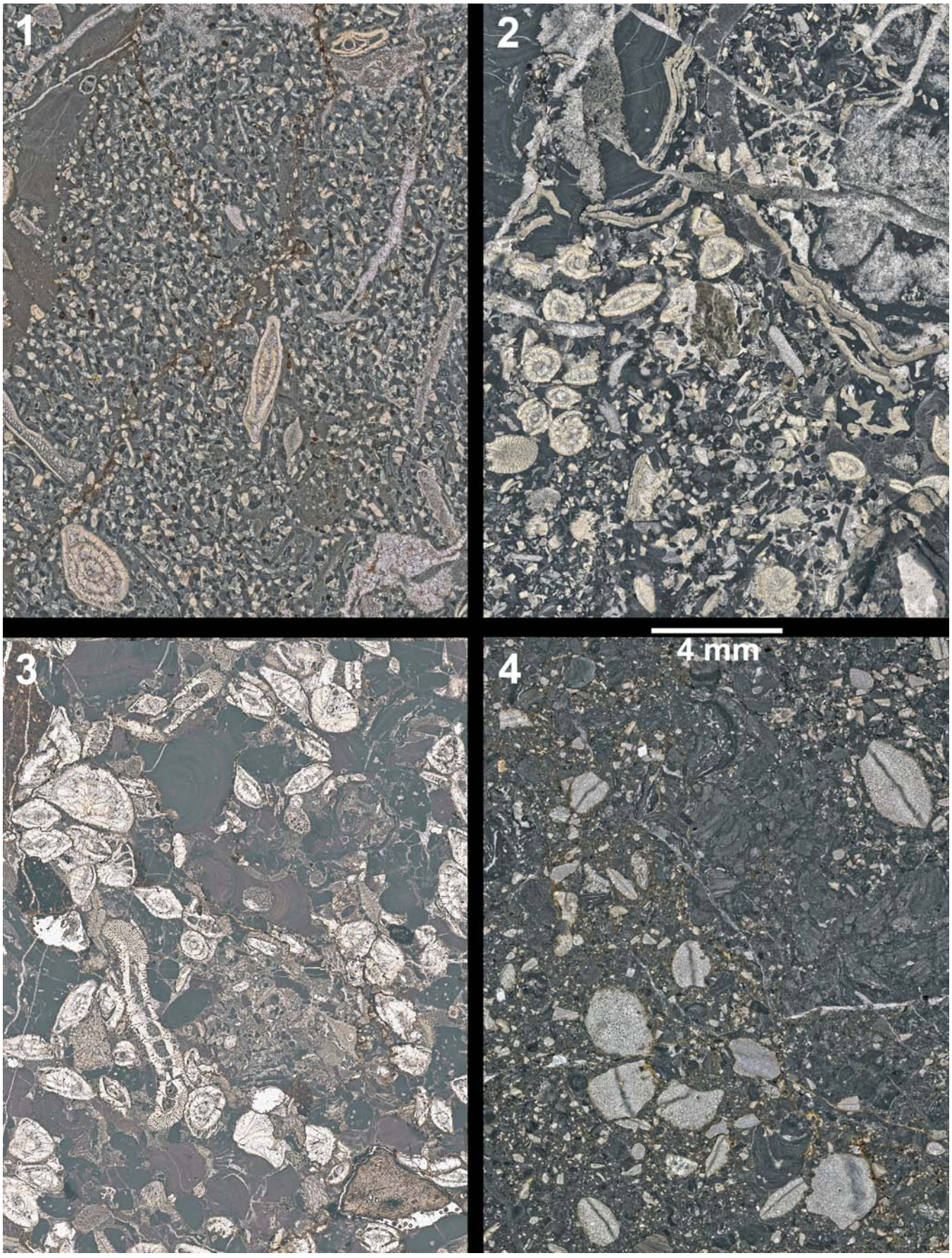
1
2
3
4
4 mm

1205, pl. 12, fig. 11, 16. – SERRA-KIEL et al. 2007, p. 380, pl. 3, g, h. 18-19, 21-23.

Remarks: thick shell, diameter/thickness = 1.8-2.5, size>2 mm, embryonic apparatus: 90-150 µn.

Neodiscocyclina weaveri (Vaughan 1929)
Plate 5, figs, 12, 17. Plate 6, fig. 14. Plate 7, figs. 14-15f Plate 8, fig. 1.

Discocyclina weaveri nov. sp. - VAUGHAN 1929, p. 5-7, pl. 1, figs. 1-2. – BUTTERLIN 1981, p. 50, pl. 26, fig. 1-2.
Discocyclina (*Discocyclina*) *weaveri* (Vaughan) COLE 1959, p. 384, pl. 33, figs. 3-5.

Remarks: test flat-lenticular, diameter/thickness = 2.5-6. Diameter = 1.5 – 4.3 mm.

Neodiscocyclina grimsdalei (Vaughan and Cole 1941)
Plate 4, fig. 14

Discocyclina grimsdalei nov. sp.- VAUGHAN and COLE 1941, p. 9, fig. 24-25, pl. 18, figs.8-9, pl.19 fig. 1-3; pl. 21, fig.3.
Neodiscocyclina grimsdalei (Vaughan and Cole). – CAUDRI 1975, p. 552, pl. 3, fig. 8, pl. 15, fig. 1-6, pl. 23, fig. 2. – CAUDRI 1996, p. 1203, pl. 12, fig. 7

Remarks: Test flat-lenticular, with a marked central depression, variable in size: 1.5 – 5 mm.

ACKNOWLEDGMENTS

We are indepted to Johannes Pignatti, Javier Escuder Viruete, and Karl Föllmi who reviewed this manuscript. Going back to the beginning of this work, we are thankful to Lukas Hottinger†. He passed us the foram virus with his enthusiasm and his enormous knowledge. Our thoughts are also with Jacques Butterlin† who determined foraminifera in our first thin sections back in 1983, now a precious part of our Caribbean LBF collection. We are also grateful to the late Bramine Caudri† for her invitations to tea in La Tour de Peilz, during her last years. Peter Jung from the Natural History Museum of Basel (NHMB) showed us his way of collecting paleontological samples during our fieldwork in Panama and Costa Rica. He opened us the doors of the Basel Museum and gave precious information from Senn's maps and drawings for field work in Barbados.

We share beautiful memories with many colleagues and friends doing fieldwork: Jorge Cortes, Percy Denyer, Marino Protti. Collaboration with Goran Andjic, Alexandre Bandini, Maximilian Bôle, David Buchs, Gianni DiMarco, Samuel Jaccard and Marc Münster was very fruitful.

We thank Michael Knappertsbusch (Natural History Museum Basel), for providing the loans of the LBF type collections and revising some of the planktonic foraminifera. We thank Raymond Ansermoz and Laurent Jacques Nicod for the high quality polishing of thin sections, and our librarian Catherine Schlegel Rey for great help searching old literature. We are thankful to Jan Kramers (University of Berne) Maximo Chiaradia (University of Geneva) for their dedication to our measurements on the multicollector ICPMS.

Equipment and part of the research was funded by the University of Lausanne, in particular the Fondation Herbette. This work was carried out in the frame of a succession of projects of the Swiss National Science Foundation (Project Numbers, 200020_162670, 200020_125130, 200020-116667, 200021-105845 and 200020_143894 all granted to P. O. B.). These projects provided funds for travel and laboratory analyses, as well as salaries for a number of PhD-students over the years.

REFERENCES

ABRARD, D., 1955. Une Operculine cordelée de l'Eocenè inférieur de la Côte-d'Ivoire. *Operculina (Nummulitoides) tessieri*, n. subgen., n. sp. *Bulletin de la Société géologique de France* (*série* 6), 5: 489–493.

ADAMS, C.G., 1967. Tertiary foraminifera in the Tethyan, American, and Indo-PacificProvinces. In: Adams, C.G. and Ager, D.V. *Aspects*

PLATE 10

Transmitted light scans of thin sections of Upper Paleocene *Ranikothalia*- and *Neodiscocyclina*-bearing limestones from Costa Rica, Scale bar = 4 mm. For sample location, see table 1.

1 Sample OA 64-6, Río Cañas, Fila Costeña, Costa Rica. LBF-coralgal rudstone, rather large, current sorted fraction. *Ranikothalia catenula* ssp.: *antillea, bermudezi, soldadensis*, geniculate corallines (20), oyster fragments, bryozoans. Bimodal grain size distribution: fine- grained "matrix" between larger bioclasts. Possibly a debris flow deposit.

2 Sample CM 806, Playa Macha Sur, Quepos. redeposidted melobesian-LBF rudstone with olivine reworked from seamount basement. Larger *Neodiscocyclina* spp. and *Ranikothalia* spp. Bimodal grain size distribution: granule-sized bioclasts in a lime-mudstone matrix, possibly a debris flow deposit reworked in the Quepos Chaotic Formation (text-fig. 6).

Figs 3, 4 – Sample CM 324, Playa Mangle, Burica Costa Rica (text-fig. 7). Allochthonous, current- sorted assemblages associated with pelagic sediments. Note fine grained, detrital soft lithoclasts of arc-derived material, deformed by compaction.

3 Thin section CM 324.02 cut at right angle to bedding, showing mostly axial sections in the well-oriented *Ranikothalia*- and *Neodiscocyclina*-bearing turbidite.

4 Thin section of same sample CM 324.09 cut parallel to bedding showing abundant equatorial sections.

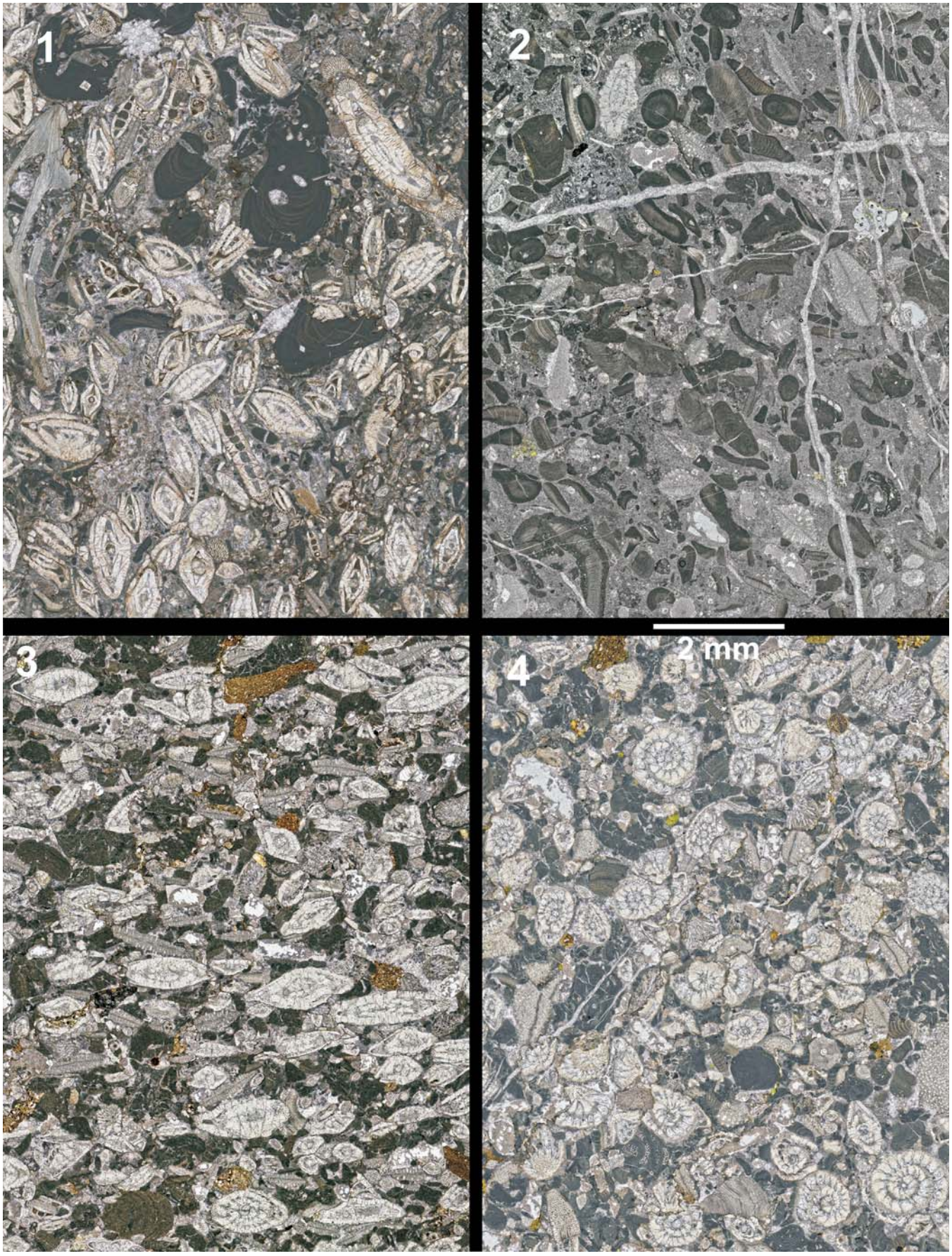
1
2
3
4
2 mm

of Tethyan Biogeography. London, Systematics Association 7: 195–217.

AGUILAR, T. and DENYER, P., 2001. Una nueva especie de Euphylia (Scleractinia: Caryophylliidae) en las calizas de Barra Honda (Paleógeno), Costa Rica. *Revista de Biología Tropical,* 2: 195–201.

ALVARADO, G. E., DENGO, C., MARTENS, U., BUNSCHUH, J., AGUILAR, T. and BONIS, S.B., 2007. Stratigraphy and geologic history. In: Bundschuh J. and Alvarado G. E., Eds., *Central America, geology, resources, hazards,* Taylor and Francis, vol.1, 345–394.

ALVARADO, G. E., DENYER, P. and SINTON, C., 1997. The 89 Ma Tortugal komatiitic suite, Costa Rica: implications for a common geological origin of the Caribbean and Eastern Pacific region from a mantle plume. *Geology,* 25: 439–442.

AMIEUX, P., 1987. Description petrographique de foraminifères par combinaison d'images en lumière naturelle et en cathodoluminescence. *Comptes rendus de l'Académie des Science*s, Paris, *Serie* 2, 304: 741–744.

ANDJIC, G. and BAUMGARTNER, P. O., 2015. Late Cretaceous siliceous deep-water formations of the Nicoya Peninsula (Costa Rica): Age and relationship of the Loma Chumico and Berrugate Formation and consequences for the terrane stratigraphy. *20th Caribbean Geological Congerence, Port of Spain Trinidad and Tobago, Conference booklet* 49.
www.thegstt.com/wp-content/uploads/2015/03/20th-CGC-Conference-Booklet.pdf

ANDJIC, G., BAUMGARTNER-MORA, C. and BAUMGARTNER, P.O., 2016. An upper Paleogene shallowing-upward sequence en the southern Sandino Forearc Basin (NW Costa Rica): Response to tectonic uplift. *Facies,* 62: 9.

———, (submitted). The Berigate Arc (Loma Chumico Formation. Late Cretaceous terrane evolution and arc initiation (Tempisque, N-Costa Rica. *International Journal of Earth Sciences*.

ARENILLAS, I., MOLINA, E. and SCHMITZ, B., 1999. Planktic foraminiferal and delta 3C isotopic changes across the Paleocene/Eocene boundary at Possagno (Italy). *International Journal of Earth Sciences,* 88: 352– 364.

ARIAS, O., 2000. "Géologie et pétrologie magmatique du Bloc Herradura (Crétacé supérieur. Eocène, Costa Rica)." PhD thesis, Univerité de Lausanne.

———, 2003. Redefinición de la Formación Tulín (Maastrichtiano-Eoceno Inferior) del Pacífico Central de Costa Rica. *Revista Geologica de América Central*, 28: 47–68.

ARNI, P., 1965a. L'évolution des Nummulitinae en tant que facteur de modification des dépôts littoraux. In: *Colloque International de Micropaléontologie*, *Mémoires BRGM*, 32: 7–20.

———, 1965b. Contribution à la systématique des *Nummulites* s.l. Colloque international de Micropaléontologie. Dakar, *Mémoires BRGM*, 32: 21–28.

———, 1966. Contribution to the history of growth of the *Chordoperculinoides* shell. *Eclogae Geologicae Helvetiae*, 59: 339–346.

ASTORGA, A., 1987. "El Cretácico Superior y el Paleógeno de la vertiente Pacífica de Nicaragua Meridional y Costa Rica Septentrional: origen y dinámica de las cuencas profundas relacionadas al margen convergente de Centroamérica." *Tesis Escuela Centroamericana de Geología,* Universidad de Costa Rica (unpublished).

AUBRY, M.-P., OUDAM, K., DUPUIS, C., BERGGREN, W. A., VAN COUVERING, J. A. and the Members of the Working Group on the Paleocene/Eocene Boundary, 2007. The Global Standard Stratotype-section and Point (GSSP) for the base of the Eocene Series in the Dababiya section (Egypt). *Episodes,* 30: 271–286.

AZÉMA, J., GLAÇON, G., TOURNON, J. and VILA, J-M., 1979. Precisiones acerca del Paleoceno de Puerto Quepos y sus alrededores, provincia de Puntarenas, Costa Rica. *Informe semestral del Instituto Geográfico Nacional*, 2: 77–78.

AZÉMA J., SORNAY, J. and TOURNON, J., 1979. Découverte d'Albien supérieur à ammonites dans le matériel volcano-sédimentaire du "Complexe de Nicoya" (Province de Guanacaste, Costa Rica). *Comptes rendus sommaires de la Société géologique de France*, 3: 71–76.

BABAZADED, S. A. 2011. New observations on biostratigraphy of *Ranikothalia sindensis* (Davies) in Early Paleogene of eastern Iran. *Revue de Paléobiologie,* 30: 313–319

BANDINI, A. N., FLORES, K., BAUMGARTNER, P. O., JACKETT, S.-J. and DENYER, P., 2008. Late Cretaceous and Paleogene radiolaria from the Nicoya Peninsula, Costa Rica: a tectonostratigraphic application. *Stratigraphy,* 5: 3–21.

BANNER, J. L., 2004. Radiogenic isotopes: systematics and applications to earth surface processes and chemical stratigraphy. *Earth-Science Reviews,* 65: 141–194.

BARBIN, V., 2000. Cathodoluminescence of carbonate shells: biochemical vs diagenetic process. In: Pagel, M. et al., Eds., *Cathodoluminescence in Geosciences*. Berlin: Springer, 303–329.

BARBIN, V., RAMSEYER K., DEBENAY, J. P., SCHEIN, E., ROUX, M. and DECROUEZ, D., 1991a. Cathodoluminescence of Recent biogenic carbonates: an environmental and ontogenetic fingerprint. *Geological Magasine,* 128: 19–26.

BARBIN, V., RAMSEYER, K., DECROUEZ D. and HERB, R., 1989. Mise en evidence par la cathodoluminescence d'indices de remaniements synsédimentaires. *Geobios,* 22: 253–259.

BARBIN, V., SCHEIN, E., ROUX, M., DECROUEZ, D. and RAMSEYER, K., 1991b. Stries de croissance révélées par cathodoluminescence dans la coquille de Pecten maximus (L.) récent de la Rade de Brest (Pectinidae, Bivalvia. *Geobios,* 24: 65–70.

BAUMGARTNER, P. O., 1986. Discovery of subduction related mélanges on Caño Island and Osa Peninsula (Pacific, Costa Rica, Central America. *Onziéme Réunion Annuelle des Sciences de la Terre.* Clermont-Ferrand, France, 12.

———, 1987. Tectónica y sedimentación del Cretácico superior en la zona pacífica de Costa Rica (América Central). *Simposio Internacional: El Cretácico de México y América Central.* Linares, México, 251–260.

BAUMGARTNER P.O., FLORES, K., BANDINI, A., GIRAULT, F. and CRUZ, D., 2008. Upper Triassic to Cretaceous radiolaria from Nicaragua and northern Costa Rica: the Mesquito composite oceanic terrane. *Ofioliti,* 33: 1–19.

BAUMGARTNER, P. O. and BAUMGARTNER-MORA, C., 2010. Chapter 5.5, Sedimentary Rocks; In: Werner et al. *Meteor-Berichte* 11-8, *CLIP. Origin of the Caribbean Large Igneous Province (CLIP) in connection with the geodynamic evolution of the Central Caribbean*, 29–34.
https://oceanrep.geomar.de/13988/1/Fahrtbericht_M81-2A_B.pdf

BAUMGARTNER, P. O. and MORA, C., 1984. Mapa Geológico de Quepos, 1:50000. *Instituto Geogràfico Nacional.* Costa Rica.

BAUMGARTNER, P. O., MORA, C., BUTTERLIN, J., SIGAL, J., GLACON, G., AZÉMA, J. and BOURGOIS, J., 1984. Sedimentación y paleogeografía del Cretácico y Cenozoico del litoral pacífico de Costa Rica. *Revista Geologica de América Central*, 1: 57–136.

BAUMGARTNER, P. O., OBANDO, J. A., MORA, C., CHANNELL, J. E. T. and STECK, A., 1989. Paleogene accretion and suspect terranes in southern Costa Rica (Osa, Burica, Central America), In: Larue, D. K. and Draper, G., Eds., *Transactions of the 12th Caribbean geological Conference*. St. Croix, U.S. Virgin Islands: 529.

BAUMGARTNER-MORA, C., 2006. Late Cretaceous-Tertiary larger foraminifera in carbonate palaeoenvironments of Costa Rica. *Forams 2006, Annuario do Instituto de Geosciencias, Universidade Federal do Rio de Janeiro,* 29: 645–646.

BAUMGARTNER-MORA, C. and BAUMGARTNER, P. O., 1994. Shell structure of fossil foraminifera studied by cathodoluminescence. *Microscopy and Analysis,* 3: 35–38.

———, 2011. Latest Miocene / early Pliocene Foraminifera and depositional environments of the carbonate bank of La Désirade Island, Guadeloupe (French Antilles. *Revue de Micropaléontologie,* 54: 183–205.

BAUMGARTNER-MORA, C., BAUMGARTNER, P. O., BUCHS, D. M., BANDINI, A. N. and FLORES, K., 2008. Palaeocene to Oligocene Foraminifera from the Azuero Peninsula (Panama): The timing of seamount formation, accretion and forearc overlap, along the Mid American Margin. *6th Swiss Geoscience Meeting*. Lugano: 116–117.

BAUMGARTNER-MORA, C., BAUMGARTNER, P. O. and TSCHUDIN, P., 2008. Late Oligocene Larger Foraminifera from Nosara (Nicoya Península, Costa Rica) and Windward (Carriacou, Lesser Antilles), calibrated by 87Sr/86Sr isotope stratigraphy. *Revista Geologica de América Central,* 38: 33–52.

BAUMGARTNER.MORA, C., BAUMGARTNER, P. O. and BARAT, F., 2013. Middle Cretaceous to Oligocene rise of the Middle American landbridge. documented by south-eastwards younging shallow water carbonates. *Geophysical Research Abstracts* 15: EGU2013-12742-2.

BAUMGARTNER-MORA, C, and DENYER, P., 2008. Upper Cretaceous (Campanian-Maastrichtian) limestone with Larger Foraminifera from Peña Bruja Rock (Santa Elena Peninsula). *Revista Geologica de América Central*, 26: 85–89.

BECKER, R., 1991. "Die Entwicklungsgeschichte des östlichen Parrita-Beckens im Tertiären Forearc-Bereich der südlichen Zentralamerikanischen Landbrücke (Costa Rica)." *Diploma thesis.* Universität Mainz, Germany, (unpublished).

BERGGREN, W. A., KENT, D. V., SWISHER, C. C. and AUBRY, M. P., 1995. A revised Cenozoic geochronology and chronostratigraphy. In: Berggren et al., Eds., *Geochronology, time scales and global stratigraphic correlation*. *Society of Economic Paleontologists and Mineralogists, Special Publication* 54: 129–212.

BERNER, R. A. and RYE, D. M., 1992. Calculations of the Phanerozoic strontium isotope record of the oceans from a carbon cycle model. *American Journal of Science,* 292: 136–148.

BERRANGÉ, J. P. and THORPE, R. S., 1988. The geology, geochemistry and emplacement of the Cretaceous Tertiary Ophiolitic Nicoya Complex of the Osa Peninsula, Southern Costa-Rica. *Tectonophysics,* 147: 193–220.

BLONDEAU, A., 1972. Les Nummulites. De l'ensegnement à la recherche. *Sciences de la Terre.* Librairie Vuibert, Paris.

BOER, J., DE, l979. The outer arc of the Costa Rican orogen (oceanic basement complexes of Nicoya and Santa Elena peninsulas. *Tectonophysics,* 56: 251-259.

BOLLI, H. M., 1957. Planktonic foraminifera from the Eocene Navet and San Fernando formations of Trinidad, B.W.I. *Bulletin U.S. National Mueum*, 215: 155-72.

BOLZ, A. and CALVO, C., 2003. Nuevos datos bioestratigráficos y sedimentológicos sobre el origen del complejo básico de Quepos. *Revista Geologica de América Central,* 2: 31-45.

BOURGOIS, J., AZEMA, J., BAUMGARTNER, P.O., TOURNON, J. and DESMET, A., 1984. The geologic history of the Caribbean Cocos plate boundary with special reference to the Nicoya Ophiolite Complex (Costa Rica) and DSDP results (Legs. 67 and 84 off Guatemala): A synthesis. *Tectonophysics,* 108: 1-32.

BRASS, G.W., 1976. The variation of the marine 87Sr/86Sr ratio during Phanerozoic time: interpretation using a flux model. *Geochimica et Cosmochimica Acta,* 40: 721-730.

BRIGUGLIO, A. and HOHENEGGER, J., 2009. Nummulitids hydrodynamics: an example using Nummulites globulus Leymerie. *Bolletino della Societá Paleontolologica Italiana,* 48:105–111.

BRIGUGLIO, A. and HOHENEGGER, J., 2011. How to react to shallow-water hydrodynamics: the larger benthic foraminifera solution. *Marine Micropaleontology,* 81: 63–76.

BRÖNNIMANN, P., 1952. Trinidad Paleocene and lower Eocene Globigerinidae. *Bulletin of American Paleontology,* 34 (143): 1-34.

BRUCKSCHEN, P., NEUSER, R.D., RICHTER, D.K., 1992. Cement stratigraphy in Triassic and Jurassic limestones of the Weserbergland (northwestern Germany). *Sedimentary Geology*, 81: 195-214.

BUCHS, D. M., ARCULUS, R. J., BAUMGARTNER, P. O., BAUMGARTNER-MORA, C., ULIANOV, A., 2010. Late Cretaceous arc development on the SW margin of the Caribbean plate: Insights from the Golfito, Costa Rica, and Azuero, Panama, complexes. *Geochemistry Geophysics Geosystems,* 11: Q07S24.

BUCHS, D. M., ARCULUS, R. J., BAUMGARTNER, P. O. and ULIANOV, A., 2011a. Oceanic intraplate volcanoes exposed: Example from seamounts accreted in Panama. *Geology,* 39: 335–338. Doi:10.1130/G31703.1.

BUCHS, D.M. and BAUMGARTNER, P.O., 2007. Comment on "From seamount accretion to tectonic erosion: Formation of Osa Mélange and the effects of Cocos Ridge subduction in southern Costa Rica" by P. Vannucchi et al. *Tectonics* 26: TC3009, doi:3010.1029/2006TC002032.

BUCHS, D. M., BAUMGARTNER, P. O., BAUMGARTNER-MORA, C., BANDINI, A. N., JACKETT, S. J., DISERENS, M. O. and STUCKI, J., 2009. Late Cretaceous to Miocene seamount accretion and melange formation in the Osa and Burica peninsulas (southern Costa Rica); episodic growth of a convergent margin. In: K. H. James, M.A. Lorente and J.L. Pindell, Eds., *The origin and evolution of the Caribbean plate*. Geological Society Special Publications 328: 411-456.

BUCHS, D. M., BAUMGARTNER, P. O., BAUMGARTNER-MORA C., FLORES K. and BANDINI A. N., 2011b. Upper Cretaceous to

Miocene tectonostratigraphy of the Azuero area (Panama) and the discontinuous accretion and subduction erosion along the Middle American margin. *Tectonophysics* 512: 31–46. Doi:10.1016/j.tecto.2011.09.010.

BUCHS, D. M., HOERNLE, K., HAUFF, F., BAUMGARTNER, P.O., 2016. Evidence from accreted seamounts for a depleted component in the early Galapagos plume. *Geology*, 44: 383-386. doi:10.1130/G37618.1

BUTTERLIN, J., 1960): Géologie générale et régionale de la République d'Haiti. *Institut Hautes Études Amerérique Latine,* Paris: 1-194.

———, 1981. Claves para la determinación de macroforaminíferos de Mexico y del Caribe del Cretacico Superior al Mioceno Medio. *Instituto Mexicano de Petróleo,* 29: 1–51.

———, 1992. Données nouvelles sur la distribution géographique des grands foraminifères du Crétacé terminal. *Geobios,* 14: 29–34.

BUTTERLIN, J. and BONET, F., 1960. Microfauna del Eoceno Inferior de la Península de Yucatan. *Paleontologia Mexicana*, Instituto de Geología, Mexico 7: 1–18.

BUTTERLIN, J. and MONOD, O., 1969. Biostratigraphie (Paléocène a l'Eocène moyen) d'une coupe dans le Taurus de Beysehir (Turquie). Etude des «Nummulites cordelées» et révision de ce groupe. *Eclogae geologicae Helvetiae,* 62: 583–604.

CALVO, C. and BOLZ, A., 1991. La Formación Espíritu Santo (Costa Rica): sistema de plataforma carbonatada autóctona del Paleoceno superior -Eoceno inferior. *Revista Geológica de América Central*, 13: 91–95.

CAPO, C., STEWART, B. W. and CHADWICK, O. A., 1998. Strontium isotopes as tracers of ecosystem processes: theory and methods. *Geoderma,* 82: 197–225.

CAUDRI, C. M. B., 1944. The larger foraminifera from San Juan de los Morros, State of Guarico, Venezuela. *Bulletins of American Paleontology, 2*8 (114): 355–404.

———, 1948. Note on the stratigraphic distribution of *Lepidorbitoides*. *Journal of Paleontology*, 22, 473–481.

———, 1972. Systematics of the American Discocyclinas. *Eclogae Geologicae Helvetiae,* 65: 211–219.

———, 1974. The larger foraminifera of Punta Mosquito, Margarita Island, Venezuela. *Verhandlungen der Naturforschenden Gesellschaft Basel,* 84: 293–318.

———, 1975. Geology and Paleontology of Soldado Rock, Trinidad (West Indies). *Eclogae Geologicae Helvetiae*, 68: 533–589.

———, 1990. A note on the type material of the genus Ranikothalia (Foraminifera. *Eclogae geologicae Helvetiae,* 83: 747–749.

———, 1996. The larger Foraminifera of Trinidad (West Indies). *Eclogae geologicae Helvetiae,* 89: 1137–1309.

CAZENAVE, S., CHAPOULIE, R. and VILLENEUVE, G., 2003. Cathodoluminescence of synthetic and natural calcite: the effects of manganese and iron on orange emission. *Mineralogy and Petrology,* 78: 243– 253.

CAZENAVE, S., DUTTINE, M., VILLENEUVE, G., CHAPOULIE, R. and BECHTEL, F., 2003. Cathodoluminescence orange (620 nm) de la calcite. I. Rôle du manganèse et du fer. *Annales de Chimie, Science des matériaux*, 28: 135–147.

CIZANCOURT, M. DE, 1948. Nummulites de l'île de la Barbade (Petites Antilles). *Mémoires de la Société géologique de France,* 57: 1–40.

———, 1951. Grandes foraminifères du Paléocène, Eocène inférieur et de l'Eocène moyen de Venezuela. *Mémoires de la Société géologique de France, nouvelle série*, 64: 1–68.

COATES, A. G., JACKSON, J. B. C., COLLINS, L. S., CRONIN, T. M., DOWSETT, H. J., BYBELL, L. M., JUNG, P. and OBANDO, L. A., 1992. Closure of the isthmus of panama : The near-shore marine record of costa rica and western panama. *Geological Society of America Bulletin*, 104: 814–828.

COLE, W. S., 1927. A foraminiferal fauna from the Guayabal formation in Mexico. *Bulletins of American Paleontology* 14 (51): 1–46.

———, 1953a. Criteria for the recognition of certain assumed camerid genera. *Bulletins of American Paleontology*, 35 (147): 28–46.

———, 1959. Faunal associations and the stratigraphic position of certain American Paleocene and Eocene larger foraminifera. *Bulletins of American Paleontology*, 39 (182): 377–393.

———, 1960. The Genus Camerina. *Bulletins of American Paleontology*, 41 (190): 189–200.

———, 1969a. Names and variation in certain American larger foraminifera, particularly the Eocene pseudophragminids. IV. *Bulletins of American Paleontology,* 56(248): 1–52.

COLE, W. S. and BERMÚDEZ, P. J., 1947. Eocene Discocyclinidae and other foraminifera from Cuba. *Bulletins of American Paleontology,* 31(125): 191–224.

COLE, W. S. and HERRICK, S. M., 1953. Two species of larger foraminifera from the Paleocene beds of Georgia. *Bulletins of American Paleontology*, 35: 6–9.

CORRIGAN, J., MANN, P. and INGLE, J. C. Jr., 1990. Forearc response to subduction of the Cocos Ridge, Panama–Costa Rica. *Geological Society of America Bulletin*, 102: 628–652.

CUSHMAN, J. A. and JARVIS, P. W., 1932. Upper Cretaceous Foraminifera from Trinidad. *Proceedings of the United States National Museum*, 80 (14): 1–60.

CUSHMAN, J. A. and RENZ, H. H., 1942. Eocene Midway Foraminifera from Soldado Rock, Trinidad. *Contributions from the Cushman Laboratory of Foramiferal Research*, 18(1), 1–14.

———, 1946. The foraminiferal fauna of the Lizard Springs Formation of Trinidad, British West Indies. *Cushman Laboratory for Foraminiferal Research Special Publication,* 18: 1–18.

DENGO, G., 1962a. Tectonic-igneous sequence in Costa Rica. Petrologic studies. A volume in honor of A. F. Buddington, 133–161.

———, 1962b. Estudio geológico de la región de Guanacaste, Costa Rica. *Instituto Geográfico Nacional, San José*: 1–112.

DENYER, P., AGUILAR, T. and MONTERO, W., 2013. Cartografía geológica de la Península de Nicoya. Mapas geológicos 1: 50000. SIEDIN, Universidad de Costa Rica, San José, C.R.

———, 2014. Cartografía geológica de la Península de Nicoya. Estratigrafía y tectonica. SIEDIN, Universidad de Costa Rica, San José, C.R.

DENYER, P. and ALVARADO, G. E., 2007. Mapa Geológico de Costa Rica 1: 400'000. Librería Francesa S.A., San José, Costa Rica.

DENYER, P. and BAUMGARTNER, P. O., 2006. Emplacement of Jurassic-Lower Cretaceous radiolarites of the Nicoya Complex (Costa Rica). *Geologica Acta*, 4: 203–218.

DENYER, P., BAUMGARTNER, P. O., and GAZEL, E., 2006. Characterization and tectonic implications of Mesozoic-Cenozoic oceanic assemblages of Costa Rica and Western Panama. *Geologica Acta*, 4: 219–235.

DENYER, P. and GAZEL, E., 2009. The Costa Rican Jurassic to Miocene oceanic complexes: Origin, tectonics and relations. *Journal of South American Earth Sciences,* 28: 429–442.

DI MARCO, G., 1994. Les terrains accrétés du Costa Rica: évolution teconostratigraphique de la marge occidentale de la Plaque Caraïbe, *Mémoires de Géologie* (*Lausanne*), 20.

DI MARCO, G., BAUMGARTNER P. O. and CHANNELL J. E. T., 1995. Late Cretaceous-early Tertiary paleomagnetic data and a revised tectonostratigraphic subdivision of Costa Rica and western Panama. Geologic and tectonic development of the Caribbean Plate boundary in southern Central America.. In: Mann, P., Ed., *Geologic and Tectonic Development of the Caribbean plate boundary in southern Central America*. *Geological Society of America Special Paper 295*: 1–27.

DROOGER, C. W., 1960. Some early rotaliid Foraminifera. *Proceedings of the Koninklijke Nederlandse Akademie van Wetenschappen*, serie B 63: 287–301.

EAMES, F. E., 1968. *Sindulites*, a new genus of the Nummulitidae (Foraminifera.) *Palaeontology,* 11: 435–438.

EHRLICH, R. N., ASTORGA, A., SOFER, Z., PRATT, L. M. and PALMER, S. E., 1996. Palaeoceanography of organic-rich rocks of the Loma Chumico Formation of Costa Rica, Late Cretaceous, eastern Pacific. *Sedimentology,* 43: 609–770.

EL ALI, A., BARABIN, V., CALAS, G., CERVELLE, B., RAMSEYER, K., BOUROULEC, J., 1993. Mn^{2+} activated luminescence in dolomite, calcite and magnesite: quantitative determination of manganese and site distribution by EPR and CL spectroscopy. *Chemical Geology,* 104: 189–202.

FAURE, G., 1986. Isotope geology of neodymium and strontium in igneous rocks. In: *Principles of Isotope Geology*, second edition. New York: John Wiley and Sons, 217–238.

FAURE, G. and MENSING, T. M., 2004. Isotopes: Principles and applications, third edition, John Wiley and Sons, New York: 1–928.

FLORES K., 2009. "Mesozoic Oceanic Terranes of Southern Central America: Geology, Geochemistry and Geodynamics." *Ph.D. thesis*, University of Lausanne, 1–290.

FLORES, K., DENYER, P. and AGUILAR, T., 2003. Nueva propuesta estratigráfica: Geología de la hoja Abangares, Guanacaste, Costa Rica. *Revista Geológica de América Central*, 29: 127–136.

FLORES, K. E., SKORA, S., MARTIN, C., HARLOW, G.E., RODRÍGUEZ, D. and BAUMGARTNER, P. O., 2015. Metamorphic history of riebeckite- and aegirine-augite-bearing high-pressure–low-temperature blocks within the Siuna Serpentinite Mélange, northeastern Nicaragua. *International Geology Review* 57: 943–977, http://dx.doi.org/10.1080/ 00206814.2015.1027747

GELDMACHER, J., HANAN, B. B., BLICHERT-TOFT, J., HARPP, K., HOERNLE, K., HAUFF, F. WERNER, R. and KERR, A. C., 2003. Hafnium isotopic variations in volcanic rocks from the Caribbean Large Igneous Province and Galápagos hot spot tracks, *Geochemistry, Geophysics, Geosystems* 4: 1062. http://dx.doi.org/10.1029/2002GC000477.

GREEN, O. R., 2001. A manual of practical laboratory and field techniques in palaeobiology. Kluwer Academic Publishers: 1–538.

HALLOCK, P., 1981. Algal symbiosis: A mathematical analysis. *Marine Biology*, 62: 249–255.

———, 1984. Distribution of selected species of living algal symbiont-bearing Foraminifera on two Pacific coral reefs. *Journal of Foraminiferal Research*, 14: 250–261.

———, 1985. Why are larger Foraminifera large? *Paleobiology*, 11: 195–208.

———, 1987. Fluctuations in the trophic resource continuum: a factor in global diversity cycles? *Paleoceanography*, 2: 457–471.

———, 1988. Interoceanic differences in Foraminifera with symbiotic algae: a result of nutrient supplies? *Proceedings Sixth International Coral Reef Symposium*, Townsville, Australia, 3: 251– 255.

HALLOCK, P., RÖTTGER, R. and WETMORE, K., 1991. Hypotheses on form and function in Foraminifera. In: Lee, J.J., and Anderson, O.R., Eds., *Biology of Foraminifera*. Academic Press, London: 41–72.

HANZAWA, S., 1937. Notes on some interesting Cretaceous and Tertiary Foraminifera from the West Indies. *Journal of Paleontology*, 11: 110–117.

HAQ, B.U. and AL-QAHTANI, A.M., 2005. Phanerozoic cycles of sea-level change on the Arabian Platform. *GeoArabia,* 10: 127–160.

HAUFF, F., HOERNLE K., BOGAARD, P., ALVARADO, G. E. and GARBE-SCHÖNBERG, D., 2000a. Age and geochemistry of basaltic complexes in western Costa Rica: Contributions to the geotectonic evolution of Central America. *Geochemistry, Geophysics, Geosystems* 1, 1069. doi.org/10.1029/1999GC000020.

HAUFF F., HOERNLE, K., SCHMINCKE H. U. and WERNER, R., 1997. A mid-Cretaceous origin for the Galapagos hotspot: volcanological, petrological and geochemical evidence from Costa Rica oceanic crustal fragments. *Geologische Rundschau*, 86: 141–155.

HAUFF, F., HOERNLE, K., TILTON G., GRAHAM D.W. and KERR, A. C., 2000b. Large volume recycling of oceanic lithosphere over short time scales: geochemical constraints from the Caribbean Large Igneous Province. *Earth and Planetary Science Letters,* 174: 247–263.

HAYNES, J. R., RACEY, A. and WHITTAKER, J. E., 2010. A revision of the Early Palaeogene nummulitids (Foraminifera) from Northern Oman, with implications for their classification. In: Whittaker, J. E., Hart, M.B., Eds., *Micropalaeontology, Sedimentary Environments and Stratigraphy: A Tribute to Dennis Curry (1912–2001). The Micropalaeontological Society Special Publication*: 29–89.

HENNINGSEN, D., 1966. Die pazifische Küstenkordillere (Cordillera Costefia) Costa Ricas und ihre Stellung innerhalb des südzentral amerikanischen Gebirge. *Geotektonische Forschungen, Stuttgart*, 23: 3–66.

HODELL, D. A., MUELLER, P. A., MCKENZIE, J. A. and MEAD, G. A., 1989. Strontium isotope stratigraphy and geochemistry of the late Neogene ocean. *Earth and Planetary Science Letters*, 92: 165–178.

HOERNLE, K. A., BOGAARD P., VAN DEN, WERNER, R., HAUFF, F., LISSINNA, B., ALVARADO, G. E. and GARBE-SCHÖNBERG, D., 2002. Missing history (16–71 Ma) of the Galapagos hotspot: Im-

plications for the tectonic and biological evolution of the Americas, *Geology*, 30: 795–798.

HOFMANN, H. J., 1994. Grain-shape indices and isometric graphs. *Journal of Sediment Research*, 64: 916–920.

HOHENEGGER, J., 1994. Distribution of living larger Foraminifera NW of Sesoko-Jima, Okinawa, Japan. *P.S.Z.N. I: Marine Ecology*, 15: 291–334.

———, 2000. Coenoclines of larger foraminifera. *Micropaleontology*, 46: 127–151.

———, 2004. Depth coenoclines and environmental considerations of western pacific larger foraminifera. *Journal of Foraminiferal Research*, 34: 9–33.

HOHENEGGER, J., YORDANOVA, E., NAKANO, Y., TATZREITER, F., 1999. Habitats of larger foraminifera on the upper reef slope of Sesoko Island, Okinawa, Japan. *Marine Micropaleontology*, 26: 109–168.

HOLLAND, H.D., 1984. The Chemical Evolution of the Atmospheres and Ocean. Princeton University, Princeton, N.J.: 1–582.

HOTTINGER, L., 1977a. Foraminifères operculiniformes. *Mémoires du Muséum National d'Histoire Naturelle*, Série C 40: 1–159.

———, 1977b. Distribution of larger Peneroplidae, *Borelis* and Nummulitidae in the Gulf of Elat, Red Sea. *Utrecht Micropaleontological Bulletins,* 15: 35–109.

———, 1983. Processes determining the distribution of larger foraminifera in space and time. *Utrecht Micropaleontological Bulletins*, 30: 239–253.

———, 2000. Functional morphology of benthic foraminiferal shells, envelopes of cells beyond measure. In: Lee, J. J. and Muller, P.H., Eds., *Advances in the Biology of Foraminifera*. *Micropaleontology*, 46: 57–86.

HOTTINGER, L., HALICZ, E., REISS, Z., 1993. Recent Foraminiferida from the Gulf of Aqaba, Red Sea. Opera SAZU, Ljubljana 33: 1–179.

HOTTINGER, L. and SCHAUB, H., 1960. Zur Stufeneinteilung des Paleocaens und des Eocaens. *Eclogae Geologicae Helvetiae*, 53: 453–479.

HSU, K. J., 1973. Mesozoic evolution of California Coast ranges; a second look. In: DeJong, K. A. and Scholten, R., Eds., *Gravity and tectonics*. New York, John Wiley and Sons: 379–396.

JACCARD, S. and MÜNSTER, M., 2001. Etude géologique multidisciplinaire de la plateforme de Barra Honda (Guanacaste, Costa Rica): Sédimentologie, isotopes stables du strontium, du carbone, de l'Oxygène et contexte géodynamique. *DEA thesis*, Université de Lausanne (unpublished).

JACCARD, S., MÜNSTER, M., BAUMGARTNER, P. O., BAUMGARTNER-MORA, C. and DENYER, P., 2001. Barra Honda (Upper Paleocene- Lower Eocene) and El Viejo (Campanian-Maastrichtian) carbonate platforms in the Tempisque area (Guanacaste, Costa Rica). *Revista Geologica de América Central,* 24: 9–28.

KAMINSKI, M. A., GRADSTEIN, F. M., BERGGREN, W. A., GEROCH, S., and BECKMANN, J. P., 1988. Flysch-type agglutinated foraminiferal assemblages from Trinidad: Taxonomy, Stratigraphy, and Paleobathymetry. In: Rogl, F., Gradstein, F.M., Eds., Second Workshop on Agglutinated Foraminifera, Vienna, 1986, *Abhandlungen der geologischen Bundesansalt,* 41: 155–227.

KELLY, D.C., BRALOWER, T.J. and ZACHOS, J.C., 1998. Evolutionary consequences of the latest Paleocene thermal maximum for tropical planktonic foraminifera. *Palaeogeography, Palaeoclimatology, Palaeoecology,* 141: 139–161.

KOŁODZIEJ, B., JURKOWSKA, A., BANAŚ, M. and IVANOVA, D., 2011. Improving detection of foraminifera by cathodoluminescence. *Facies*, 57: 571–578.

KUGLER, H. G. and CAUDRI C. M. B., 1975. Geology and Paleontology of Soldado Rock, Trinidad (West Indies. Part 1: Geology and Biostratigraphy. *Eclogae Geologicae Helvetiae*, 68: 365–430.

LUNDBERG, N., 1982. Evolution of the slope landward of the Middle America Trench, Nicoya Peninsula, Costa Rica. In: Leggett, J.K., Ed., *Trench-forearc geology.* Geological Society, London, Special Publications 10: 131–147.

LY, A. and ANGLADA, R., 1991. Le bassin sénégalo-mauritanien dasn l'évolution des marges pèriatlantiques au Tertiaire. *Cahiers de Micropaléontologie*, 6/2; 23–47.

MACHEL, H. G, MASON, R. A, MARIANO, A. N, and MUCCI, A., 1991. Causes and emission of luminescence in calcite and dolomite. In: Barker, C.E. and Kopp, O.C., Eds., *Luminescence Microscopy: Quantitative and Qualitative Aspects*. *Soc. Econn. Paleontol. Mineral. Short Course Notes,* 25: 9–25.

MADRIGAL, O. GAZEL, E., FLORES, K., BIZIMIS, M. and JICHA, B., 2016. Record of massive upwellings from the Pacific large low shear velocity province. *Nature Communications*, 7: 13309. DOI: 10.1038/ncomms13309

MALAVASSI, E., 1967. Informe geológico de la hoja Candelaria. *Informes Ministerio Economía, Industria y Comercio*: 1–16.

———, 1961a. Some Costa Rican larger foraminifera localities. *Journal of Paleontology*, 35: 498–501.

———, l96lb. *Pseudogloborotalia velascoensis* (Cushman), especie índice del Paleoceno Superior en Punta Guiones, Guanacaste. *Informes Departamento de Geología, Minas y Petróleo*, 1 (1 l): l–5.

MANN, P., 2007. Overview of the tectonic history of northern Central America. Geologic and tectonic development of the Caribbean Plate boundary in northern Central America. In: Geologic and tectonic development of the Caribbean Plate boundary in northern Central America. In: Mann, P., Ed., *Geological Society of America Special Paper*, 428: 1–19,

MARSHALL, D. J., 1988. Cathodoluminescence of geological materials. Allen and Unwin Inc, USA, Massachusetts: 1–146.

MARTINI, R., AMIEUX, P., GANDIN, A. and ZANINETTI, L., 1987. Triassic foraminifers from Punta Tonnara (SW Sardinia) observed in cathodoluminescence. *Revue de Paléobiologie,* 6: 23–27.

MASSIEUX, M. and DENIZOT, M., 1964. Rapprochement du genre *Pseudolithothamnium* Pfender avec le genre actuel *Ethelia* Weber Van Bosse (Algues Florideae, Squamariaceae). *Revue de Micropaléontologie,* 7: 31–42.

MCARTHUR, J. M., 1994. Recent trends in strontium isotope stratigraphy. *Terra Nova*, 6: 331–358.

———, 1998. Strontium isotope stratigraphy. In: Doyle, P. and Bennett, M.R., Eds., *Unlocking the stratigraphical record*. *Advances in modern stratigraphy.* Chichester: John Wiley and Sons, 221–241.

MCARTHUR, J. M., HOWRATH, R. J. and BAILLEY, T. R., 2001. Strontium Isotope Stratigraphy: LOWESS version 3: Best fit to the

marine Sr-Isotope curve for 0-509 Ma and accompanying look-up table for deriving numerical age. *Journal of Geology*, 109: 155–170.

MELLO E SOUSA E, S. H., FAIRCHILD, T. R. and TIBANA, P., 2003. Cenozoic biostratigraphy of larger foraminifera from the Foz Do Amazonas basin, Brazil. *Micropaleontology*, 49: 253–266.

MESCHEDE, M. and FRISCH, W., 1994. Geochemical characteristics of basaltic rocks from the Central American ophiolites. *Profil*, 7: 71–85.

MEYBECK, M., 1987. Global chemical weathering of surficial rocks estimated from river dissolved loads. *American Journal of Science*, 287: 401– 428.

MEYERS, W. J., 1974. Carbonate cement stratigraphy of The Lake Valley Formation (Mississippian) Sacramento Mountains, New Mexico. *Journal of Sedimentary Petrology*, 44: 837–861.

———, 1978. Carbonate cement: their regional distribution and interpretation in Missippian limestones of southwestern New Mexico. *Sedimentology*, 25; 371–400.

MONTES, C., CARDONA, A., MCFADDEN, R., MORÓN, S. E., SILVA, C. A., RESTREPO-MORENO, S., RAMÍREZ, D. A., HOYOS, N., WILSON, J., FARRIS, D., BAYONA, G. A., JARAMILLO, C. A., VALENCIA, V., BRYAN, J. and FLORES, J.A., 2012a. Evidence for middle Eocene and younger emergence in Central Panama: implications for Isthmus closure. *Geological Society of America Bulletin*, 124: 780–799. doi.org/10.1130/B30528.1.

MORA, C., BAUMGARTNER, P. O. and HOTTINGER, L., 1989. Eocene shallow-water carbonate facies with larger foraminifera in the Caño Accretionary Complex, Caño Island and Osa Peninsula (Costa Rica, Central America). *12th Caribbean Geological Conference, St. Croix* (USVI): 122.

MORA, S., 1981. Barra Honda. *Editorial Universidad Estatal a Distancia, Serie Educación Ambiental*, 5, San José: 1–94.

NAGAPPA, Y., 1959. Foraminiferal Biostratigraphy of the Cretaceous. Eocene succession in the India. Pakistan. Burma region. *Micropalenotology*, 5:145–192.

OBANDO RODRIGUEZ, J. A., 1986. Sedimentología y tectónica del Cretacico y Paleógeno de la región de Golfito, Península de Burica y Península de Osa, Provincia de Puntarenas, Costa Rica. *Tesis de Licenciatura*. Escuela Centroamericana de Geología, Universidad de Costa Rica (unpublished).

PAK, D. K. and MILLER, K. G., 1992. Paleocene to Eocene benthic foraminiferal isotopes and assemblages: implications for deepwater circulation. *Paleoceanography*, 7: 405–422,

PALMER, D. K., 1934. Some large fossil Foraminifera from Cuba. *Memorias de la Sociedad Cubana de Historia Natural*, 8 (4): 235–264.

PALMER, M. R. and EDMOND, J. M., 1989. The strontium isotope budget of the modern ocean. *Earth and Planetary Science Letters*, 92: 11–26.

PALMER, M. R. and OSMOND, J. M., 1992. Controls over the Sr isotope composition of river water. *Geochimica et Cosmochimica Acta*, 56: 2099–2111.

PEYBERNÈS, B., FONDECAVE-WALLEZ, M.-J., HOTTINGER, L., EICHÈNE, P. and SÉGONZAC, G., 2000. Limite Crétacé-Tertiaire et biozonation paléontologique du Danien-Sélandien dans le Béarn et la Haute-Soule (Pyrénées-Atlantiques). *Geobios*, 33: 35–48.

PONS, J. and SCHMIDT-EFFING, R., 1998. Upper Cretaceous rudists from Guanacaste province, Costa Rica, Central América. *Terra Nostra*, 16: 124–125.

PONS, J., VICENS, E. and SCHMIDT-EFFING, R., 2016. Campanian rudists (Hippuritida, Bivalvia) from Costa Rica (Central America). *Journal of Paleontology*, 90: 211–238.

PRATURLON, A., 1966. Algal assemblages from Lias to Paleocene in Southern Latium-Abruzzi: a review. *Bollettino della Società Geologica Italiana*, 85: 167–194.

PROKOPH, A., SHIELDS, G. A. and VEIZER, J., 2008. Compilation and time-series analyses of a marine carbonate $\delta^{18}O$, $\delta^{13}C$, $^{87}Sr/^{86}Sr$ and $\delta^{34}S$ database through Earth history. *Earth Science Reviews*, 87: 113–133.

RANERO, C. R. and VON HUENE, R., 2000. Subduction erosion along the Middle America convergernt margin. *Nature*, 404: 748–752.

RAYMO, M. E., RUDDIMAN, W. F. and FROELICH, P. N., 1988. Influence of late Cenozoic mountain building on ocean geochemical cycles. *Geology*, 1: 649–653.

RIVIER, F., 1983. Síntesis geológica y mapa geológico del ârea del Bajo Tempisque Guanacaste, Costa Rica. *Instituto Geografico Nacional*, *Informe semestral,* Costa Rica: 7–30.

ROBINSON, E. and WRIGHT, R. M., 1993. Jamaican Paleogene larger foraminifera. In: Wright, R.M., Robinson, E., Eds., *Biostratigraphy of Jamaica*. *Geological Society of America, Memoir* 182: 283–345.

SACHS, K. N. Jr., 1957. Restudy of some Cuban larger Foraminifera. *Contributions from the Cushman Foundation for Foraminiferal Research*, 8: 106–120.

SCHINDLBECK, J. C., KUTTEROLF, S., FREUNDT, A., STRAUB, S. M., WANG, K. L., JEGEN, M., HEMMING, S. R., BAXTER, A. T. and SANDOVAL, M. I., 2015. The Miocene Galápagos ash layer record of Integrated Ocean Drilling Program Site Legs 334 and 344: Ocean-island explosive volcanism during plume- ridge interaction. *Geology*, 43: 599–602.

SCHMIDT-EFFING, R., 1975. El primer hallazgo de amonites en América Central Meridional y notas sobre las facies cretacicas en dicha region. *Instituto Geogrâfico Nacional, Informe semestral*, Costa Rica: 53–61.

———, 1979. Alter und Genese des Nicoya-Komplexes, einer ozeanischen Palaokruste (Oberjura bis Eozän) im südlichen Zentralamerika: *Geologische Rundschau*, 68: 457–494 .

SCHOLLE, P. A. and ULMER-SCHOLLE, D. S., 2003. A Color Guide to the Petrography of Carbonate Rocks: Grains, textures, porosity, diagenesis: Tulsa, OK, A Color Guide to the Petrography of Carbonate Rocks: Grains, Textures, Porosity, Diagenesis. *American Association of Petroleum Geologists Memoir* 77: 1–474.

SCHREIBNER, C. and SPEIJER, R.P., 2009. Recalibration of the Tethyan shallow-benthic zonation across the Paleocene- Eocene boundary: the Egyptian record. *Geologica Acta*, 7: 195–214.

SERRA-KIEL, J., HOTTINGER, L., CAUS, E., DROBNE, K., FERRÀNDEZ, C., JAUHRI, A.K., LESS, G., PAVLOVEC, R., PIGNATTI, J., SAMSÓ, J.M., SCHAUB, H., SIREL, E., STROUGO, A., TAMBAREAU, Y., TOSQUELLA, J. and ZAKREVSKAYA, E., 1998. Larger foraminiferal biostratigraphy of the Tethyan Paleocene and Eocene. *Bulletin de la Societé géologique de France*, 169: 281– 299.

SEYFRIED, H. and SPRECHMANN, P., 1985. Acerca de la formación del Puente Istmo Centroamericano Meridional con énfasis en el desarrollo acaecido desde el Campaniense al Eoceno. *Revista geológica de América Central*, 2: 63–87.

SHIELDS, G. A., 2007. A normalized seawater strontium curve: possible implications for Neoproterozoic-Cambrian weathering rates and the further oxygenation of the Earth. *Earth*, 2: 35–42.

SINTON, C. W., DUNCAN, R. A. and DENYER, P., 1997. Nicoya Peninsula, Costa Rica: A single suite of Caribbean oceanic plateau magmas. *Journal of Geophysical Research*, 102: 507–520.

SOMMER, S. E., 1972. Cathodoluminescence of carbonates: 1. Characterization of cathodoluminescence from carbonate solid solutions. *Chemical Geology*, 9: 257–273.

SPRECHMANN, P., Editor, 1984. Manual de Geología de Costa Rica. *Editorial Univarsidad de Costa Rica*, San José: 1–320.

SPRECHMANN, P., ASTORGA, A., BOLZ, A., CALVO, C., 1987. Estratigrafía del Cretacico de Costa Rica. *Actas de la Facultad de Ciencias de la Tierra U.A.N.L*. Linares, 2: 69–83.

TOSQUELLA, J., SERRA-KIEL, J., FERRÀNDEZ-CAÑADELL, C. and SAMSÓ, J. M., 1998. Las biozonas de nummulítidos del Paleoceno Superior -Eoceno Inferior de la Cuenca Pirenaica. *Acta Geologica Hispanica,* 31: 23–36.

TRELA, J., VIDITO, C., GAZEL, E., HERZBERG, C., CLASS, C., WHALEN, W., JICHA, B., BIZIMIS, M., ALVARADO, G. E., 2015. Recycled crust in the Galápagos Plume source at 70 Ma: Implications for plume evolution. *Earth and Planetary Science Letters*, 425: 268–277.

URQUHART, E., GARDIN, S., LECKIE, R. M., WOOD, S.A., PROSS, J., GEORGESCU, M. D., LADNER, B., and TAKATA, H., 2007. A paleontological synthesis of ODP Leg 210, Newfoundland Basin. *Proceedings of the Ocean Drilling Program, Scientific Results,* 210: 1–53.

VAUGHAN, T. W., 1929. Description of new species of foraminifera of the genus Discocyclina from the Eocene of Mexico. *Proceedings of the United States Natural History Museum,* 76, 1–18.

———, 1932. The Foraminiferal Genus *Orbitolina* in Guatemala and Venezuela. *Proceedings of the National Academy of Sciences of the United States of America*, 18: 609–610.

———, 1945. American Old and Middle Tertiary larger Foraminifera and Corals. Part I. American Paleocene and Eocene larger foraminifera. *Geological Society of America Memoir*, 9: 1–175.

VAUGHAN, T.W. and Cole, W.S., 1941. Preliminary report on the Cretaceous and Tertiary larger foraminifera of Trinidad, British West Indies. *Geological Society of America Special Papers*, 30: 1–137.

VEIZER, J., 1989. Strontium isotopes in seawater through time. *Annual Review of Earth and Planetary Sciences*, 17: 141–167.

VEIZER, J. and MACKENZIE, F.T., 2003. Evolution of sedimentary rocks. In: Mackenzie, F. T., Ed., *Treatise of Geochemistry*, *7*, *Sediments, diagenesis and sedimentary rocks*. 369–407.

VÉRARD, C., HOCHARD, C., BAUMGARTNER, P. O., STAMPFLI, G. M., 2015. Geodynamic evolution of the Earth over the Phanerozoic: Plate tectonic activity and paleoclimatic indicators. *Journal of Palaeogeography*, 4: 60–81.

VICEDO, V., BERLANGA, J.A. and SERRA-KIEL, J., 2014. Paleocene larger foraminifera from the Yucatán Peninsula (SE Mexico. *Carnets de Géologie*, 14 (4): 41–67.

VICEDO, V., BERLANGA, A., SERRA-KIEL, J. and CAUS, E., 2013. Architecture and age of the foraminiferal genus *Taberina* Keijzer, 1945. *Journal of Foraminiferal Research*, 43: 170–181.

VIERS, J., DUPRÉ, B., BRAUN, J-J., DEBERT, S., ANGELETLI, B., NDAMNGOUPAYOU, J. and MICHARD, A. 2000. Major and trace element abundances, and strontium isotopes in the Nyong basin rivers (Cameroon): constraints on chemical weathering processes and elements transport mechanisms in humid tropical environments. *Chemical Geology*, 169: 211–241.

WEBER, P. J. N., 2013. Assessing sedimentary evolution by means of Sr-isotope ratios: 3 case studies on the Caribbean Plate (Cretaceous: Nicoya Peninsula, Costa Rica, Tertiary: Hess Rise, and La Désirade, Guadeloupe, France. *Ph.D. thesis*, University of Lausanne: 1–176.

WINSEMANN, J., 1992. Tiefwasser-Sedimentationsprozesse und -produkte in den Forearc-Becken des mittelamerikanischen Inselbogensystems: Eine sequenzstratigraphische Analyse. *Dissertation an der Universität Stuttgart*, *Profil*, 2: 1–218.